1995

# Studies on the chemical composition and thermo-mechanical processings of high performance steels

Thomas John Todaro
*Lehigh University*

# STUDIES ON THE CHEMICAL COMPOSITION AND THERMO-MECHANICAL PROCESSING OF HIGH PERFORMANCE STEELS

by

Thomas John Todaro

A Thesis

Presented to the Graduate and Research Committee

of Lehigh University

in Candidacy for the Degree of

Master of Science

in

Materials Science and Engineering

Lehigh University

May 1995

This thesis is accepted and approved in partial fulfillment of the requirements for the degree of Master of Science.

5/1/95
Date

Dr. R. D. Stout
Thesis Advisor

Dr. J.H. Gross
Thesis Advisor

Dr. K. Tarby
Faculty Advisor

Dr. D. B. Williams
Chairperson of the Materials Science and Engineering Department

## Acknowledgments

The work being reported was conducted at Lehigh University's Advanced Technology for Large Structural Systems (ATLSS) Engineering Research Center. Dr. J.W. Fisher is the director of ATLSS. I would like to thank ATLSS for the financial support and the use of the facility.

Special thanks are due to Dr. Robert D. Stout and Dr. John H. Gross who guided the research. I would also like to thank Dr. Eric Kaufmann and Dr. Bruce Sommers for their technical support, Dave Schnalzer who helped to run and guide laboratory testing, and Carl Chrisbacher and Tony Magee who helped run the experimental tests.

I would also like to thank my parents, Josephine and Thomas, my sisters Josette and Janine, and Jennifer L. Koza for their support and understanding throughout my education.

## Table of Contents

## List of Tables

## List of Figures

# Abstract

The need to improve the infrastructure has influenced the use of thermo-mechanical controlled processed (TMCP) steels in construction. Previous work on high strength steels, at Lehigh University's Advanced Technology for Large Structural Systems (ATLSS), determined that lowering the carbon content would eliminate the need to preheat weldments and that the resulting loss in strength could be offset by controlled-rolling and direct quenching (CRDQ). Further studies showed that controlled-rolling, air cooling, and off-line heat treatment (CRAQ) improved toughness as compared to the CRDQ processing, but gains in strength were not as significant. ATLSS has continued this work on high performance steels to optimize the compositions and properties of 100 ksi and 70 ksi steels suitable for construction applications such as bridges.

Steel compositions were obtained at nominal carbon levels of 0.065% to meet 100 ksi and 70 ksi minimum yield strengths in the following three processed conditions: 1. CRDQ, 2. Control-Rolled and Air-cooled (CRA), and 3. Hot-Rolled and Air-cooled (HRA). Initial mechanical property tests showed that CRA processed plates had reduced strength but improved toughness as compared to the CRDQ processed plates. In an attempt to improve property levels, two additional plates for each composition were processed: 1. CRDQ finished rolled at a higher temperature and 2. CRA finished rolled at a lower temperature. The purpose of the additional plates was to regain toughness in the CRDQ processed plates by permitting recrystallization of the microstructures and to improve strength in the CRA processed plates by adding deformation to the

microstructure. Mechanical tests showed that CRA off-line heat treated plates had better strength-toughness relationships than CRDQ processed plates and that the roll-finishing temperature did little to improve properties. In addition, weldability tests showed that steels with carbon contents held well below 0.10% had high resistance to hydrogen induced HAZ cracking without a preheat.

# 1. Introduction

## 1.1 Purpose of Present Investigation

The need to improve the United States infrastructure is well documented in the literature.[1,2] Reports indicate that the development of a new era of high strength steel is essential for high performance applications.[3] This concern has spurred the development of High Performance Steels (HPS) for applications in large structures such as bridges. These new steels differ from traditional high strength steels because they provide improved properties such as weldability, toughness, yield strength, and corrosion resistance. If these HPS steels were utilized, gauge thickness could be reduced and strict welding procedures could be eliminated. These advancements would be cost effective during all stages of the construction process.[4]

Traditional high strength steels developed for bridge construction have serious limitations. For example, A514 Steel is limited because its weldments must be preheated which increases the cost of fabrication[5]. Improvement of weldability in high performance steels can be achieved by reducing carbon content and offsetting the resultant loss in hardenability/strength with a Thermo-Mechanical Controlled Practice (TMCP).[6] Lowering the carbon content reduces the heat affected zone (HAZ) hardness, thus minimizing the susceptibility to hydrogen induced HAZ cracking. As a result, preheating may be eliminated or minimized which enhances productivity. Therefore, TMCP high

performance steels can be welded at a substantially lower cost than conventional high strength steels. This advantage combined with excellent mechanical properties makes these steels extremely important to U.S. manufactures. To take full advantage of these properties, ATLSS initiated this study to optimize low carbon steel compositions coupled with advanced TMCP treatments to develop improved high performance bridge steels.

## 1.2 Development of TMCP at ATLSS

As part of the Fleet of the Future Project (FFP), ATLSS began a study of TMCP high performance steels as replacements for the Navy's HY 100 ksi series steels.[7] The intent of this project was to investigate the possibility of improving weldability in a low cost, low alloy 100 ksi minimum yield strength steel. The study showed that by reducing carbon content from the current HY level of 0.14% minimum down to 0.065%, the need to preheat weldments would be eliminated and the resulting loss in strength could be offset by TMCP.

The TMCP used in the FFP project consisted of controlled-rolling and direct quenching (CRDQ). There were two main drawbacks of the CRDQ process. First, the lack of existing facilities in the United States would require a large monetary investment. Second, ATLSS showed that the increased strengths of the CRDQ processed plates were accompanied by poor toughness. ATLSS initiated a Special Studies Program to examine the previously studied Navy steels evaluated in the FFP project.[8] The scope of the Special Studies Program was three fold:

1. Determine the reason for the poor toughness of the CRDQ plates.

2. Investigate the possibility of recovering toughness with an additional off-line heat treatment applied to the CRDQ plates.
3. Evaluate a TMCP process which consists of controlled-rolling, air cooling, and off-line heat treating (CRAQ).

An encouraging advantage of CRAQ processing is that this TMCP can be readily applied by US manufacturers with their existing equipment.

The conclusions of this study were:

1. CRDQ produced elongated grains in the direction of rolling. This anisotropic microstructure caused poor toughness and high strength in the transverse testing direction.
2. A second off-line heat treatment was effective in improving the toughness of the CRDQ plates but the strength gains were minimized.
3. The strengths of CRAQ steels were nearly as good as the strengths of CRDQ steels, while its toughness was superior to that of the CRDQ processed plates.

## 1.3 Scope of the Present Work

The objective of the present work was to optimize a TMCP based on the FFP project that could be applied to steels suitable for bridge applications. This would be done to improve weldability while retaining strength in order to reduce the cost of fabrication. Although the first studies at ATLSS on TMCP were not directed toward bridge applications, the TMCP developed served as an evolutionary step in the proposed direction. Beyond that objective, the ultimate goal was to develop suitable low cost, low

alloy 100 ksi and 70 ksi steels which could be utilized as High Performance Steels and which would meet the American Association of State Highway Transportation (AASHTO) requirements, shown in Table I and II, for bridge fabrication.

The present investigation covered three areas: steel composition, roll-finishing temperature, and quenching practice. Two steel compositions from the FFP project were examined for construction applications. They were modified A514 and A710 steels with aim minimum yield strength of 100 ksi. In addition, three compositions of modified A852 were chosen to bracket a suitable composition with aim minimum yield strength of 70 ksi. The compositions of the A514, A710, and A852 types steels are shown in Table III. Previous mechanical property tests suggested that the roll-finishing temperature might affect the strength and toughness levels of control-rolled plates. Increasing the roll-finishing temperature allows additional time for recrystallization of the microstructure, resulting in a tougher steel. Similarly, by decreasing roll-finishing temperature, the effect of deformation persists, thereby strengthening the steel. Therefore, roll-finishing temperatures were investigated as a means of improving the mechanical properties of control-rolled plates. The final stage of the investigation was to match quench rates associated with direct quench facilities abroad in an effort to adopt an improved quenching technique for off-line heat treatment. In summary, compositions, roll-finishing temperatures, and quench rates were investigated to develop viable 100 and 70 ksi yield strength construction steels that could be welded without preheat.

## 1.4 Thermo-Mechanical Controlled Processing

Thermo-mechanical controlled processing (TMCP) is defined as any combination of mechanical and thermal production processes aimed at obtaining desired properties in a material. This is achieved by controlling plastic deformation within the hot-working temperature range. The ultimate goal is to improve mechanical properties beyond those normally attainable by conventional means[9]. Some examples of TMCP treatments are schematically represented in Figure 1.

Traditional alloy steels of similar grades to those discussed in this paper are typically conventionally hot rolled and off-line heat treated[9]. These high strength steels, such as A514, A710, and A852 steels, are off-line heat treated to improve strength and toughness beyond what would be normally be attainable by air-cooling. To increase economic potential, these steels are rolled to desired thickness at high temperature and air-cooled to room temperature. The steel plates are then off-line austenitized and quenched, usually in water, to achieve a desired microstructure consisting of low temperature transformation products. The quenched plates are later tempered below the Ae1 to obtain the desired strength and toughness levels. Although, these steels provide high strength, good toughness, and better weldability than most steels, they require considerable alloying and to obtain good weldability costly preheating.

Thermo-mechanically control-rolled steels, like the CRDQ and CRAQ steels discussed in this paper, are lower in carbon than most high strength steels and are strengthened by a combination of thermal and mechanical processes in lieu of expensive

alloy additions. Controlled-rolling, unlike hot rolling, follows a pre-determined schedule of rolling and temperature control to ensure a fine and uniform microstructure upon completion of the processing. The steels are first rolled in the high temperature region where the plate can easily be reduced in thickness, similar to hot rolling. But unlike hot rolling these plates are not rolled to final gage during this stage (usually only to 2T). The final rolling occurs in the in the nonrecrystallization region where the austenite grains are deformed. After rolling, the control-rolled plates are then cooled by a variety of methods and further heat treating may be necessary. The added deformation improves micro-structure, thus making it possible for TMCP steels to have improved weldability (due to the low carbon content) at the same strength and toughness levels of conventional high strength steels. The mechanisms in which improved properties of TMCP steels are obtained are discussed below.

Although the thermo-mechanical controlled process is defined as any thermal or mechanical process aimed at improving the properties of a material beyond those conventionally obtained, the complete TMCP in its fullest extension can be described by four comprehensive stages. These four stages are defined by Tanaka[10] as:

1. Hot rolling to cause deformation in the high temperature austenite region to attain grain refinement through repeated recrystallization.
2. Hot rolling to cause deformation in the non-recrystallized austenite region to increase nucleation sites via deformed austenite grains combined with deformation bands.
3. Hot rolling to increase strength through ferrite deformation in the two-phase austenite /ferrite region.

4. Cooling of the plates during the austenite/ferrite transformation by accelerated cooling to yield a fine grained structure.

The first three stages of the complete thermo-mechanical controlled process are designed to control microstructure through rolling to a strict schedule that coordinates rolling passes with temperature. The fourth stage is aimed at microstructural control through accelerated cooling. In accelerated cooling the plate is cooled immediately after completion of the rolling schedule at the onset of ferrite transformation. Accelerated cooled plates are quenched rapidly through the transformation temperatures and at a predetermined temperature the quench is terminated. The plate is then left to air-cool to room temperature. This allows the plate to self-temper without any further need of heat treatment.

High strength low alloy TMCP steels with improved strength and superior weldability can be produced by the optimum combination of the aforementioned stages [10]. The more conventional controlled-rolling, as employed in this study, is slightly more simplified than the Tanaka's four stage process. Here the scheduled rolling is performed above the Ae3 with little or no rolling occurring in the two-phase region. The rolling schedule is now defined as a two stage process:

1. Hot rolling in the recrystallization austenite region to attain a fine grained structure via controlled deformation and recystallization [10,11].
2. Hot rolling to cause deformation of austenite grains in the nonrecrystallization temperature range[10,11].

In stage one of the controlled-rolling operation, the coarse austenite grains are refined by repeated recrystallization. This is accomplished by successive hot rolling passes which causes sufficient deformation above the recrystallization temperature. The strength of the steel is increased in this stage through grain refinement. The second stage starts when recrystallization of austenite is no longer possible. The austenitic structure is flattened by additional hot rolling to form pancake shaped grains. These pancaked austenite grains have expanded surfaces that provide large numbers of site for fine grained transformation products to nucleate.

Once the rolling schedule is complete the plates are either direct quenched or air cooled. Direct quenching, the extreme of accelerated cooling, is equivalent to reheat quenching in that both processes have the same cooling rate through transformation[12,13]. In direct quenching the plate is rapidly cooled to room temperature by a facility in-line with the rolling mill. The goal is to quench fast enough to ensure that the austenite transforms to fine grained low temperature products consisting of martensite and bainite. This formation strengthens the steel and eliminates the need for an additional austenitizing and quenching treatment. The plates then only require a temper to achieve optimum strength and toughness. The air cooled plates require an off-line austenitizing and quenching treatment. The slow air-cooling after rolling allows for the formation of high temperature products usually ferrite and pearlite. After quenching the steel plates consist of fine grained banite and ferrite. The steels are then tempered to optimum strength and toughness.

Neither in-line accelerated cooling or direct quenching facilities exist at the production level in the United States. However, these facilities are being used for production operations abroad. In Japan, Kawasaki Corporation is producing both accelerated cooled and direct quenched steels for a number of uses[14]. Kawasaki has published accelerated cooling rates in the range of 9°F/sec to 35°F/sec and direct quench rates in the range 18°F/sec to 180°F/sec[14] (Figure 2). This variety of cooling is performed by innovative spray quenching systems. Since in-line direct quenching facilities do not exist in the U.S., there is significant interest in improved off-line spray quenching facilities. The additional control of spray quenching can be used to compliment the control-rolled and off-line heat treatment process. The combination of these processes, controlled-rolling and off-line heat treating, will enable competitive TMCP steels to be produced domestically.

# 2. Experimental procedures

## 2.1 Melting and Rolling

Five five-hundred pound heats were melted by the United States Steel Technical Center in Pittsburgh, Pennsylvania. These steels were identified as Steels N, P, R, S, and T. Steels N and P were modeled after A514 and A710 respectively and were melted with an aim minimum yield strength of 100 ksi. Steels R, S, and T were modeled after A852 in order of increasing carbon content from 0.065% to 0.14% and were melted with an aim minimum yield of 70 ksi. The compositions are shown in Table IV.

Each melt was cast into an 7 x 13 x 20 inch ingot and subsequently slabbed to 3.5 x 13 x 40 inches. The slab was then cut into three 10-inch and two 5-inch long pieces. The three 10-inch pieces were cross-rolled to plates 1 x 10 x 36 inches through one of the following processes:

1. Control-Rolled using a 2T practice 1600°F and Direct Quenched (CRDQ1600)
2. Control-Rolled using a 2T practice to 1600°F and Air-cooled (CRA1600)
3. Conventionally Hot-Rolled to about 1900°F and Air-cooled (HRA)

After initial mechanical property tests of these plates the remaining two 5-inch pieces were cross-rolled to plates 1 x 5 x 36 inches through one of the following processes:

1. Control-Rolled using a 2T practice to 1725°F and direct Quenched (CRDQ1725)
2. Control-Rolled using a 2T practice to 1500°F and Air-cooled (CRA1500)

Rolling schedules are illustrated in Figures 3 and 4.

## 2.2 Quenching Practice.

The HRA and CRA processed plates were off-line austenitized at 1650°F and water quenched. The water quench was carried out by immersion or spray quenching. The spray quench was employed to simulate the quench rate associated with commercial direct quench facilities. A small scale spray quench facility, designed to control the cooling rate during quenching, was constructed at ATLSS. Cooling rates were controlled in the spray quench facility by varying nozzle size, spray pressure, spray volume, and nozzle to plate distances. Where faster quenching rates were required, an immersion quench facility was employed. See Figures 5 through 8 for photographs of the spray and immersion quench facilities. Typical cooling curves for the United States Steel Technical Center direct quench facility, the ATLSS spray quench facility, and the immersion quench facility are shown in Figures 9 and 10.

### 2.2.1 Cooling Rate Studies

The quenching rate studies were conducted on A36 steel test plates. The specimen consisted of an 8 x 10 inch plate of either .5, 1, or 2 inch thickness. The test plates were soaked at 1650°F, removed from the furnace, placed vertically in the spray quench facility, and water sprayed. The cooling rates were traced by an imbedded thermo-couple and documented by an x-y recorder. Cooling rates were then calculated over the temperature range of 932°F to 1472°F.

## 2.3 Mechanical Property Tests

### 2.3.1 Tempering and Hardness Surveys

Tempering surveys were conducted for each particular composition and/or TMCP condition. The survey served as a guide to the tempering temperature that should produce the most advantageous mechanical properties. A series of 0.5 x 0.5 x 1 inch blocks was cut from quenched plates and tempered between 950°F and 1350°F. The hardness of the tempered blocks was determined and correlated to yield strength. From these surveys, the temperatures were selected to temper 1 x 2 x 5 inches as-quenched pieces for mechanical tests. The hardness testing was performed with a Rockwell hardness testing machine on 'a' setting (HRa). HRa employs a *brale* diamond indenter loaded by a minor load of 10 kg and a major load of 60 kg.

### 2.3.2 Tensile Tests

Two standard tensile specimens were machined from each tempered steel plate and tested at room temperature according to ASTM E8-91 specifications. Either .505 or .252 inch standard tensile specimen geometries were employed. The .505 inch tensile specimens were machined from the mid-thickness of the plate, whereas the .252 inch specimens were machined from the quarter thickness. Tensile specimens were machined from plates in the transverse direction, and in some cases two additional tensile specimens were machined in the longitudinal direction to reveal anisotropic effects. The .505 and .252 inch tensile specimens were punch-marked with a 2 or 1 inch gauge length,

respectively, and initial cross sectional diameters were measured. A graph of the load versus displacement was obtained. The yield and tensile strengths were then calculated from the load versus displacement graph. The percent reduction in cross sectional area, percent elongation, fracture strength, and the yield-to-tensile ratio were also recorded.

### 2.3.3 Charpy V-Notch Tests

Eight standard Charpy V-Notch specimens were machined from each tempered steel plate and tested according to ASTM E23-92 specifications. Charpy V-Notch specimens were machined from plates in the transverse direction, and when desired eight additional Charpy V-Notch specimens were machined in the longitudinal direction to reveal anisotropic effects. The Charpy V-Notch specimens were notched in the through-plate thickness direction. Test temperatures ranged between -120°F and 150°F. Specimens tested below room temperature were liquid nitrogen cooled in a stirred ethanol bath. Specimens tested above room temperature were heated in a stirred water bath. The energy absorbed, lateral expansion, and fracture appearance data were recorded for each specimen.

### 2.3.4 Jominy Hardenability Tests

Standard Jominy end-quench specimens were machined from HRA plates and tested according to ASTM E255-89 specifications. The specimens were austenitized at 1650°F and held for one hour. They were then removed individually from the furnace and end quenched in a standard Jominy end-quench apparatus. Once the far end of the specimen opposite quenching had cooled to 500°F the specimen was removed from the

quenching apparatus and immersed in water. Two diametrically opposed axial flats were then ground on each specimen and hardness tests (HRa) were taken at 1/16 inch intervals from the quenched end for the first inch and every 1/8 inch thereafter for the remainder of the bar. Plots of hardness versus distance from the quenched end were then prepared from the hardness data.

## 2.4 Weldability Tests

### 2.4.1 Implant Tests

Implant specimens were machined from the transverse direction of each CRDQ1600 steel plate and tested. The implant specimen consisted of a .242 inch diameter bar of test steel with a helical notch machined 0.02 inches deep, 28 threads per inch.[15] Each specimen was cleaned of any contaminants and slip fitted into a cleaned .245 inch hole drilled through a 1-inch thick steel plate so that the specimen end was flush with the plate rear surface. A weld bead was deposited on the rear surface of the plate and over the hole containing the specimen at a heat input of 35 kJoule/inch. Within 60 seconds of the weld bead passing over the specimen, the weldment was dead loaded with the implant specimen in tension. The load was maintained for 24 hours or until failure. Tests were conducted on each material for two welding practices over a range of loads beginning near the yield strength of the steel. Tests were carried out by decreasing the load until the load could be maintained for 24 hours, constituting a run-out. Each run-out was confirmed by an additional test and at least 4 tests were performed on each material for each welding process. Load and time to failure were recorded for each test and the

fracture surfaces were examined. A cross section representing each welding process was mounted and microhardness profiles were made perpendicular to the fusion line. The microhardness testing was performed with a Leco hardness tester, using a Vickers diamond pyramid indenter loaded with 300 gm for 15 seconds (VHN).

The welding practices employed in the implant tests were shielded metal arc welding (SMAW) and flux cored arc welding (FCAW). Weld beads were deposited at about 35 kJoules/inch. The SMAW procedure used an 3/16 inch E110-18 electrode with welding parameters of 21 volts, 240 amps, and 8.2 inches per minute travel speed. The FCAW procedure used an 0.052 inch E91T1-K2 electrode with welding parameters of 30 volts, 275 amps, and 14.1 inches per minute travel speed. The electrodes were handled in accordance with low hydrogen specifications.[16]

### 2.4.2 Diffusible Hydrogen Tests

Two standard diffusible hydrogen test specimens were taken from HSLA 80 steel for each welding process and tested according to AWS A4.3-92 specifications. Specimen geometry consisted of an 0.5 x 1 x 3 inch block of steel, which was cleaned in acetone, weighed, and clamped into a copper fixture before being welded. The weld bead was deposited running the length of the specimen. Once welded, the weldment was plunged into an ice bath and transferred to a liquid nitrogen bath for storage. The specimens were thoroughly cleaned, dried, and placed in a glycerin filled eudiometer held at 113°F. The amount of hydrogen evolved in 72 hours was recorded and the specimen weighed. The diffusible hydrogen content was then calculated from recorded data for each process.

## 2.5 Metallographic Preparation

Metallographic specimens were machined from test plates so that the longitudinal short plane could be examined. Selected metallographic specimens were examined in as-received, quenched, and tempered conditions. Specimens were etched with a 50/50 mixture of 2% nital and 4% picral solutions. Micrographs were taken at 400X to illustrate both rolling orientation and microstructure.

## 2.6 Fractographic Preparation

Steel N tensile fracture surfaces were observed with a Scanning Electron Microscope (SEM) to detect the presence of microvoid coalescence which was associated with fracture. The specimens processed by the CRDQ and CRAQ practices were observed in both the transverse and longitudinal directions. The photographs were taken at 1000X magnification, 20 mm working distance and 20 keV accelerating potential.

Steel R implant fracture surfaces were observed with a SEM to study the characteristics associated with hydrogen induced heat affected zone (HAZ) cracking. The specimen was welded using the SMAW process and loaded to failure. The photographs were taken at various magnification, 20 mm working distance, and 20 keV accelerating potential to show detail.

# 3. Results and Discussion

## 3.1 Mechanical Properties

Tensile and Charpy V-Notch (CVN) specimens were machined from tempered plates. The results of the tensile and CVN tests are presented in Tables IV through IX. Selected values are compared in Figure 11 through 20. As illustrated, CRDQ processing increased the strength of all five steels as compared to CRAQ and HRAQ processing. However, CRDQ processing resulted in poor toughness as compared to HRAQ and CRAQ processed plates. The CRDQ processed 100 ksi steels suffered a greater loss in toughness than the 70 ksi steels.

Steel N in the HRAQ (Immersion quenched) and both CRDQ conditions had a toughness below 30 Ft-lbs at -40°F, while both CRAQ plates climbed above 45 Ft-lbs, when properly tempered. The CRDQ plates had yield strengths above 115 ksi while the CRAQ and HRAQ plates tempered at 1275°F had yield strengths of 105 and 110 ksi, respectively.

For Steel P, the improvement in toughness of the CRAQ and HRAQ plates over the CRDQ plates is more pronounced than for Steel N. Tempered at 1275°F, CRDQ plates had toughness of 42 Ft-lbs at -40°F, while HRAQ and CRAQ plates were above 97 Ft-lbs. However, HRAQ plates tempered at 1275°F did not make the 100 ksi aim yield

strength. All control-rolled plates (CRDQ and CRAQ) were near 110 ksi yield strength at the 1275°F tempering temperature.

For Steel R, HRAQ and both CRAQ plates showed improved toughness over the CRDQ plates. The off-line heat treated plates had toughness between 120 and 240 Ft-lbs at -40°F, while the CRDQ plates were between 45 and 120 Ft-lbs. CRAQ and HRAQ plates had yield strengths above 70 ksi when properly tempered, while CRDQ plates were in excess of 75 ksi.

Steels S and T showed similar trends to that of Steel R. The additional carbon content decreased toughness in all processed plates when compared to Steel R, but yield strengths were significantly increased in Steels S and T. CRDQ plates had yield strengths above 80 and 82 ksi for steels S and T, respectively. The off-line heat treated plates had yield strengths above 70 and 76 ksi for Steels S and T, respectively.

Steel N would have to be control-rolled and off-line heat treated to make AASHTO specifications for 100 ksi construction steels. Steel P would make specifications in all TMCP conditions if properly tempered. All TMCP conditions for Steels R, S, and T exceed AASHTO specifications for A852 when properly tempered. These results indicate that there is no advantage to CRDQ treatments of these steels to meet AASHTO specifications for constructions steels.

The relationship between yield strength and CVN energy absorbed at -40°F is compared in Figure 21 for Steels N and P, and in Figure 22 for Steels R, S, and T. Generally, as strength increased toughness decreased. Figure 21 illustrates that the strength-toughness relationship is slightly better for Steel P than for Steel N. This may be

primarily due to the harmful effect of boron. Boron is added to steel to improve hardenability by suppressing ferrite transformation[17], but the addition of boron has also been suspected to cause embrittlement in low carbon steels such as Steel N [18]. Steels R, S, and T show satisfactory strength-toughness relationships for all processes. However, CRAQ processed steels show the best strength-toughness relationship for all experimental compositions.

To study anisotropic effects inherent in HRAQ, CRAQ, and CRDQ processing, tensile and CVN specimens were machined from plates tempered at 1275°F in both the transverse and longitudinal directions. The results of these tests are illustrated in Tables IV through XI. The yield strength and CVN energy absorbed at -40°F are also compared in Figures 23 through 32.

The effects are most apparent in the CRDQ processed plates. In this case, the anisotropy is a result of large austenite deformed grains whose effect persists after tempering. The yield strengths of CRDQ processed Steels N and P are over 8 ksi higher in the transverse testing direction than in the longitudinal testing direction. Likewise, transverse yield strengths are 3, 13, and 10 ksi stronger than longitudinal yield strengths for CRDQ Steels R, S, and T, respectively. Additionally, transverse CVN energy absorbed at -40°F are 9 and 68 Ft-lbs lower for Steels N and P, respectively. CVN energy absorbed at -40°F for Steels R, S and T are over 39 Ft-lbs lower for transverse specimens than for longitudinal specimens.

Anisotropy in the HRAQ and CRAQ plates affects toughness. The longitudinal toughness of Steels N and P is slightly higher than the transverse toughness in both CRAQ

and HRAQ plates. CVN energy absorbed at -40°F for CRAQ processed Steels R, S, and T are 69, 22, and 13 Ft-lbs higher for longitudinal specimens than for transverse specimens, respectively. Steels R, S and T in the HRAQ condition were 80, 65, and 35 Ft-lbs higher for longitudinal specimens than for transverse specimens. These effects should be considered when determining the suitability of processed steels for construction applications.

The yield strength to tensile strength ratios (yield-tensile ratios) for the 100 ksi steels were high. They ranged from .92 to .98, which is unacceptable for most construction applications.[19] The yield-tensile ratios of the 70 ksi steels are significantly better than the ratios of 100 ksi steels. The yield-tensile ratios of Steels R, S, and T are in the range 0.83 to 0.89, which is suitable for construction steels of this grade. Yield-tensile ratios of less than 0.9 are desired in construction steels (especially in earthquake areas) to ensure sufficient yielding of the structure before fracture[20].

Figure 33 illustrates the fracture surfaces of Steel N tensile specimens for both CRDQ and CRAQ processing. These SEM micrographs show typical ductile microvoid coalescence initiated fracture.[21] Both transverse and longitudinal tensile specimens are illustrated for comparison. The CRDQ fracture surfaces morphology consists of fine elongated dimples accompanied by large voids, whereas the CRAQ morphology exhibits rounder and somewhat coarser dimples. Fracture surfaces of longitudinal specimens appear to be coarser and contain more large voids than transverse tensile specimens. This suggests that the finer dimpled structure may be superior in strength and lower in ductility.

## 3.2 Hardenability Results

The Jominy end-quench curves for Steels N, P, R, S, and T are illustrated in Figure 34. The distances from the quenched end, which correspond to commercial quenching rates for 1, 2, 3, and 4 inch thick plates, are also shown on these curves. The horizontal lines at 60 and 52 HRa correspond roughly to yield strengths of 100 ksi and 70 ksi respectively. These correlations are derived from Figure 35, which shows the yield strength-hardness relationships of the experimental test steels. The data illustrated in Figure 31 is a compilation of the yield strengths from tensile tests versus the Rockwell HRa tests performed on tempered plates. It was determined from this curve that 60 and 52 HRa corresponded to yield strengths of 100 and 70 ksi for the steels being investigated.

The Jominy curves suggest that Steel N is suitable with regard to strength for applications up to 4 inches thick in the HRAQ condition. Steel P would only be useful up to 2 inches thick, unless a proper TMCP was applied to increase strength in thicker gauges. As expected, the hardenability of Steels R, S, and T was significantly influenced by the carbon content. The Jominy curves illustrate that Steel T is the most hardenable of the 70 ksi steels. Steel T could meet minimum yield strength of 70 ksi for gauges exceeding 4 inches in thickness. Conventionally rolled Steels R and S are expected to be useful in plates up to 2 and 2.5 inches thick, respectively. The fact that Steel R exhibited such high toughness, even in the CRDQ condition, suggests that Steel R, like Steel P, might be useful in gauges thicker than 2 inches if effective TMCP could be applied.

## 3.3 Effects of Roll-Finishing Temperature on Properties

Initial tests showed CRDQ1600 processed plates were stronger but less tough than plates control-rolled to 1600°F and off-line heat treated (CRAQ1600). As a result, additional plates were control-rolled to 1725°F and direct quenched (CRDQ1725). The aim was to improve toughness by promoting recrystallization of austenite prior to direct quenching. Similarly, additional plates were control-rolled to 1500°F and air cooled (CRA1500). It was hoped that the effect of deformation would persist after air cooling and off-line heat treatment and, thereby, improve strength.

The effects of roll-finishing temperature on yield strength and CVN energy absorbed at -40°F are compared graphically in Figures 11 through 20. Increasing the finishing temperature from 1600°F to 1725°F did little to raise the toughness of the CRDQ processed plates. Steels N, R, S, and T showed slight increases in toughness, whereas Steel P showed none. For Steel N, CVN energy absorbed at -40°F increased from values as low as 4 Ft-lbs to 25-30 Ft-lbs. Steel R recovered 20 Ft-lbs at -40°F. Steel T only recovered 10 Ft-lbs at -40°F. Similarly, decreasing the roll-finishing temperature from 1600°F to 1500°F in the CRA plates was ineffective for the purpose of increasing strength. Any trends that may be assumed are obscured by experimental scatter. In general, roll-finishing temperature does not influence strength or toughness significantly.

## 3.4 Quenching Rates

### 3.4.1 Quenching Rate Studies

The ATLSS spray quench facility used two nozzles per side to ensure uniform coverage of the test plate (Figure 7). Water volume was controlled by using different capacity solid spray pattern nozzles and by controlling spray pressure. Spray pressures were in the range of 20 to 80 psig. It was determined that the higher end of this range ensured a uniform droplet size and spray pattern. Nozzle capacities ranged from 1 to 6 gal/min per nozzle. Figure 36 illustrates the calibration of the nozzles used in quenching. Quenching rates were calculated between 932°F and 1472°F. Spray quench data obtained for the 0.5, 1, and 2 inch plates are compared in Table X. Table X also includes immersion quench data.

Studies show that quenching rates achieved by direct quench facilities such as the one at Kawasaki Steel Corporation could be duplicated in off-line heat treatment. Figure 2 illustrates cooling rates used at the Kawasaki Steel Corporation direct quench facility in Japan. Kawasaki direct quench rates for 0.5, 1, and 2 inch plate were 90, 44, and 21 °F/s respectively.[14] Those obtained by the ATLSS off-line spray quench facility were 82, 45, and 21 °F/s for 0.5, 1, and 2 inch plate, respectively. Typical cooling curves for 0.5, 1, and 2 inch thick test plates obtained at the ATLSS spray quench facility are illustrated in Figure 37.

Considerable scatter occurred in these tests. This unpredictability resulted from plate surface conditions or from the recalescence of ferrite during spray quenching. Oxide scale accumulated on the test plate surfaces during the heating cycle. The degree of scaling was dependent on the initial plate surface quality and the duration of heating cycle. The scale acted to insulate the test plate from the sprayed water. As a result of the scale the test plate could not transfer heat efficiently to the water spray. Hence, cooling rates were slowed in an unpredictable manner. The effect of the heat of transformation released during cooling was an additional source of irreproducibility, which varied with steel composition. Therefore, slight variations in test plate composition and spray quench parameters could cause varying amounts of heat to be evolved, affecting quenching rates. It is necessary to conduct extensive tests on the effects of recalescence and plate surface conditions on cooling rates to determine the exact cause and extent of the irreproducibility.

### 3.4.2 2-inch plate Simulation

Based on Kawasaki data (Figure 2) CRA1500 plates were spray quenched at 20°F/s to simulate the direct quench rate for 2-inch thick plate. This enabled 2-inch thick plate properties to be simulated in the available 1-inch thick experimental steel plates. These results are also shown in Table IV through IX. Strengths in the 100 ksi grades were reduced when spray quenched at 20°F/s, but still reached 100 ksi minimum yield strength as Jominy end-quench hardenablity data suggested. Although, Steel N showed

adequate hardenability, it demonstrated little hope of meeting ASSHTO toughness requirements in any gauge thicker than one inch in the CRAQ condition. Steel N in the CRAQ condition quenched at 20°F/s had CVN energy of 5 Ft-lbs at -40°F. Toughness remained adequate in Steel P up above 70 Ft/lbs at -40°F, showing no marked reduction in toughness compared to the plates spray quenched at 45°F/s.

Mechanical properties show that Steels R, S, and T made minimum yield strength of 70 ksi. Steel R, the lowest in carbon at 0.065%, had strengths in excess of 70 ksi and retained more than adequate toughness when properly tempered. This suggests that CRAQ processed Steel R may be useful in plates over 2 inches, in keeping with hardenablity results. The two inch plate thickness simulation demonstrated that Steels P, R, S, and T have promising strength-toughness combinations in the CRAQ condition for 2-inch plate thickness.

## 3.5 Weldability

### 3.5.1 Diffusible Hydrogen Tests

The SMAW process, which used an E110-18 electrode, had a diffusible hydrogen level of 1 ml per 100 gram sample. The FCAW process, which used an E91T1-K2 electrode, had a diffusible hydrogen level of 4.6 ml per 100 gram sample. By using both of these processes, it was possible to demonstrate the effects of higher hydrogen levels on the threshold stress associated with hydrogen induced cold cracking.

### 3.5.2 Implant tests

The weldability of the experimental steels was assessed by implant tests. Welds were deposited at 35 kJoules/inch by SMAW and FCAW processes with a room temperature preheat. The results are illustrated in Figures 38 through 42. The significant feature of the implant tests was the effect of carbon content on critical stress. Steels N, P, and R, nominal 0.065% carbon steels, had critical stresses near or above their yield strength. By contrast Steels S and T, with carbon contents of 0.10% and 0.14%, respectively, had critical stresses that dropped well below their yield strength.

The threshold stresses, compared in Table XI, showed that SMAW produced weldments had superior resistance to hydrogen induced cold cracking to that of FCAW weldments for Steels R, S, and T. Steels N and P showed excellent resistance to hydrogen assisted cracking for both processes. Steel R did not achieve the same resistance to hydrogen induced cracking in the FCAW weldments as did Steels N and P. The poor performance of Steel R may be due to the limited number of experimental tests performed and would be expected to behave similarly to Steels N and P.

Diffusible hydrogen tests showed FCAW hydrogen levels were 3.6 ml per 100 gram specimen higher than levels produced by SMAW (4.6 ml vs. 1 ml). Hence more hydrogen was available to assist cracking. Figures 43 through 47 illustrate hardness profiles performed on cross sections of failed implant specimens. Heat affected zones produced by FCAW for Steels S and T were 50 VHN harder than those produced by SMAW (The HAZ hardness of Steel S was 325 and 375 VHN for SMAW and FCAW,

respectively. The HAZ hardness of Steel T was 390 and 440 VHN for SMAW and FCAW, respectively). Steels N, P, and R HAZ hardness values, around 350 VHN, were nearly the same for both welding processes. This demonstrates that the higher carbon steels have harder heat affected zones, especially when welded by the FCAW process. A susceptible microstructure combined with the increased hydrogen levels was deleterious to performance. These results show that carbon levels must be held well below 0.10% to improve weldability with room temperature preheat.

Figures 48 and 49 show micrographs of the SMAW and FCAW cross sections of failed implant specimens. The micrographs show that hydrogen induced cracks initiated in the highly stressed notched area of the HAZ proceeded along the coarse grain heat affected zone and ran into the weld metal. Once the net section was reduced, overload occurred and specimens failed in tension.

Figures 50 and 51 illustrate the implant fracture surface morphology of Steel R welded by the SMAW process. This specimen failed after 327 minutes at a stress of 90 ksi. The micrographs illustrate the initiation region, coarse grain HAZ, and weld metal. SEM observations of fracture initiation region revealed the presence of intergranular facets, which is indicative of hydrogen cracking.[22] The area of final fracture showed evidence of ductile microvoid coalescence, which is typical of tensile failure.

## 3.6 Metallographic Evaluation

### 3.6.1 Air Cooled Microstructures

The HRA and CRA1500 micrographs are compared in Figures 52 and 53. The microstructures of Steels N and P consisted of bainite containing relatively little carbide and many small islands of martensite.[23] In Steel P, the bainitic structure was accompanied by some occasional areas of proeutectoid ferrite which were more obvious in the CRA1500 and CRA1600 than the HRA processing (Figure 54). This suggests that finishing at 1900°F allows sufficient time for recrystallization whereas finishing at 1500°F or 1600°F does not. The CRA and HRA microstructure of Steels R, S, and T consisted of large amounts of proeutectiod ferrite with fine pearlite colonies. Within the pearlite colonies there were trace amounts of granular bainite that formed from austenite remnants at the completion of pearlite transformation.[23] The amount of ferrite decreased from Steel R to Steel T and gave way to increased amounts of pearlite and bainite. The CRA processed steels exhibited banding of the ferrite/pearlite structures. Banding was more pronounced in the 1500°F than the 1600°F CRA plates. This structure is most apparent in Steel T, illustrated in Figure 54. In all steels, the prior austenite grains boundaries in the HRA plates were equiaxed, whereas, in the CRA plates, they were highly elongated. The CRA1500 were slightly more elongated than the CRA1600. These microstructures are illustrated in Figures 52 through 54.

### 3.6.2 As Quenched Microstructures

The CRDQ1600 and CRAQ1600 micrographs are compared in Figures 55 and 56. The CRDQ processing resulted in elongated prior austenite grains which were deformed in the direction of rolling. This anisotropic microstructure significantly increased the strength of the steels, but resulted in embrittlement. The elongated microstructure created an easy path for crack propagation of transversely tested CVN specimens, elevating transition temperatures.

The microstructure of CRDQ Steels N and P were mostly bainitic with trace amounts of low carbon martensite. The structures of CRDQ Steels R, S, and T were mainly bainitic with some plate like martensite in the grain proper with fine ferrite formed at the elongated prior austenite grain boundaries. The ferrite at the prior austenite grain boundaries impeded crack propagation in Steels R, S and T and resulted in adequate toughness.

Figures 57 and 58 compare the microstructures of CRAQ1500 and HRAQ processed plates. The micrographs of the CRAQ1500 show that the elongated and banded structure present in the CRA processed microstructure has been obliterated by the off-line heat treatment. The microstructure of Steels N and P consisted of fine grained bainite with trace amounts of martensite, whereas the microstructures of Steels R, S, and T consisted of a mixture of fine grained ferrite and bainite. As Jominy hardenablity data would suggest, there are decreasing amounts of high temperature transformation products apparent in the structures from Steel R to Steel T. Figures 57 and 58 illustrate that the microstructures of HRAQ plates are slightly coarser than that of CRAQ plates, but both

HRAQ and CRAQ microstructures are much finer than the CRDQ microstructures. This finer equiaxed structure improved the toughness of the steels as compared to the CRDQ processed plates.

The effect of spray quenching on the CRA1500 microstructure is illustrated in Figures 59 and 60. These micrographs compare the CRA1500 spray quenched at 45°F/s to those spray quenched at 20°F/s. The microstructures of CRA1500 plates spray quenched at 20°F/s were combinations of fine grained bainite and ferrite. The microstructures of Steels N and P consisted of fine grained bainite with some ferrite, whereas the microstructures of Steels R, S, and T consisted of a mixture of fine grained bainite and somewhat coarser ferrite.

### 3.6.3 Tempered Microstructures

Figures 61 and 62 compare tempered CRDQ microstructures to the as-received CRDQ microstructures. The elongated and deformed grains are still very apparent in the tempered plates and are altered only by carbide precipitation. The microstructures of Steels N and P consist mainly of tempered bainite and some tempered martensite. Steels R, S, and T consist of tempered bainite with fine ferrite at the prior austenite grain boundaries.

Figures 63 and 64 compare the tempered CRAQ and HRAQ microstructures of Steels N, P, R, S, and T. They consist primarily of tempered bainite and martensite with small areas of ferrite. The primary effect of the tempering was to coalesce carbide particles

# 4. Conclusions

## 4.1 Merits and Limitations of CRDQ, CRAQ, and HRAQ

1. CRDQ can be used to increase strength of construction steels; however the composition must be optimized to retain adequate toughness after direct quenching.
2. CRAQ can be used as a mean of producing HPS without the costly installation of direct quench facilities.
3. CRAQ processing results in better toughness than CRDQ processing at nearly the same strength levels.
4. Strength gains in CRDQ were excessive at the expense of toughness as compared to HRAQ and CRAQ processing.
5. The anisotropic behavior of processed plates must be taken into account in design. To be conservative, transverse Charpy V-Notch and longitudinal tensile tests must be considered in evaluating mechanical properties.
6. CRAQ and HRAQ require a costly off-line heat treatment
7. Installation of direct quench facilities would be costly to US manufactures.
8. CRDQ processing is less effective in raising strength as thickness increases and could not be expected to be useful in thicker gauges.
9. Controlled-rolling slows productivity, by requiring additional time on rolling platforms to administer the lower than normal temperature mechanical treatment.

## 4.2 Summary Conclusions

The main objective of this study was to optimize a thermo-mechanical practice and chemistry that would produce improved 100 ksi and 70 ksi steels for HPS applications. The main conclusions of this study were as follows:

1. The low temperature toughness obtained by controlled-rolling , air cooling and off-line quenching and tempering for all experimental steels met or exceeded AASHTO specifications with proper tempering.
2. Conventionally hot-rolled and off-line heat treated plates, with the exception of the 0.065% carbon A514 steel, met AASHTO specifications for construction steels when properly tempered.
3. Controlled-rolling followed by direct quenching raised the strengths of the experimental steels, above that obtained by off-line heat treatment, but the toughness was inferior.
4. The 0.065 carbon A710 and A852 steels had good toughness, even when processed in the CRDQ condition and met AASHTO specifications for 1 inch plate thickness.
5. Control-Rolled finishing temperatures had little effect on mechanical properties.
6. Spray quenching successfully achieved cooling rates associated with direct quench facilities and is an suitable means of quenching off-line heat treated steels.
7. Controlled-rolling, air-cooling and off-line heat treating proved to be a viable alternative to controlled-rolling and direct quenching as a means of processing high performance steels for construction applications.

8. To eliminate the need to preheat above room temperature for welding, the carbon content of the steel must be held well below 0.10%.
9. It was confirmed that boron is detrimental to notch toughness of low carbon steels, especially in the presence of high temperature transformation products.

Table I - AASHTO Charpy requirements for A514 steel

| Zone | Charpy Requirements * |
|---|---|
| 1 (0F &above) | 35 ft-lb at 0F |
| 2 (-1F to -30F) | 35 ft-lb at 0F |
| 3 (-31F to -60F) | 35 ft-lb at -30F |

*Up to 4" thick mechanically fastened or up to 2.5" thick welded.

Table II - AASHTO Charpy requirements for A852 steel

| Zone | Charpy Requirements * |
|---|---|
| 1 (0F &above) | 35 ft-lb at 20F |
| 2 (-1F to -30F) | 35 ft-lb at 20F |
| 3 (-31F to -60F) | 35 ft-lb at -30F |

*Up to 4" thick mechanically fastened, welded

Table III - Compositions of A514, A710, and A852 Type Steels

| | 100ksi | | | | 70ksi | | | |
|---|---|---|---|---|---|---|---|---|
| Steels | A514 | N | A710 | P | A852 | R | S | T |
| C | 0.15-0.021 | 0.065 | 0.070 | 0.065 | 0.19max | 0.065 | 0.100 | 0.150 |
| Mn | 0.80-1.10 | 1.000 | 0.40-0.70 | 1.000 | 0.80-1.35 | 1.250 | 1.250 | 1.250 |
| P | 0.035 | 0.009 | 0.025max | 0.009 | 0.04max | 0.009 | 0.009 | 0.009 |
| S | 0.040 | 0.005 | 0.025max | 0.005 | 0.05max | 0.005 | 0.005 | 0.005 |
| Si | 0.40-0.80 | 0.025 | 0.40max | 0.250 | 0.20-0.65 | 0.250 | 0.250 | 0.250 |
| Cu | NA | 0.300 | 1.00-1.30 | 1.000 | 0.20-0.40 | 0.300 | 0.300 | 0.300 |
| Ni | NA | 0.750 | 0.70-1.00 | 0.750 | 0.50max | 0.300 | 0.300 | 0.300 |
| Cr | 0.50-0.80 | 0.500 | 0.60-0.90 | 0.500 | 0.40-0.70 | 0.500 | 0.500 | 0.500 |
| Mo | 0.18-0.28 | 0.500 | 0.15-0.25 | 0.500 | NA | NA | NA | NA |
| V | NA | 0.060 | NA | 0.060 | 0.02-0.10 | 0.060 | 0.060 | 0.060 |
| Al | NA | 0.030 | NA | 0.030 | NA | 0.030 | 0.030 | 0.030 |
| N | NA | 0.060 | NA | 0.060 | NA | 0.060 | 0.060 | 0.060 |
| Cb | NA | 0.015 | 0.02min | 0.015 | NA | 0.015 | 0.015 | 0.015 |
| Ti | NA | 0.040 | NA | NA | NA | NA | NA | NA |
| B | .0025max | 0.002 | NA | NA | NA | NA | NA | NA |

Table IV - Chemical Composition for 100ksi and 70ksi steels

| Steel | C | Mn | P | S | Si | Cu | Ni | Cr | Mo | V | Al | N | Cb | Ti | B |
|---|---|---|---|---|---|---|---|---|---|---|---|---|---|---|---|
| N | 0.064 | 1 | 0.01 | 0.005 | 0.24 | 0.29 | 0.74 | 0.5 | 0.5 | 0.06 | 0.033 | 0.07 | 0.017 | 0.03 | 0.002 |
| P | 0.062 | 1.01 | 0.008 | 0.005 | 0.25 | 1.02 | 0.75 | 0.48 | 0.5 | 0.07 | 0.033 | 0.07 | 0.015 | NA | NA |
| R | 0.066 | 1.26 | 0.008 | 0.006 | 0.29 | 0.29 | 0.3 | 0.49 | NA | 0.07 | 0.031 | 0.07 | 0.014 | NA | NA |
| S | 0.1 | 1.25 | 0.008 | 0.006 | 0.25 | 0.29 | 0.3 | 0.51 | NA | 0.06 | 0.038 | 0.07 | 0.015 | NA | NA |
| T | 0.14 | 1.26 | 0.009 | 0.006 | 0.26 | 0.29 | 0.31 | 0.51 | NA | 0.06 | 0.03 | 0.07 | 0.015 | NA | NA |

comp.wb1

## Table V - Mechanical Properties of Steel N

| *N-STEEL* | *Tensile Properties* | | | | | *Charpy V-Notch* Transition Temperature, deg. F | | | | | *Charpy V-Notch Energy* | | | | | Quench Rate |
|---|---|---|---|---|---|---|---|---|---|---|---|---|---|---|---|---|
| *Processing Condition* *Temperature, deg. F* | Y.S. ksi | T.S. ksi | EL. % | R.A. % | Y.S. T.S. | 20 ft-lb | 35 ft-lb | 60 ft-lb | 15 mils | 50% FAT | 70 F | 0 F | -40 F | -80 F | -120 F | *F/sec* |
| ***TRANSVERSE TESTS*** | | | | | | | | | | | | | | | | |
| CRDQ 1600 As Q | 95 | 132 | 19 | 67 | 0.72 | +15 | +25 | +70 | 0 | +85 | 60 | 16 | 12 | - | - | DQ@26 |
| CRDQ 1600+1200T | 121 | 129 | 21 | 67 | 0.94 | 0 | +45 | +100 | +40 | >+100 | 45 | 16 | 15 | 5 | - | DQ@26 |
| CRDQ 1600+1275T | 120 | 124 | 20.5 | 69 | 0.97 | +30 | +55 | +90 | +70 | >+100 | - | 6 | 4 | - | - | DQ@26 |
| CRDQ 1600+1300T | 115 | 119 | 21.5 | 69 | 0.97 | +5 | +25 | +55 | 0 | +70 | 72 | 27 | 4 | - | - | DQ@26 |
| | | | | | | | | | | | | | | | | |
| CRDQ 1725+1275T 1hr | 126 | 130 | 21.5 | 64 | 0.96 | -20 | +15 | +60 | +10 | +55 | - | 30 | 15 | 5 | - | DQ@30 |
| CRDQ 1725+1275T 4hr | - | - | - | - | - | <-80 | -15 | +40 | -80 | +20 | 80 | 46 | 31 | 23 | - | DQ@30 |
| CRDQ 1725+1300T 4hr | 115 | 118 | 21 | 66 | 0.97 | -40 | -10 | +40 | -55 | +30 | 72 | 40 | 22 | 14 | - | DQ@30 |
| | | | | | | | | | | | | | | | | |
| CRA 1500+1650 SQ+1275T 1hr | 109 | 114 | 26 | 70 | 0.95 | -90 | -60 | -20 | -90 | 0 | - | 73 | 48 | 26 | 12 | SQ@45 |
| CRA 1500+1650 SQ+1175T 1hr | 126 | 132 | 23 | 69 | 0.96 | -35 | -10 | +20 | -30 | +40 | 80 | 45 | 15 | - | - | SQ@45 |
| CRA 1500+1650 SQ+1225T | 120 | 130 | 23 | 69 | 0.93 | -75 | -60 | -20 | -70 | +15 | 100 | 68 | 47 | 16 | - | SQ@45 |
| CRA 1500+1650 SQ+1150T | 112 | 122 | 24 | 69 | 0.92 | +70 | >+70 | >+70 | >+70 | >+70 | 16 | 2 | - | - | - | SQ@20 |
| CRA 1500+1650 SQ+1250T | 106 | 112 | 26 | 73 | 0.95 | +25 | +60 | >+70 | 0 | >+70 | 46 | 14 | - | - | - | SQ@20 |
| | | | | | | | | | | | | | | | | |
| CRA 1600+1650 IQ+1275T | 112 | 114 | 22 | 70 | 0.98 | -80 | -50 | -20 | -65 | +10 | 98 | 92 | 44 | 18 | 10 | IQ@52 |
| CRA 1600+1650 SQ+1275T | 109 | 116 | 22.5 | 71 | 0.93 | -85 | -60 | -35 | -100 | -25 | 109 | 56 | 52 | 22 | - | SQ@40 |
| | | | | | | | | | | | | | | | | |
| | | | | | | | | | | | | | | | | |
| HRA+1650 IQ+1225T | 119 | 121 | 22.5 | 71 | 0.98 | -20 | +5 | +35 | -20 | +45 | 91 | 28 | 10 | - | - | IQ@52 |
| HRA+1650 IQ+1275T | 104 | 108 | 22.5 | 71 | 0.97 | +40 | >+80 | >+80 | +30 | >+80 | 37 | 12 | 7 | 3 | - | IQ@52 |
| HRA+1650 IQ+1275T | 103 | 108 | 23 | 71 | 0.95 | +30 | +70 | +105 | +30 | +140 | 35 | 10 | - | - | - | IQ@52 |
| HRA+1650 SQ+1275T | 110 | 113 | 22.5 | 71 | 0.97 | -90 | -45 | 0 | -60 | +30 | 109 | 55 | 41 | 23 | 4 | SQ@40 |
| | | | | | | | | | | | | | | | | |
| ***LONGITUDINAL TESTS*** | | | | | | | | | | | | | | | | |
| CRDQ 1725+1275T 4hr | 118 | 122 | 22 | 70 | 0.97 | -75 | -45 | -15 | -65 | +30 | 116 | 77 | 40 | 17 | - | DQ@26 |
| CRA 1500+1650 SQ+1275T | 106 | 111 | 25 | 75 | 0.95 | -105 | -65 | -45 | -100 | -20 | - | 97 | 53 | 24 | 9 | SQ@45 |
| HRA+1650 IQ+1275T | 102 | 109 | 23 | 71 | 0.94 | +50 | - | - | +70 | >+70 | 25 | 15 | - | - | - | IQ@52 |
| | | | | | | | | | | | | | | | | |

## Table VI - Mechanical Properties of Steel P

| *P-STEEL* Processing Condition Temperature, deg. F | *Tensile Properties* | | | | | *Charpy V-Notch* Transition Temperature, deg. F | | | | | *Charpy V-Notch Energy* | | | | | Quench Rate |
|---|---|---|---|---|---|---|---|---|---|---|---|---|---|---|---|---|
| | Y.S. ksi | T.S. ksi | EL. % | R.A. % | Y.S. T.S. | 20 ft-lb | 35 ft-lb | 60 ft-lb | 15 mils | 50% FAT | 70 F | 0 F | -40 F | -80 F | -120 F | *F/sec* |
| ***TRANSVERSE TESTS*** | | | | | | | | | | | | | | | | |
| CRDQ 1600 As Q | 86 | 126 | 20 | 62 | 0.68 | -90 | -40 | +5 | -70 | +30 | 58 | 71 | 29 | 24 | 15 | DQ@26 |
| CRDQ 1600+1200T | 117 | 126 | 21 | 63 | 0.93 | -65 | -30 | +25 | -30 | +60 | 78 | 20 | 33 | 13 | - | DQ@26 |
| CRDQ 1600+1275T | 110 | 116 | 22.5 | 67 | 0.94 | -75 | -50 | -20 | -65 | +25 | 95 | 74 | 43 | 15 | - | DQ@26 |
| CRDQ 1600+1300T | 108 | 113 | 24 | 71 | 0.96 | -95 | -90 | -60 | -95 | +25 | 97 | 83 | 67 | 50 | 4 | DQ@26 |
| | | | | | | | | | | | | | | | | |
| CRDQ 1725+1275T 1hr | 112 | 119 | 22.2 | 68 | 0.94 | -50 | -25 | +30 | -60 | +50 | 70 | 50 | 20 | 10 | 2 | DQ@30 |
| CRDQ 1725+1275T 4hr | - | - | - | - | - | -120 | -65 | -10 | -85 | +50 | 100 | 69 | 43 | 26 | - | DQ@30 |
| CRDQ 1725+1300T 4hr | 97 | 105 | 23.5 | 71 | 0.92 | -80 | -60 | -45 | -90 | +10 | 123 | 118 | 72 | 20 | 15 | DQ@30 |
| | | | | | | | | | | | | | | | | |
| CRA 1500+1650 SQ+1275T 1hr | 94 | 104 | 26 | 73 | 0.91 | <-120 | -120 | -100 | <-120 | -20 | - | 114 | 118 | 82 | 35 | SQ@45 |
| CRA 1500+1650 SQ+1175T 1hr | 117 | 126 | 20 | 68 | 0.93 | -110 | -70 | -20 | -110 | +25 | 105 | 70 | 50 | 30 | 15 | SQ@45 |
| CRA 1500+1650 SQ+1225T | 109 | 116 | 28 | 73 | 0.94 | -119 | -117 | -80 | -117 | -6 | - | 103 | 63 | 60 | 18 | SQ@45 |
| CRA 1500+1650 SQ+1150T | 103 | 117 | 28 | 74 | 88 | -90 | -70 | -50 | -40 | +65 | 130 | 104 | 70 | 26 | 7 | SQ@20 |
| CRA 1500+1650 SQ+1250T | 92 | 105 | 30 | 74 | 88 | <-120 | <-120 | -90 | -110 | -10 | >180 | 174 | 102 | 68 | 14 | SQ@20 |
| | | | | | | | | | | | | | | | | |
| CRA 1600+1650 IQ+1275T | 98 | 108 | 25 | 73 | 0.91 | <-120 | <-120 | -115 | >-120 | -40 | 138 | 122 | 99 | 68 | 61 | IQ@52 |
| CRA 1600+1650 IQ+1225T | 104 | 112 | 25.5 | 72 | 0.93 | -85 | -75 | -35 | -80 | +10 | 108 | 89 | 56 | 24 | 8 | IQ@52 |
| CRA 1600+1650 SQ+1225T | 104 | 112 | 22.5 | 70 | 0.92 | -110 | -100 | -80 | -115 | -15 | - | 109 | 95 | 56 | 4 | SQ@40 |
| | | | | | | | | | | | | | | | | |
| | | | | | | | | | | | | | | | | |
| HRA+1650 IQ+1250T | 101 | 108 | 25.8 | 72 | 0.94 | <-120 | <-120 | -120 | <-120 | -55 | 145 | 140 | 115 | 85 | 60 | IQ@52 |
| HRA+1650 IQ+1275T | 98 | 106 | 27.5 | 77 | 0.92 | <-120 | <-120 | -100 | <-120 | -40 | - | 135 | 110 | 75 | 45 | IQ@52 |
| HRA+1650 SQ+1225T | 102 | 110 | 24.5 | 73 | 0.93 | <-120 | <-120 | -115 | <-120 | -40 | 140 | 125 | 110 | 90 | 55 | IQ@52 |
| HRA+NORM@1650+1000T | 80 | 113 | 26.2 | 65 | 0.79 | -10 | +20 | +60 | -15 | +60 | 57 | 21 | 9 | - | - | SQ@40 |
| | | | | | | | | | | | | | | | | |
| ***LONGITUDINAL TESTS*** | | | | | | | | | | | | | | | | |
| CRDQ 1725+1275T 4hr | 103 | 111 | 26 | 74 | 0.93 | -90 | -80 | -70 | -85 | +25 | 140 | 116 | 111 | 46 | 4 | DQ@26 |
| CRA 1500+1650 SQ+1275T | 94 | 103 | 24 | 77 | 0.92 | <-120 | <-120 | <-120 | <-120 | -90 | - | 148 | 131 | 125 | 100 | SQ@45 |
| HRA+1650 IQ+1275T | 97 | 104 | 24 | 78 | 0.92 | <-120 | <-120 | <-120 | <-120 | -65 | - | 160 | 135 | 110 | 90 | IQ@52 |
| | | | | | | | | | | | | | | | | |

## Table VII - Mechanical Properties of Steel R

| *R-STEEL* | *Tensile Properties* | | | | | *Charpy V-Notch* Transition Temperature, deg. F | | | | | *Charpy V-Notch Energy* | | | | | Quench Rate |
|---|---|---|---|---|---|---|---|---|---|---|---|---|---|---|---|---|
| Processing Condition Temperature, deg. F | Y.S. ksi | T.S. ksi | EL. % | R.A. % | Y.S. T.S. | 20 ft-lb | 35 ft-lb | 60 ft-lb | 15 mils | 50% FAT | 70 F | 0 F | -40 F | -80 F | -120 F | *F/sec* |
| ***TRANSVERSE TESTS*** | | | | | | | | | | | | | | | | |
| CRDQ 1600 As Q | 70 | 108 | 25 | 66 | 0.65 | -35 | 0 | +30 | -45 | +40 | 82 | 22 | 29 | 13 | - | DQ@26 |
| CRDQ 1600+1200T | 88 | 100 | 25.5 | 70 | 0.88 | -70 | -65 | -45 | -55 | +50 | 112 | 78 | 66 | 3 | - | DQ@26 |
| CRDQ 1600+1275T | 84 | 94 | 25.2 | 73 | 0.89 | -100 | -85 | -55 | -100 | -40 | 120 | 99 | 51 | 56 | 4 | DQ@26 |
| CRDQ 1600+1300T | 79 | 90 | 28.5 | 73 | 0.88 | -115 | -100 | -70 | -115 | 0 | 152 | 112 | 102 | 39 | - | DQ@26 |
| | | | | | | | | | | | | | | | | |
| CRDQ 1725+1275T 1hr | 84 | 96 | 23.5 | 74 | 0.86 | -80 | -70 | -60 | -65 | +5 | 150 | 115 | 85 | 20 | - | DQ@30 |
| CRDQ 1725+1275T 4hr | - | - | - | - | - | -78 | -77 | -70 | -77 | >+70 | 120 | 108 | 90 | 3 | - | DQ@30 |
| CRDQ 1725+1300T 4hr | 75 | 86 | 28 | 77 | 0.87 | -100 | -90 | -80 | -90 | -30 | - | 163 | 117 | 104 | 8 | DQ@30 |
| | | | | | | | | | | | | | | | | |
| CRA 1500+1650 SQ+1275T 1hr | 67 | 80 | 34 | 78 | 0.83 | <-120 | <-120 | <-120 | <-120 | <-105 | - | 177 | 155 | 133 | 97 | SQ@45 |
| CRA 1500+1650 SQ+1175T 1hr | 74 | 86 | 29 | 79 | 0.86 | <-120 | <-120 | <-120 | <-120 | -35 | - | 170 | 115 | 95 | 85 | SQ@45 |
| CRA 1500+1650 SQ+1225T | 70 | 82 | 35 | 79 | 0.85 | <-120 | <-120 | <-120 | <-120 | -82 | - | 183 | 183 | 110 | 101 | SQ@45 |
| CRA 1500+1650 SQ+1150T | 66 | 80 | 35 | 80 | 0.83 | <-120 | <-120 | <-120 | <-120 | -90 | 200 | 200 | 180 | 160 | 80 | SQ@20 |
| CRA 1500+1650 SQ+1250T | 64 | 76 | 40 | 80 | 0.84 | <-120 | <-120 | <-120 | <-120 | -120 | 240 | 240 | 221 | 186 | 122 | SQ@20 |
| | | | | | | | | | | | | | | | | |
| CRA 1600+1650 IQ+1275T | 68 | 79 | 33 | 80 | 0.86 | <-120 | <-120 | <-120 | <-120 | -85 | 231 | 193 | 136 | 170 | 116 | IQ@52 |
| CRA 1600+1650 SQ+1275T | 67 | 77 | 34.4 | 76 | 0.86 | <-120 | <-120 | <-120 | <-120 | -100 | - | 240+ | 215 | 155 | 144 | IQ@52 |
| CRA 1600+1650 SQ+1150T | 73 | 82 | 31.2 | 76 | 0.89 | <-120 | <-120 | <-120 | <-120 | -60 | 168 | 162 | 148 | 110 | 103 | SQ@40 |
| | | | | | | | | | | | | | | | | |
| | | | | | | | | | | | | | | | | |
| HRA+1650 IQ+1150T | 72 | 84 | 30.8 | 76 | 0.86 | <-120 | <-120 | <-120 | <-120 | -30 | 175 | 145 | 130 | 125 | 115 | IQ@52 |
| HRA+1650 IQ+1275T | 70 | 81 | 34.5 | 81 | 0.86 | <-120 | <-120 | <-120 | <-120 | -110 | - | 230 | 160 | 135 | 120 | IQ@52 |
| HRA+1650 SQ+1250T | 65 | 74 | 35.8 | 81 | 0.88 | <-120 | <-120 | <-120 | <-120 | -90 | 240 | 240 | 240 | 230 | 160 | IQ@52 |
| HRA+NORM@1650 | 52 | 71 | 39.5 | 79 | 0.74 | <-120 | <-120 | <-120 | <-120 | -115 | 200 | 240 | 240 | 176 | 146 | SQ@40 |
| | | | | | | | | | | | | | | | | |
| ***LONGITUDINAL TESTS*** | | | | | | | | | | | | | | | | |
| CRDQ 1725+1275T 4hr | 81 | 91 | 23 | 74 | 0.89 | -100 | -80 | -60 | -100 | -30 | - | 177 | 124 | 33 | 5 | DQ@26 |
| CRA 1500+1650 SQ+1275T | 67 | 79 | 29 | 80 | 0.85 | <-120 | <-120 | <-120 | <-120 | -120 | - | 240 | 224 | 197 | 132 | SQ@45 |
| HRA+1650 IQ+1275T | 72 | 82 | 34 | 82 | 0.86 | <-120 | <-120 | <-120 | <-120 | <-120 | - | 240 | 240 | 205 | 170 | IQ@52 |
| | | | | | | | | | | | | | | | | |

## Table VIII - Mechanical Properties of Steel S

| *S-STEEL* | *Tensile Properties* | | | | | *Charpy V-Notch* Transition Temperature, deg. F | | | | | *Charpy V-Notch Energy* | | | | | Quench Rate |
|---|---|---|---|---|---|---|---|---|---|---|---|---|---|---|---|---|
| Processing Condition<br>Temperature, deg. F | Y.S. ksi | T.S. ksi | EL. % | R.A. % | Y.S. / T.S. | 20 ft-lb | 35 ft-lb | 60 ft-lb | 15 mils | 50% FAT | 70 F | 0 F | -40 F | -80 F | -120 F | *F/sec* |
| ***TRANSVERSE TESTS*** | | | | | | | | | | | | | | | | |
| CRDQ 1600 As Q | 76 | 118 | 21.5 | 55 | 0.64 | -30 | +10 | +80 | -50 | +70 | 55 | 35 | 21 | 14 | - | DQ@26 |
| CRDQ 1600+1200T | 92 | 104 | 23.5 | 67 | 0.88 | -60 | -25 | +30 | -50 | +60 | 82 | 47 | 30 | 6 | - | DQ@26 |
| CRDQ 1600+1275T | 85 | 98 | 23.5 | 70 | 0.87 | -60 | -20 | +10 | -65 | +40 | 110 | 53 | 40 | 15 | - | DQ@26 |
| CRDQ 1600+1300T | 80 | 93 | 27.5 | 72 | 0.86 | -70 | -55 | -35 | -75 | +40 | 106 | 79 | 61 | 4 | - | DQ@26 |
| | | | | | | | | | | | | | | | | |
| CRDQ 1725+1275T 1hr | 94 | 105 | 24 | 68 | 0.9 | -90 | -70 | -40 | -85 | +70 | 100 | 95 | 60 | 30 | 3 | DQ@30 |
| CRDQ 1725+1275T 4hr | - | - | - | - | - | -78 | -68 | -48 | -77 | - | - | 82 | 67 | 13 | - | DQ@30 |
| CRDQ 1725+1300T 4hr | 80 | 91 | 26.5 | 73 | 0.88 | -95 | -85 | -75 | -85 | +15 | 118 | 97 | 93 | 58 | 7 | DQ@30 |
| | | | | | | | | | | | | | | | | |
| CRA 1500+1650 SQ+1275T 1hr | 70 | 84 | 36 | 79 | 0.84 | <-120 | <-120 | <-120 | <-120 | -55 | - | 164 | 142 | 98 | 83 | SQ@45 |
| CRA 1500+1650 SQ+1175T 1hr | 78 | 92 | 26 | 74 | 0.85 | <-120 | <-120 | <-120 | <-120 | -60 | - | 120 | 105 | 90 | 75 | SQ@45 |
| CRA 1500+1650 SQ+1225T | 74 | 86 | 34 | 76 | 0.86 | <-120 | <-120 | <-120 | <-120 | -48 | - | 156 | 130 | 103 | 82 | SQ@45 |
| CRA 1500+1650 SQ+1150T | 72 | 85 | 35 | 77 | 0.84 | <-120 | <-120 | <-120 | <-120 | -35 | 200 | 180 | 120 | 80 | 60 | SQ@20 |
| CRA 1500+1650 SQ+1250T | 68 | 81 | 36 | 79 | 0.84 | <-120 | <-120 | <-120 | <-120 | -50 | 230 | 200 | 150 | 115 | 85 | SQ@20 |
| | | | | | | | | | | | | | | | | |
| CRA 1600+1650 IQ+1275T | 74 | 85 | 30 | 75 | 0.87 | <-120 | <-120 | <-120 | <-120 | -40 | 139 | 138 | 110 | 83 | 70 | IQ@52 |
| CRA 1600+1650 SQ+1275T | 72 | 82 | 26.5 | 73 | 0.88 | <-120 | <-120 | <-120 | <-120 | -60 | - | 170 | 150 | 125 | 88 | IQ@52 |
| CRA 1600+1650 SQ+1150T | 79 | 92 | 26.8 | 71 | 0.86 | <-120 | <-120 | -90 | <-120 | -50 | 126 | 116 | 88 | 60 | 54 | SQ@40 |
| | | | | | | | | | | | | | | | | |
| | | | | | | | | | | | | | | | | |
| HRA+1650 IQ+1150T | 81 | 92 | 29 | 75 | 0.89 | <-120 | <-120 | <-120 | <-120 | -30 | 135 | 120 | 90 | 75 | 60 | IQ@52 |
| HRA+1650 IQ+1275T | 75 | 87 | 31 | 77 | 0.86 | <-120 | <-120 | <-120 | <-120 | -50 | - | 140 | 105 | 80 | 65 | IQ@52 |
| HRA+1650 SQ+1250T | 68 | 79 | 34.8 | 78 | 0.86 | <-120 | <-120 | <-120 | <-120 | -70 | 175 | 175 | 170 | 120 | 90 | IQ@52 |
| HRA+NORM@1650 | 58 | 76 | 35 | 75 | 0.76 | <-120 | <-120 | <-120 | <-120 | -30 | 176 | 156 | 120 | 108 | 59 | SQ@40 |
| | | | | | | | | | | | | | | | | |
| ***LONGITUDINAL TESTS*** | | | | | | | | | | | | | | | | |
| CRDQ 1725+1275T 4hr | 81 | 95 | 24.5 | 73 | 0.85 | <-120 | <-120 | <-120 | <-120 | -10 | - | 118 | 106 | 100 | 22 | DQ@26 |
| CRA 1500+1650 SQ+1275T | 69 | 83 | 30 | 83 | 83 | <-120 | <-120 | <-120 | <-120 | -80 | - | 172 | 164 | 133 | 72 | SQ@45 |
| HRA+1650 IQ+1275T | 73 | 85 | 33 | 81 | 0.86 | <-120 | <-120 | <-120 | <-120 | -85 | - | 180 | 170 | 135 | 105 | IQ@52 |
| | | | | | | | | | | | | | | | | |

## Table IX - Mechanical Properties of Steel T

| *T-STEEL* | *Tensile Properties* | | | | | *Charpy V-Notch* Transition Temperature, deg. F | | | | | *Charpy V-Notch Energy* | | | | | Quench Rate |
|---|---|---|---|---|---|---|---|---|---|---|---|---|---|---|---|---|
| Processing Condition Temperature, deg. F | Y.S. ksi | T.S. ksi | EL. % | R.A. % | Y.S. / T.S. | 20 ft-lb | 35 ft-lb | 60 ft-lb | 15 mils | 50% FAT | 70 F | 0 F | -40 F | -80 F | -120 F | *F/sec* |
| ***TRANSVERSE TESTS*** | | | | | | | | | | | | | | | | |
| CRDQ 1600 As Q | 88 | 137 | 17 | 37 | 0.64 | +20 | +70 | +100 | +30 | +90 | 31 | 21 | 10 | - | - | DQ@26 |
| CRDQ 1600+1200T | 100 | 113 | 20 | 62 | 0.88 | +10 | +20 | >+100 | +35 | +100 | 50 | 7 | - | - | - | DQ@26 |
| CRDQ 1600+1275T | 94 | 107 | 21.5 | 65 | 0.88 | -50 | +10 | +50 | -75 | +50 | 69 | 32 | 30 | 13 | - | DQ@26 |
| CRDQ 1600+1300T | 86 | 100 | 24.5 | 65 | 0.86 | -60 | -30 | 0 | -65 | 0 | 96 | 65 | 35 | 6 | - | DQ@26 |
| | | | | | | | | | | | | | | | | |
| CRDQ 1725+1275T 1hr | 96 | 109 | 22 | 62 | 0.88 | -50 | -30 | -5 | -40 | +40 | 85 | 65 | 25 | 5 | - | DQ@30 |
| CRDQ 1725+1275T 4hr | - | - | - | - | - | -58 | -43 | -17 | -60 | - | 93 | 60 | 45 | 16 | - | DQ@30 |
| CRDQ 1725+1300T 4hr | 82 | 94 | 26 | 67 | 0.86 | -90 | -80 | -40 | -90 | +40 | 102 | 87 | 54 | 34 | 7 | DQ@30 |
| | | | | | | | | | | | | | | | | |
| CRA 1500+1650 SQ+1275T 1hr | 78 | 92 | 29 | 75 | 0.85 | <-120 | <-120 | -120 | <-120 | -60 | - | 118 | 115 | 64 | 66 | SQ@45 |
| CRA 1500+1650 SQ+1175T 1hr | 88 | 102 | 24 | 70 | 0.86 | <-120 | <-120 | -60 | <-120 | -50 | - | 95 | 75 | 50 | 40 | SQ@45 |
| CRA 1500+1650 SQ+1225T | 85 | 97 | 26 | 72 | 0.88 | <-120 | <-120 | -69 | <-120 | -25 | - | 116 | 88 | 52 | 38 | SQ@45 |
| CRA 1500+1650 SQ+1150T | 84 | 97 | 30 | 71 | 0.86 | <-120 | <-120 | <-120 | <-120 | -20 | 130 | 120 | 110 | 80 | 30 | SQ@20 |
| CRA 1500+1650 SQ+1250T | 78 | 92 | 34 | 73 | 0.85 | <-120 | <-120 | <-120 | <-120 | -30 | 160 | 150 | 110 | 60 | 35 | SQ@20 |
| | | | | | | | | | | | | | | | | |
| CRA 1600+1650 IQ+1275T | 76 | 88 | 28.5 | 72 | 0.86 | <-120 | <-120 | -90 | <-120 | -35 | 122 | 117 | 81 | 63 | 48 | IQ@52 |
| CRA 1600+1650 SQ+1275T | 76 | 90 | 26.5 | 71 | 0.85 | <-120 | <-120 | -90 | <-120 | -60 | - | 111 | 92 | 60 | 47 | IQ@52 |
| CRA 1600+1650 SQ+1150T | 88 | 101 | 25 | 66 | 0.87 | <-120 | -90 | -45 | <-120 | -40 | 85 | 82 | 66 | 37 | 28 | SQ@40 |
| | | | | | | | | | | | | | | | | |
| | | | | | | | | | | | | | | | | |
| HRA+1650 IQ+1150T | 91 | 104 | 24 | 68 | 0.88 | -120 | -90 | -35 | <-120 | +10 | 110 | 75 | 60 | 40 | 20 | IQ@52 |
| HRA+1650 IQ+1275T | 77 | 91 | 29 | 76 | 0.84 | <-120 | <-120 | -115 | <-120 | -40 | 135 | 130 | 115 | 80 | 55 | IQ@52 |
| HRA+1650 SQ+1250T | 74 | 85 | 29.2 | 75 | 0.87 | <-120 | <-120 | -95 | <-120 | -45 | - | 115 | 95 | 70 | 55 | IQ@52 |
| HRA+NORM@1650 | 60 | 82 | 32.5 | 66 | 0.73 | <-120 | <-120 | <-120 | -70 | -20 | 133 | 106 | 90 | 74 | 47 | SQ@40 |
| | | | | | | | | | | | | | | | | |
| ***LONGITUDINAL TESTS*** | | | | | | | | | | | | | | | | |
| CRDQ 1725+1275T 4hr | 86 | 100 | 25.3 | 70 | 0.86 | -90 | -85 | -70 | -90 | +45 | 110 | 100 | 78 | 53 | 13 | DQ@26 |
| CRA 1500+1650 SQ+1275T | 77 | 90 | 29.5 | 78 | 0.85 | <-120 | <-120 | <-120 | <-120 | -80 | - | 137 | 128 | 109 | 70 | SQ@45 |
| HRA+1650 IQ+1275T | 76 | 91 | 32 | 77 | 0.84 | <-120 | <-120 | <-120 | <-120 | -85 | - | 170 | 150 | 115 | 70 | IQ@52 |
| | | | | | | | | | | | | | | | | |

Table X - Spray and Immersion Quench Rates for .5, 1, and 2 inch Thick Plates

| Nozzle | Pressure (psig) | Cooling Rate (F/s) | | |
|---|---|---|---|---|
| | | 0.5" | 1" | 2" |
| | | | | |
| SQ 5 | 50 | | 14 | |
| | 60 | | 15 | |
| | 70 | 16 | 20 | 9 |
| | | | | |
| SQ 10 | 20 | | | 8 |
| | 30 | | 17 | |
| | 40 | 28 | | 14 |
| | 60 | | 22 | |
| | 70 | 30 | 35 | 15 |
| | | | | |
| SQ 18 | 40 | | 23 | |
| | 50 | | 27 | |
| | 60 | | 45 | |
| | 70 | 52 | | 19 |
| | | | | |
| SQ29 | 50 | | 40 | |
| | 70 | 82 | 50 | 21 |
| | 80 | | 51 | |
| | | | | |
| IQ | | 114 | 52 | 19 |
| | | | | |

Table XI - Implant Threshold Stresses - SMAW and FCAW

| | Y. S. | Process | SMAW | FCAW |
|---|---|---|---|---|
| Steel | ksi | % Carbon | Critical Stress, ksi | |
| | | | | |
| N | 100 | 0.064 | 98 | 98 |
| | | | | |
| P | 100 | 0.062 | 95 | 95 |
| | | | | |
| R | 70 | 0.066 | 93 | 60 |
| | | | | |
| S | 70 | 0.1 | 76 | 44 |
| | | | | |
| T | 70 | 0.14 | 72 | 42 |

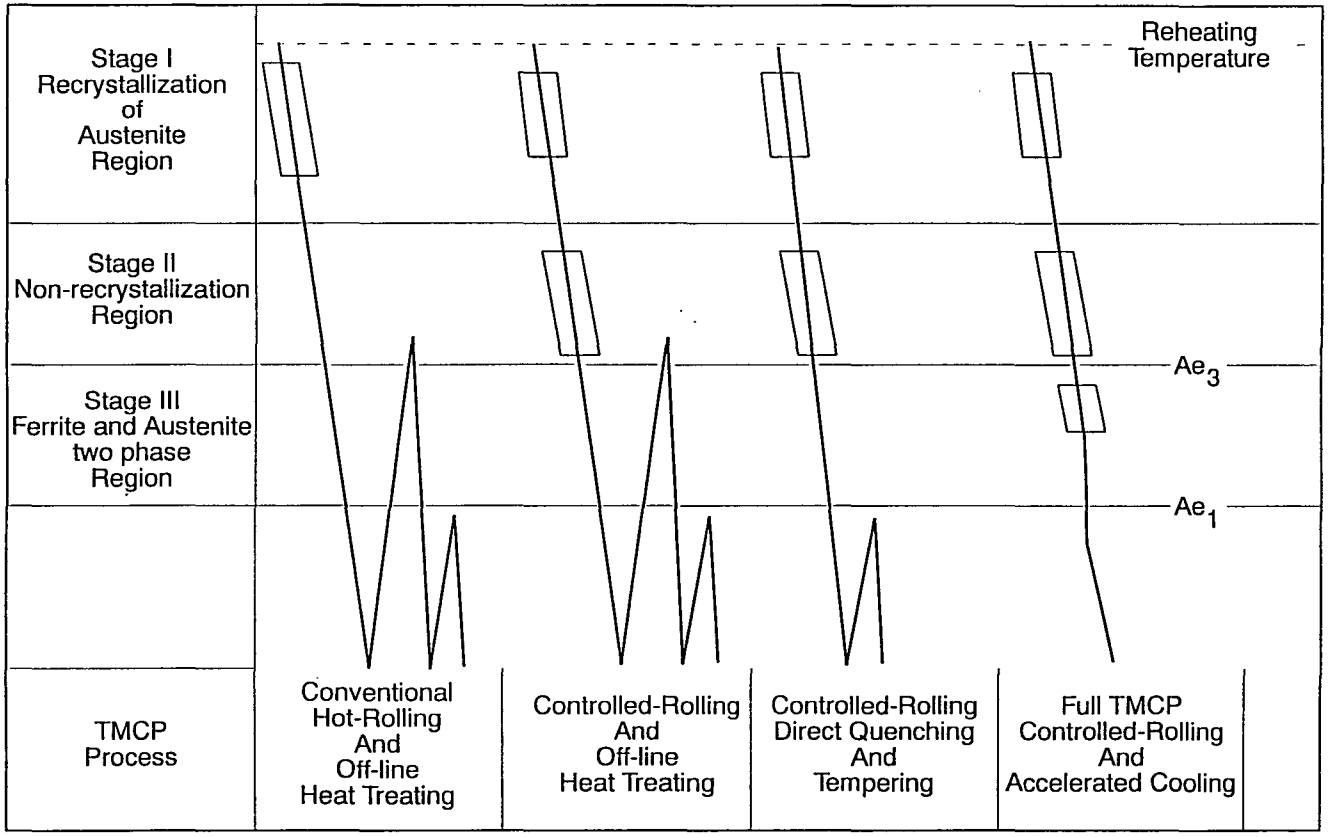


Figure 1 - Schematic representation of TMCP treatments

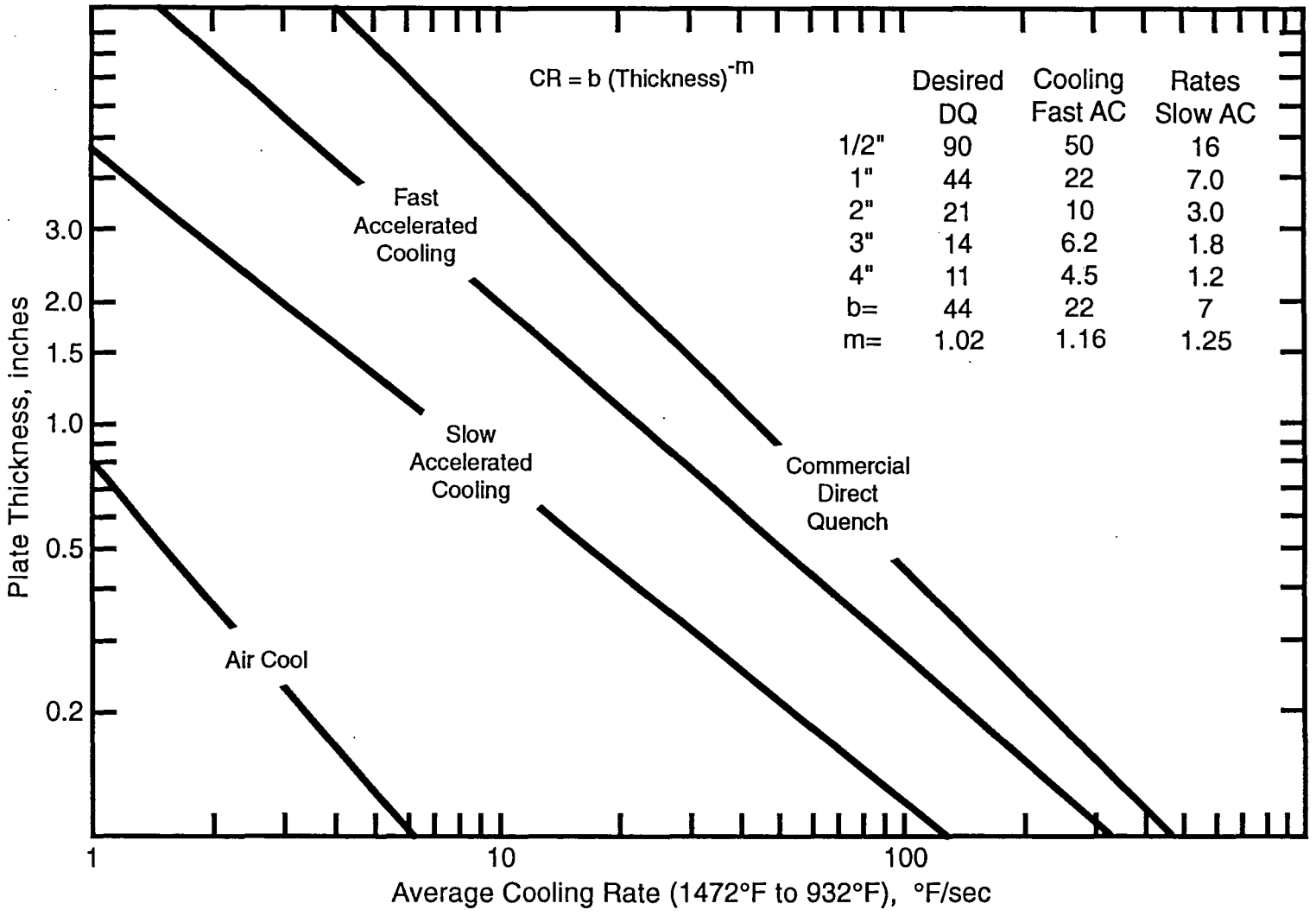


Figure 2 - Kawasaki Average Cooling Rate (932°F - 1472°F), °F/sec

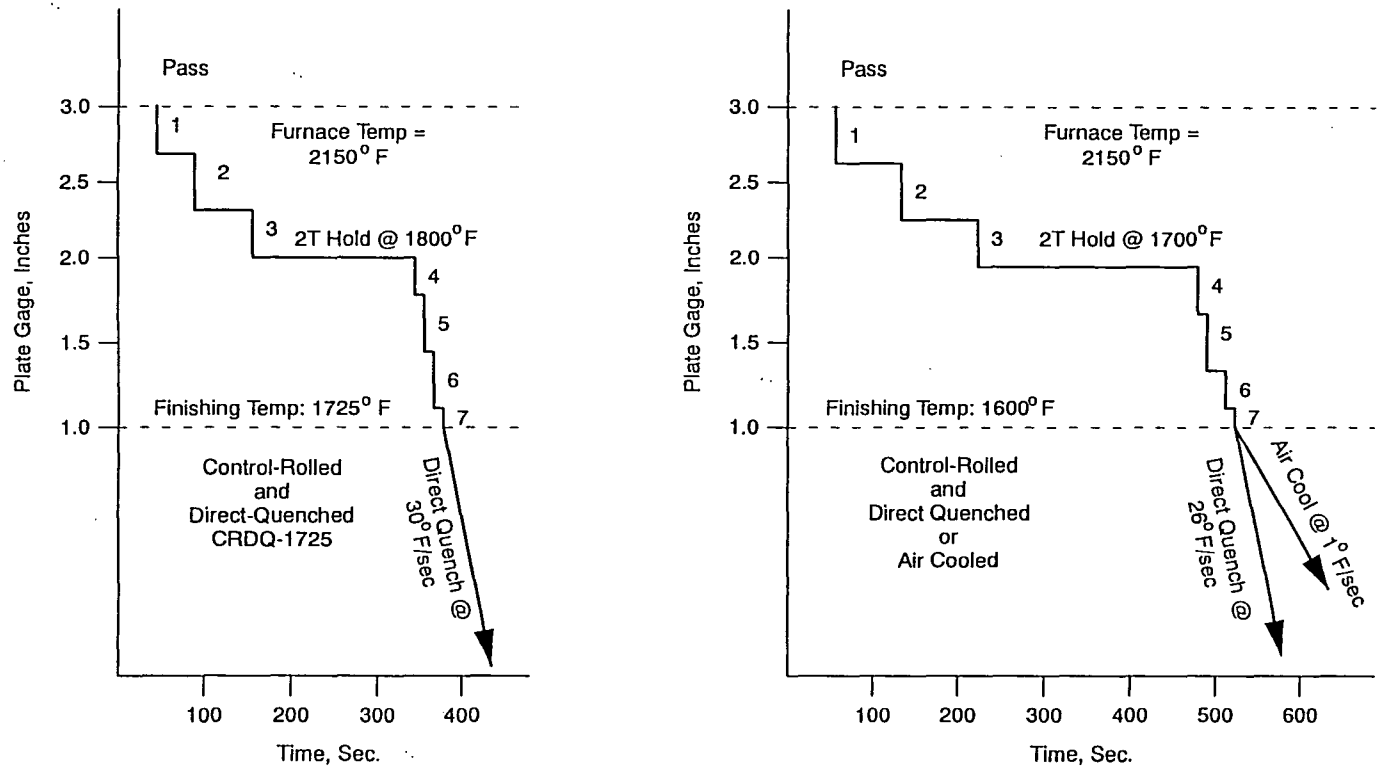


Figure 3 - Rolling schedule for CRDQ 1725, CRDQ 1600, and CRA 1600

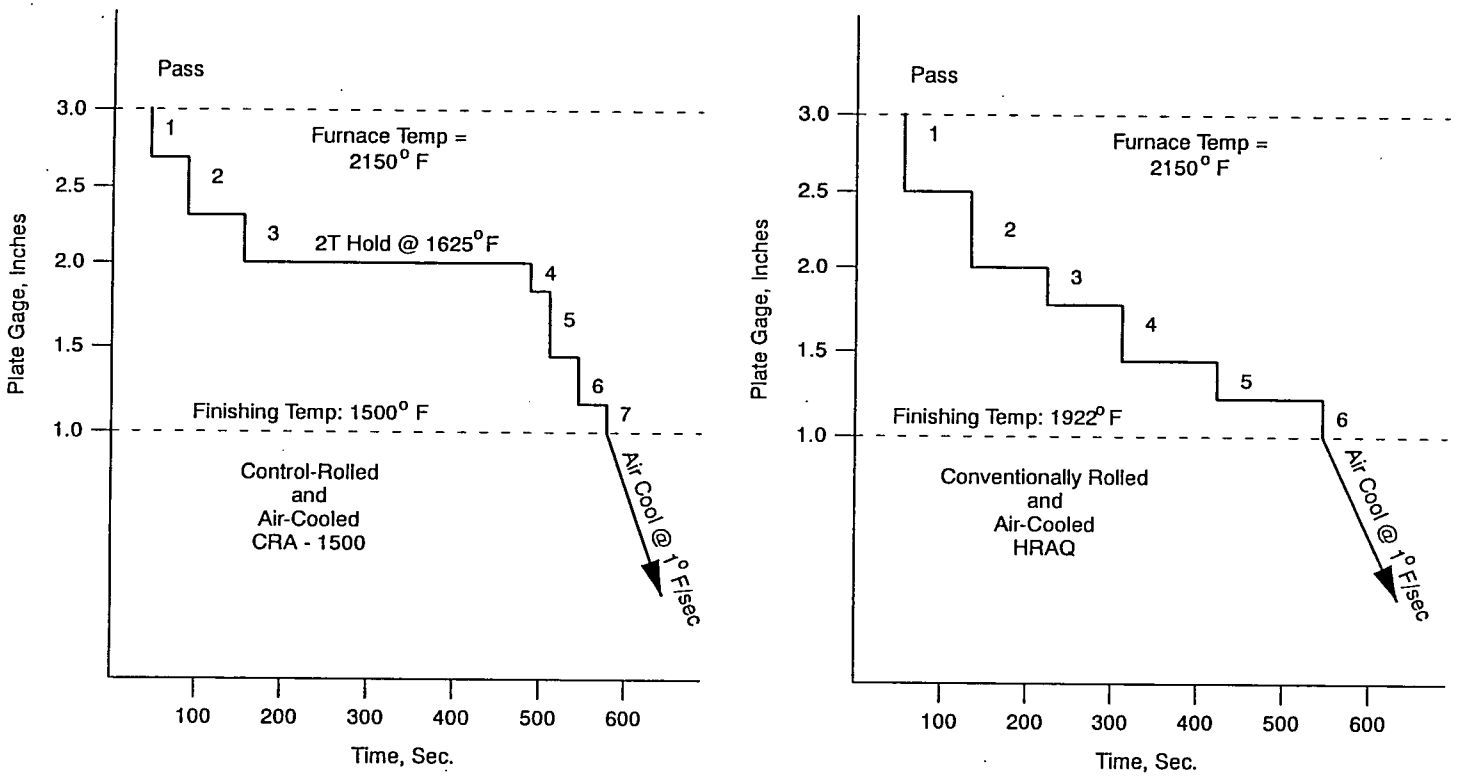


Figure 4 - Rolling schedule for CRA 1500 and HRA 1900

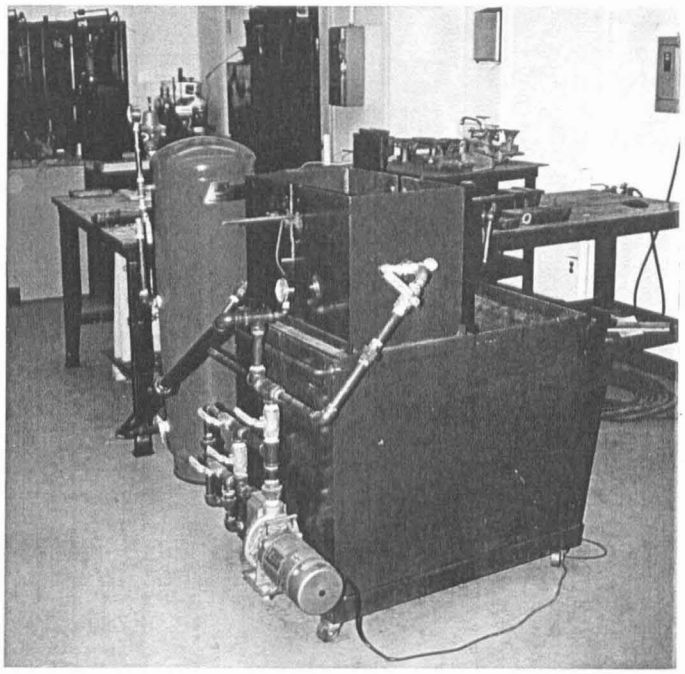

Figure 5 - Details of ATLSS spray quench facility

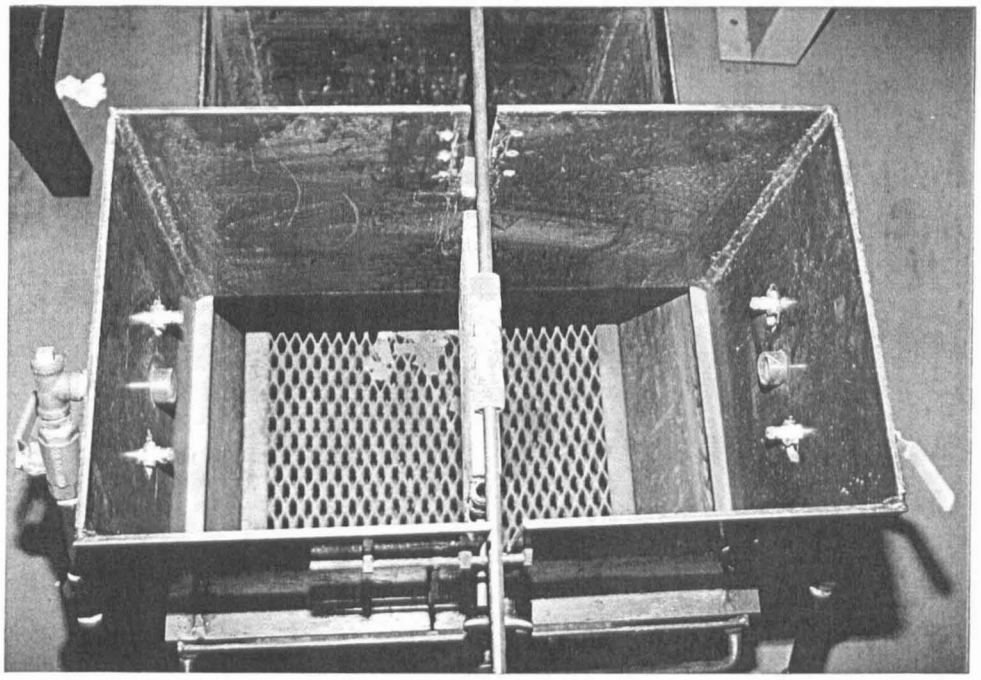

Figure 6 - Spray nozzle configuration

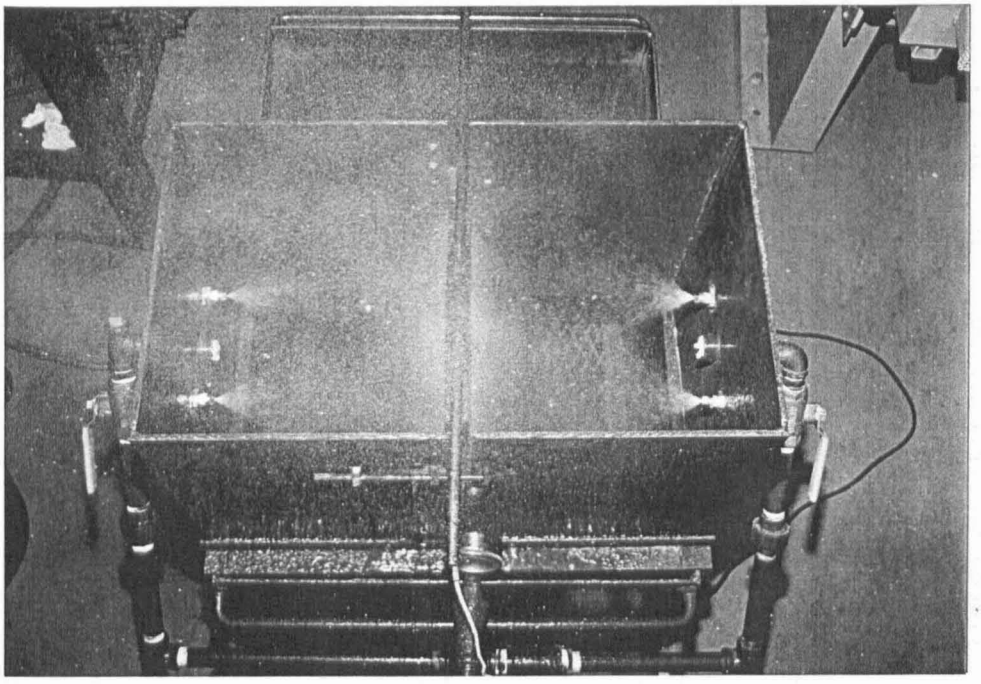

Figure 7 - Plate being spray quenched

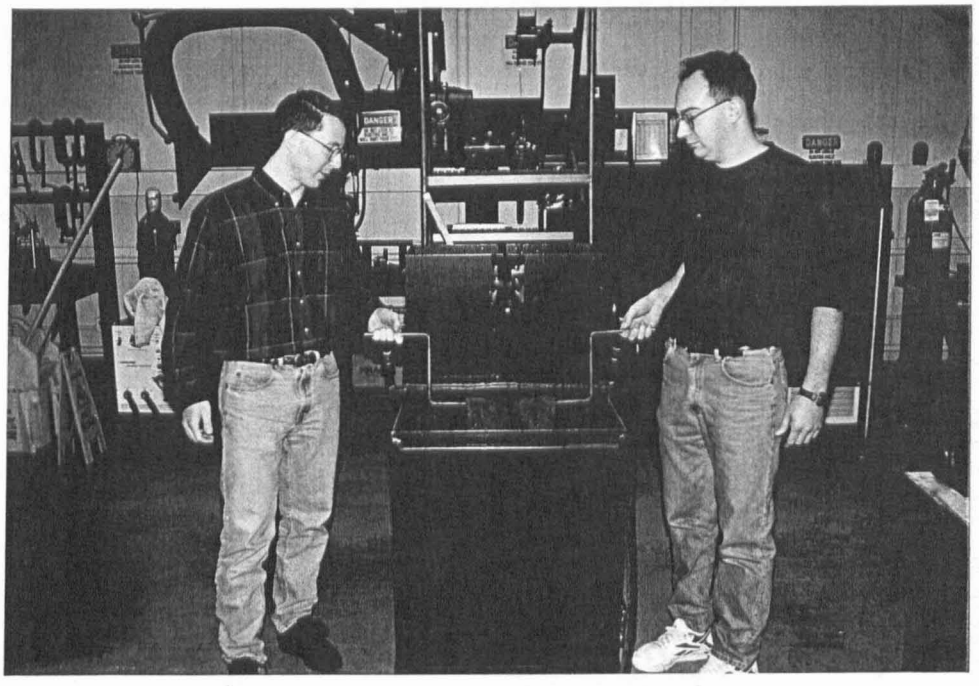

Figure 8 - Plate being placed in the immersion quench facility

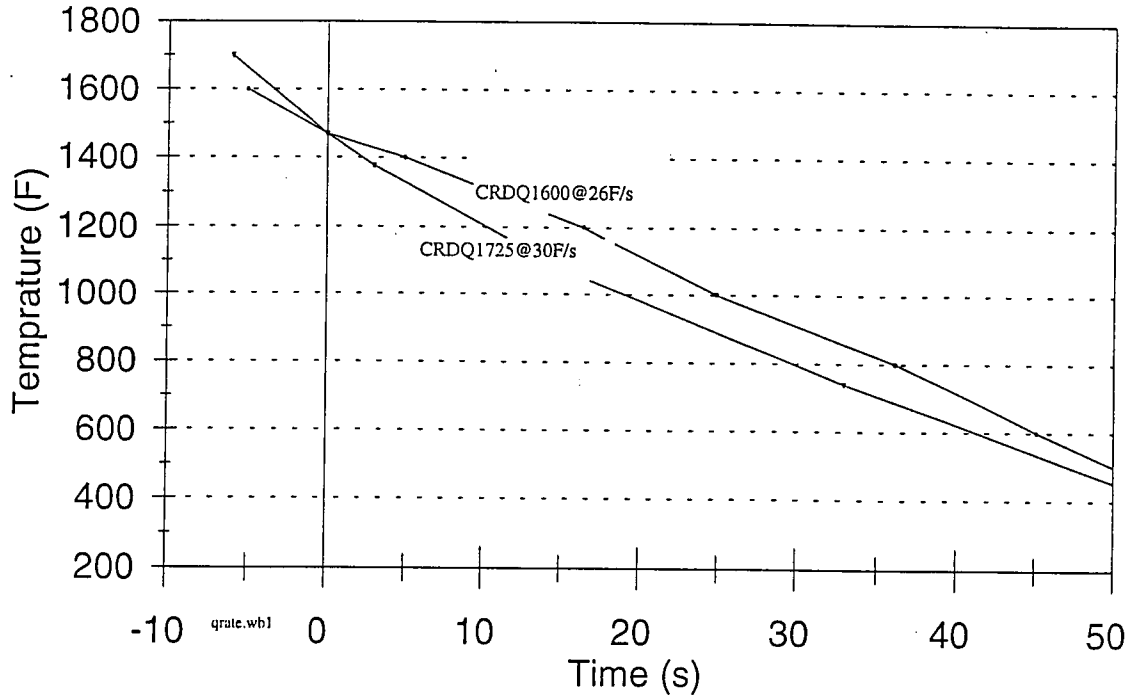


Figure 9 - Typical direct-quench cooling curves provided by US Steel

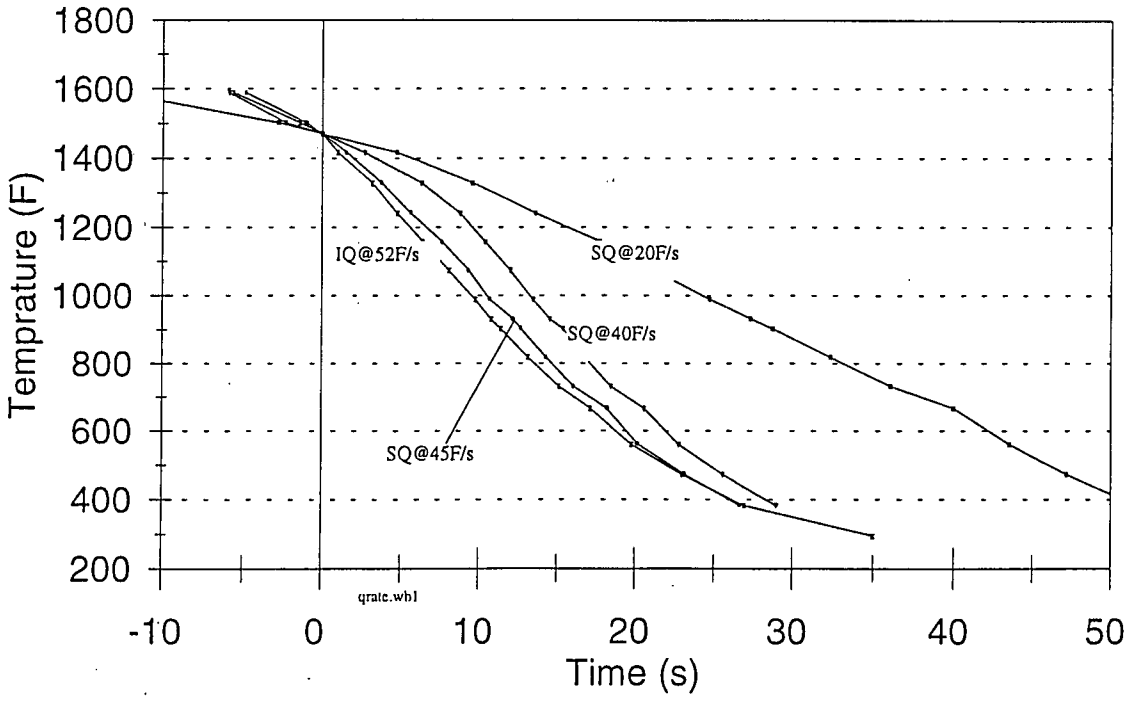


Figure 10 - Spray and immersion quenching curves employed in tests

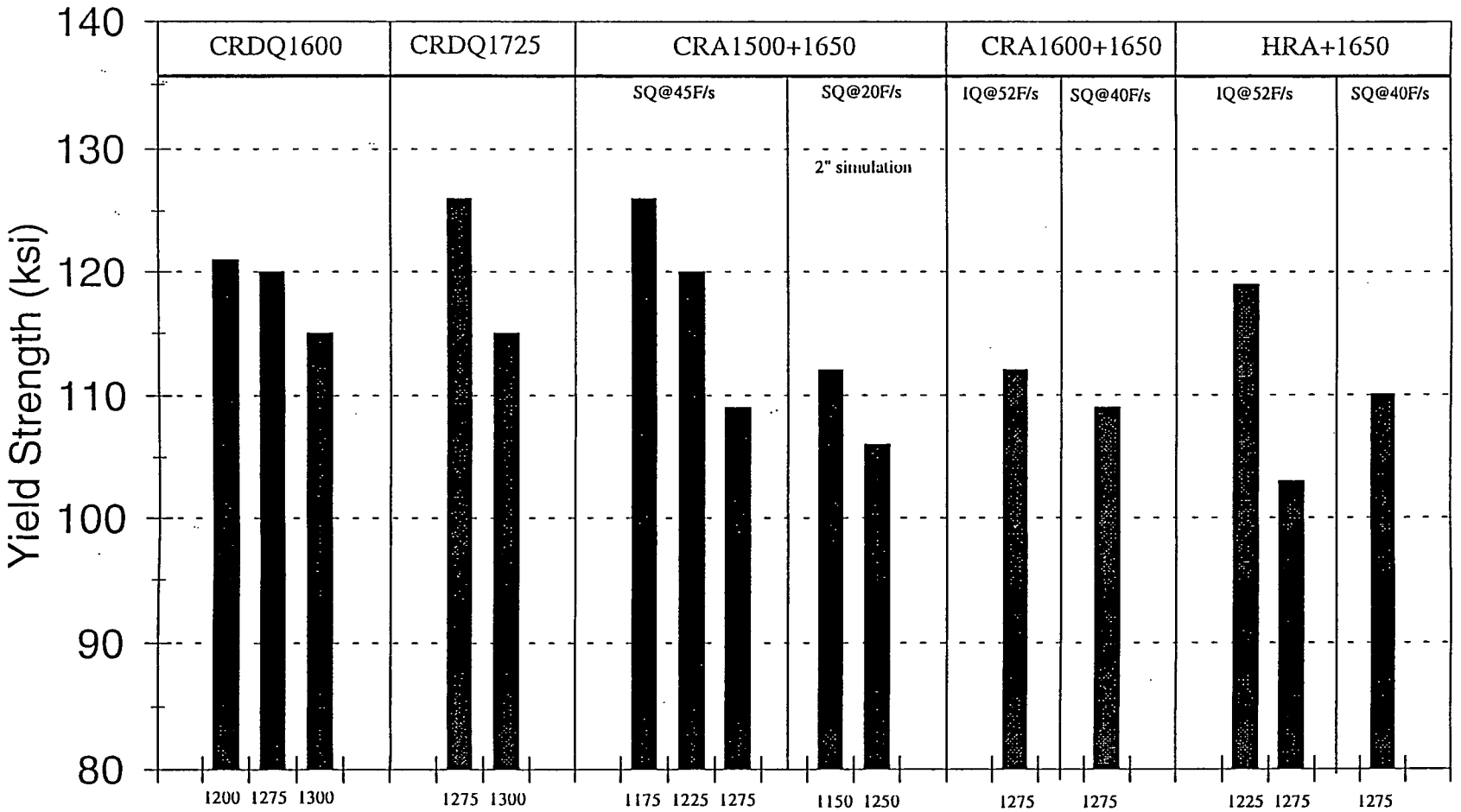


Figure 11 - Steel N yield strength at specified tempering temperatures for all TMCP practices.

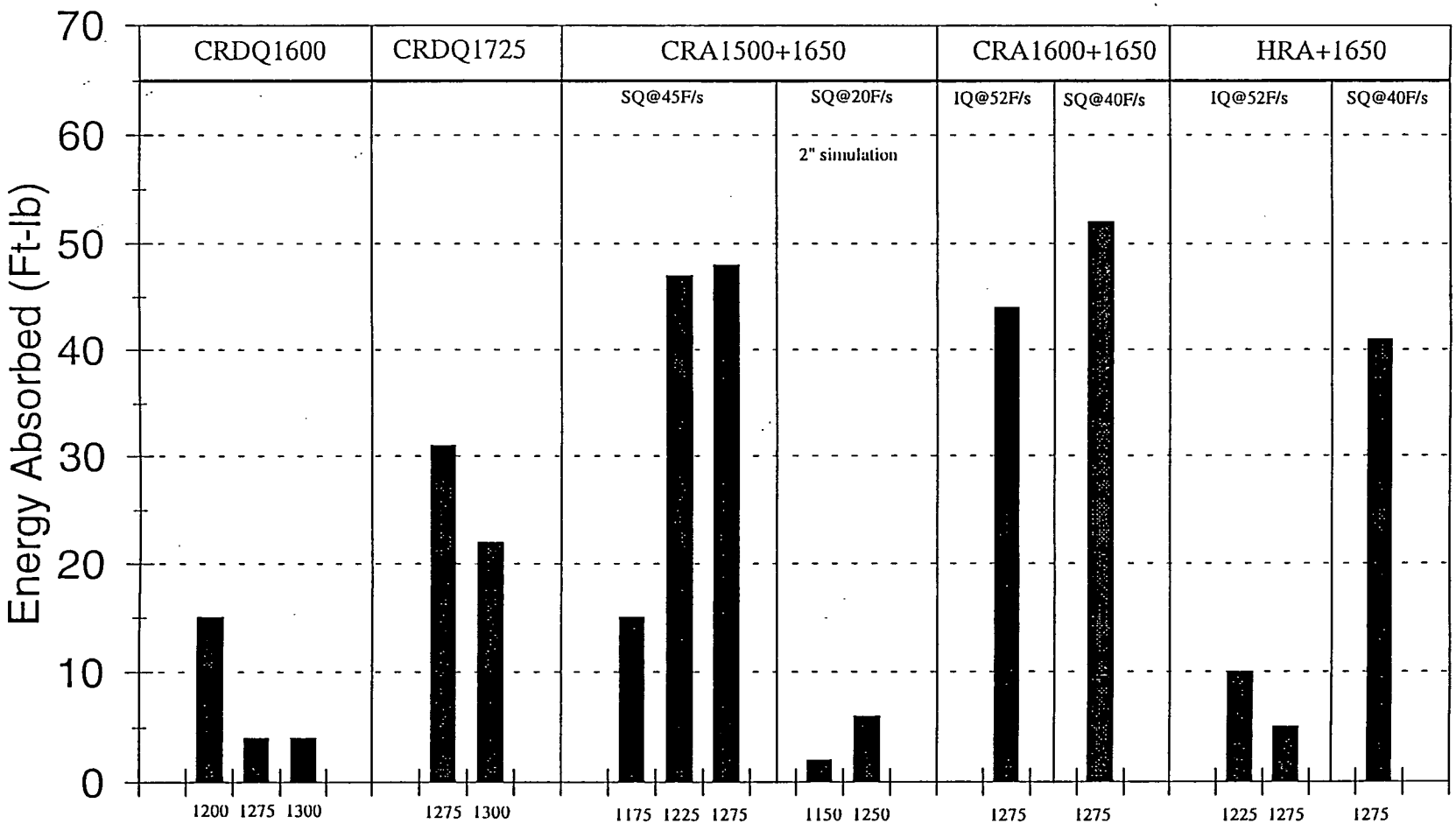


Figure 12 - Steel N -40F Charpy energy at specified tempering temperatures for all TMCP practices.

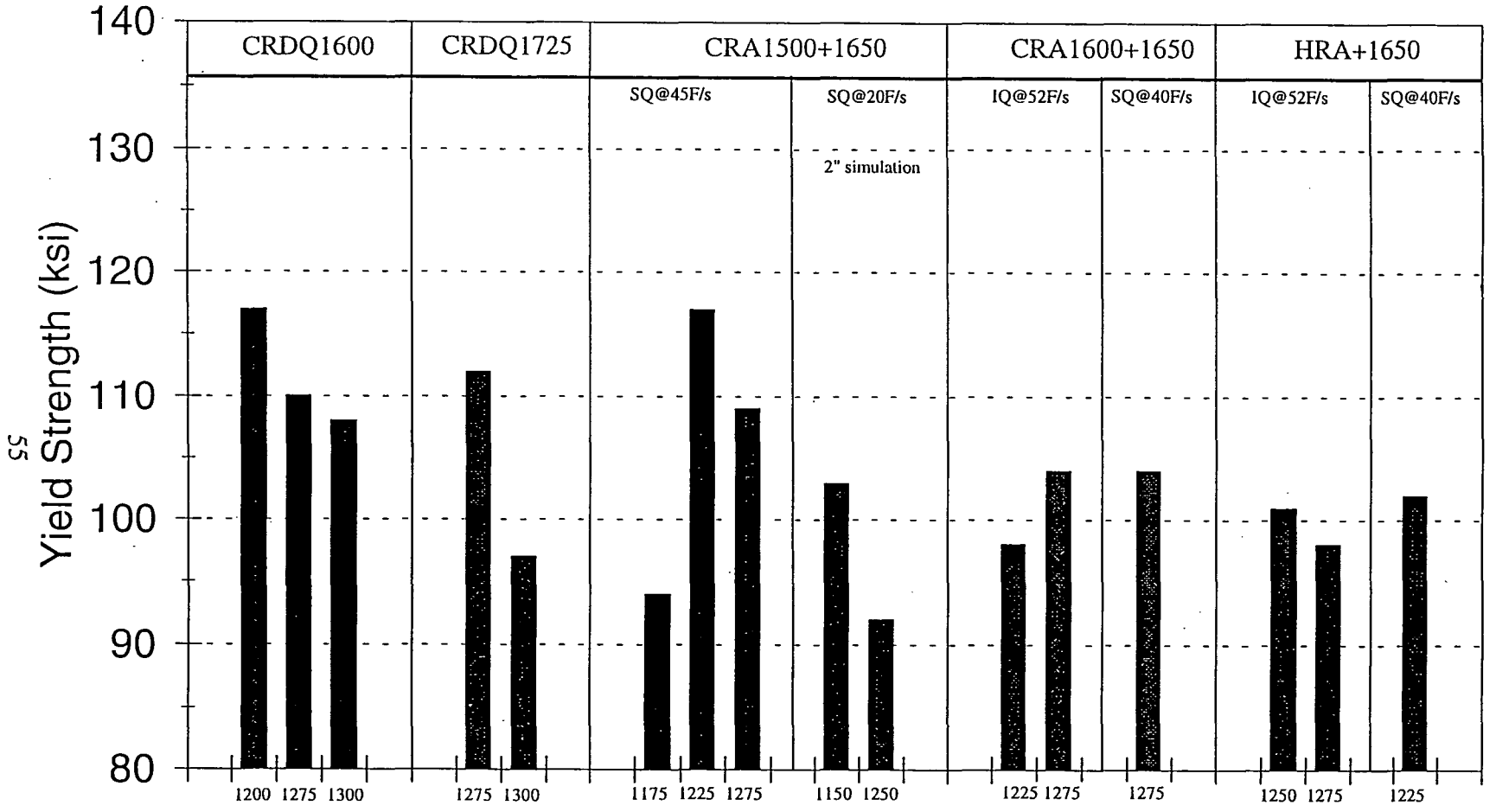


Figure 13 - Steel P yield strength at specified tempering temperatures for all TMCP practices.

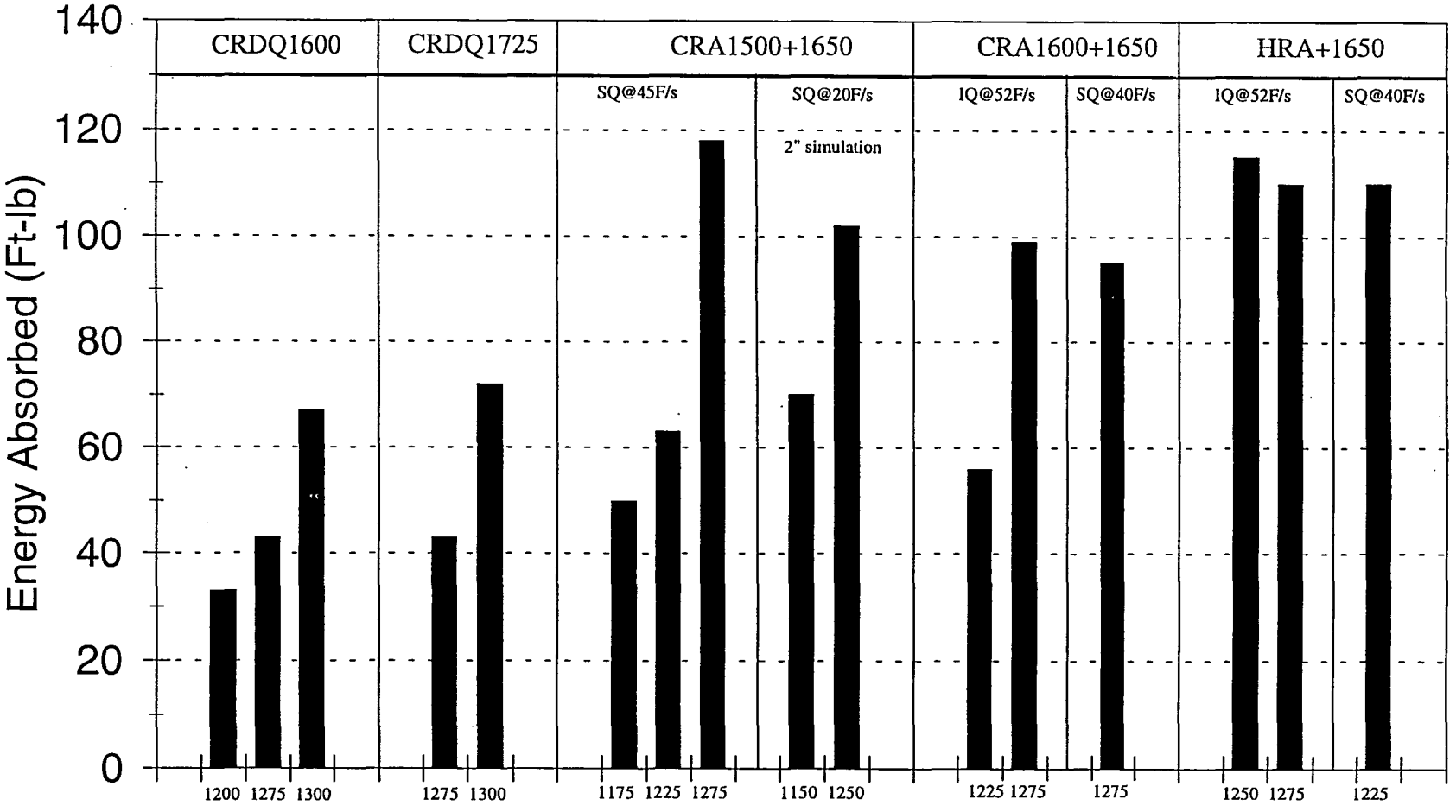


Figure 14 - Steel P -40F Charpy energy at specified tempering temperatures for all TMCP practices.

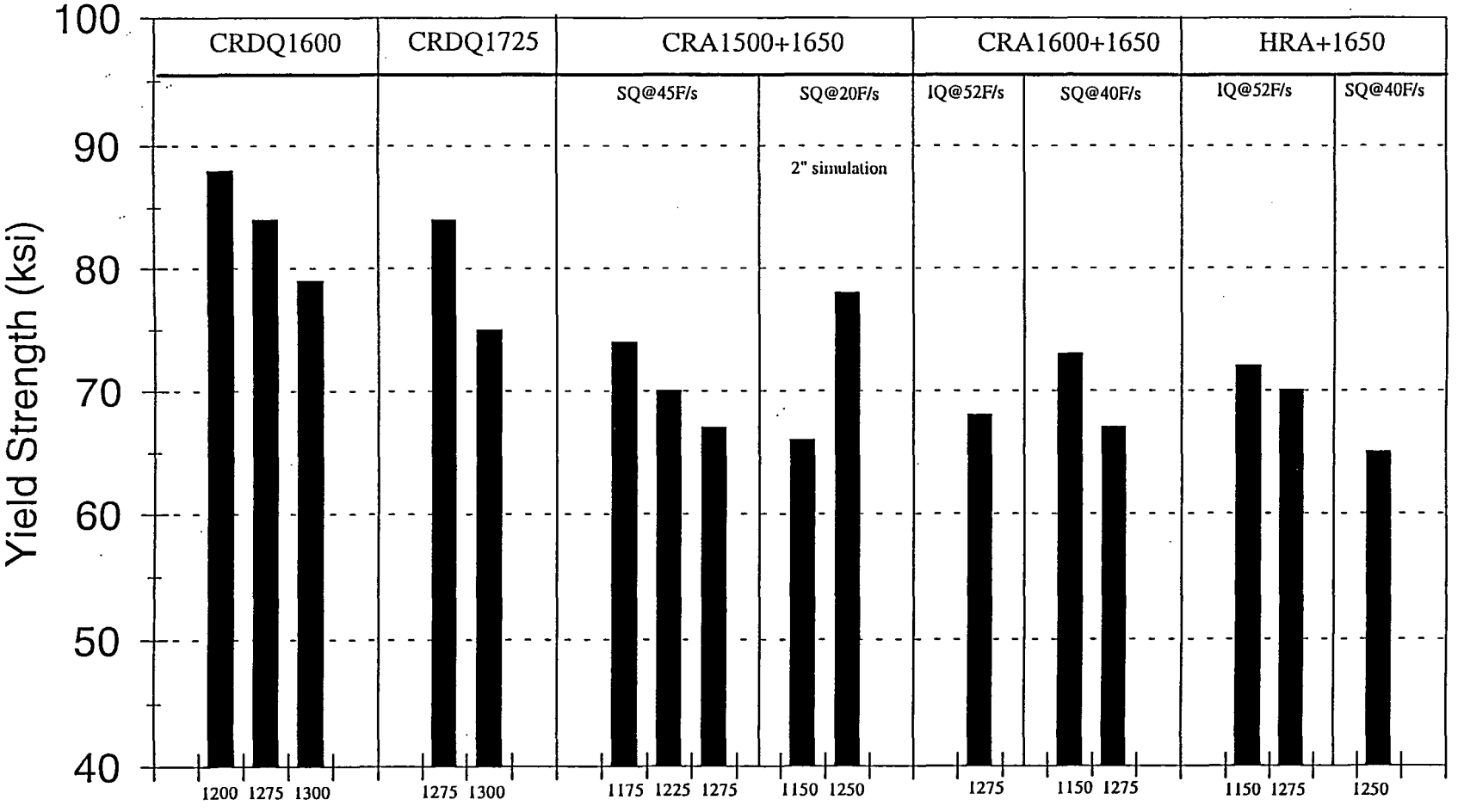


Figure 15 - Steel R yield strength at specified tempering temperatures for all TMCP practices.

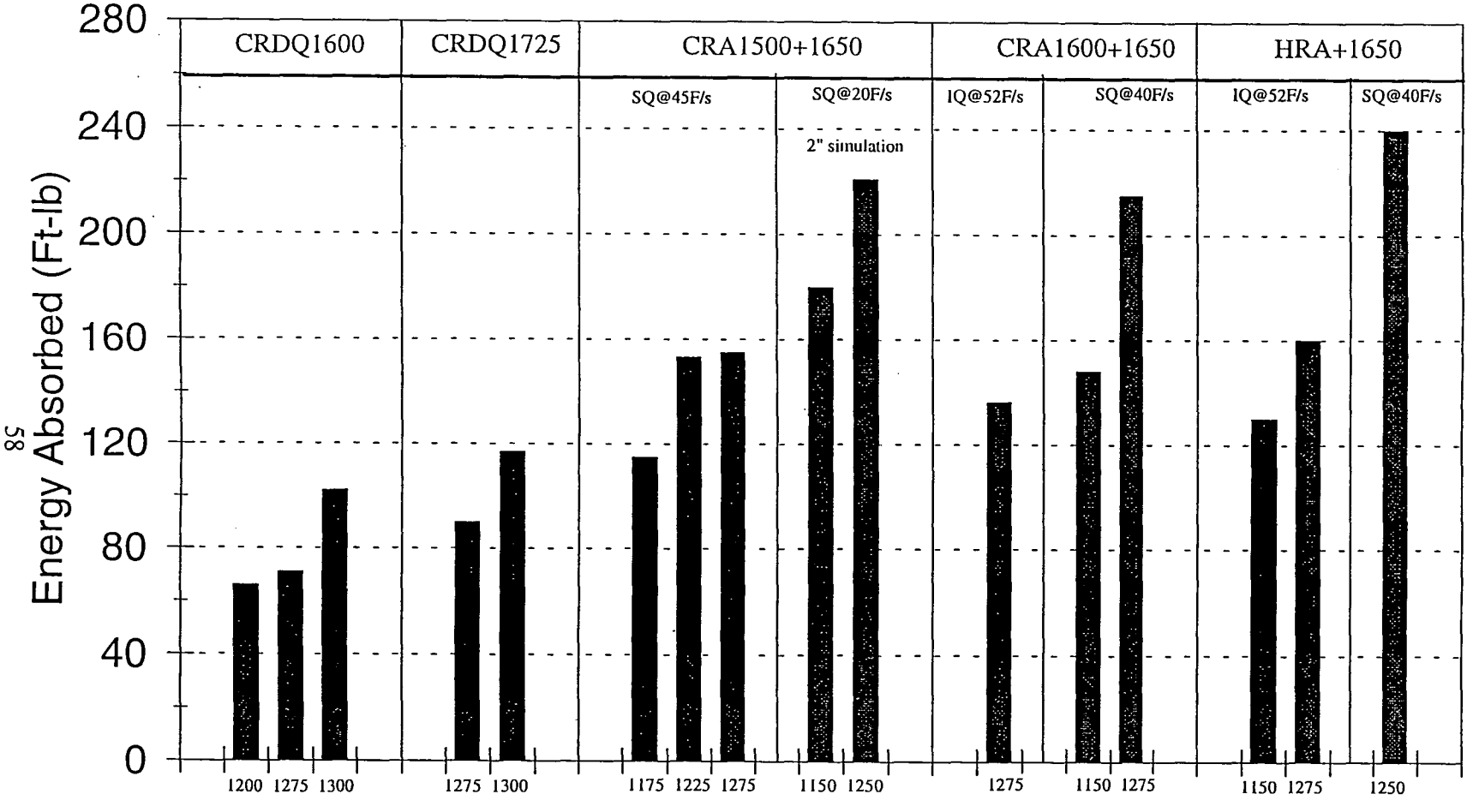


Figure 16 - Steel R -40F Charpy energy at specified tempering temperatures for all TMCP practices.

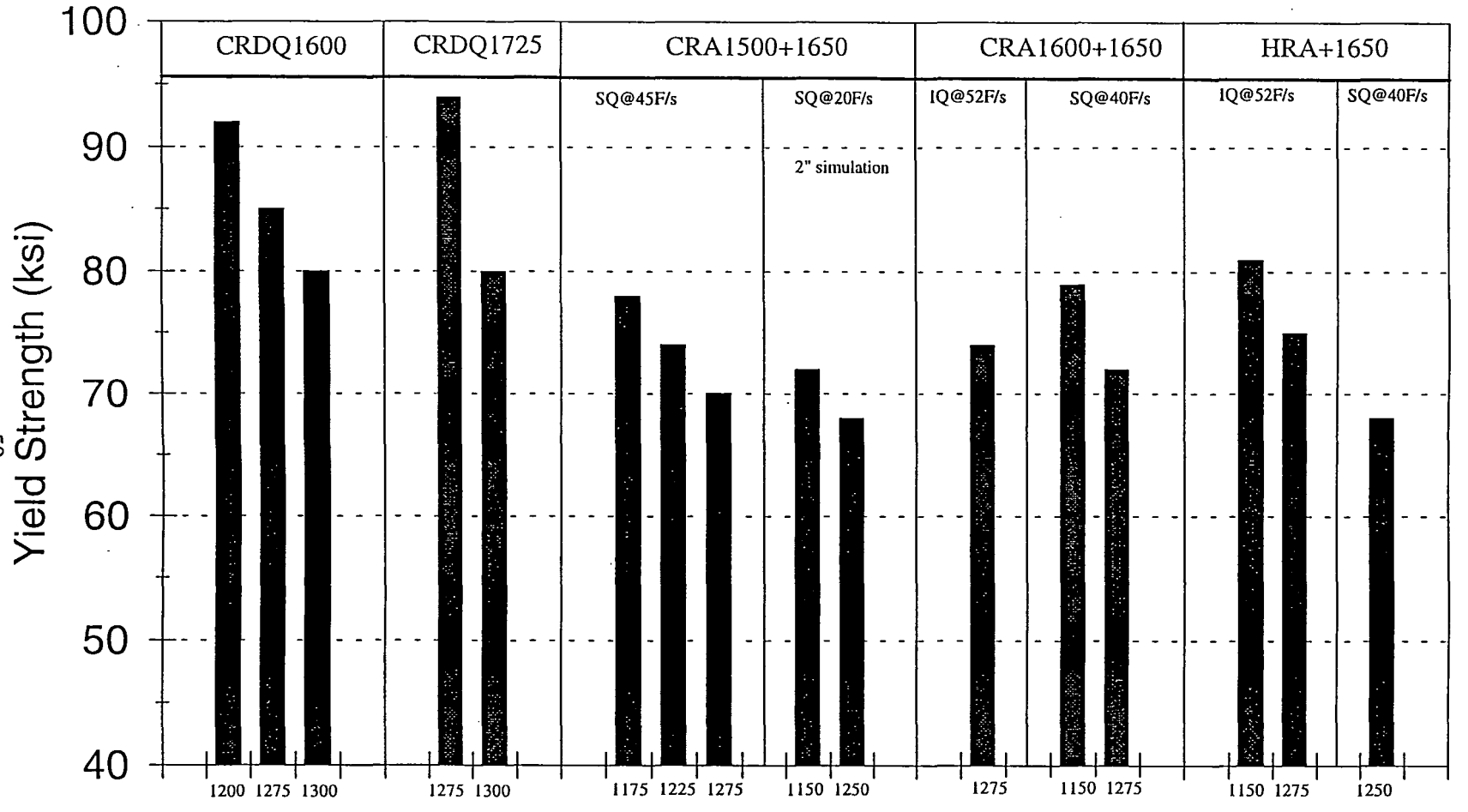


Figure 17 - Steel S yield strength at specified tempering temperatures for all TMCP practices.

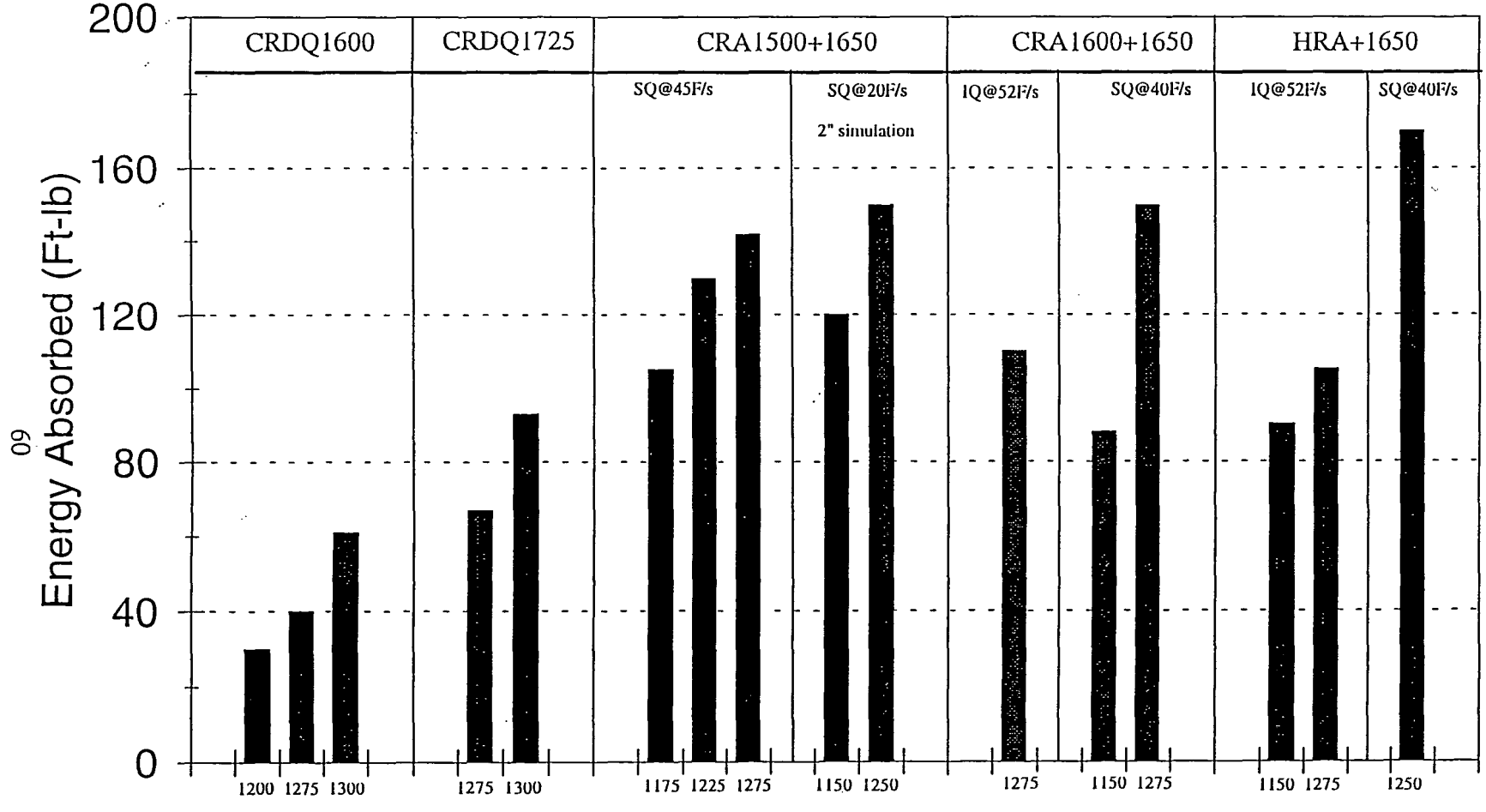


Figure 18 - Steel S -40F Charpy energy at specified tempering temperatures for all TMCP practices.

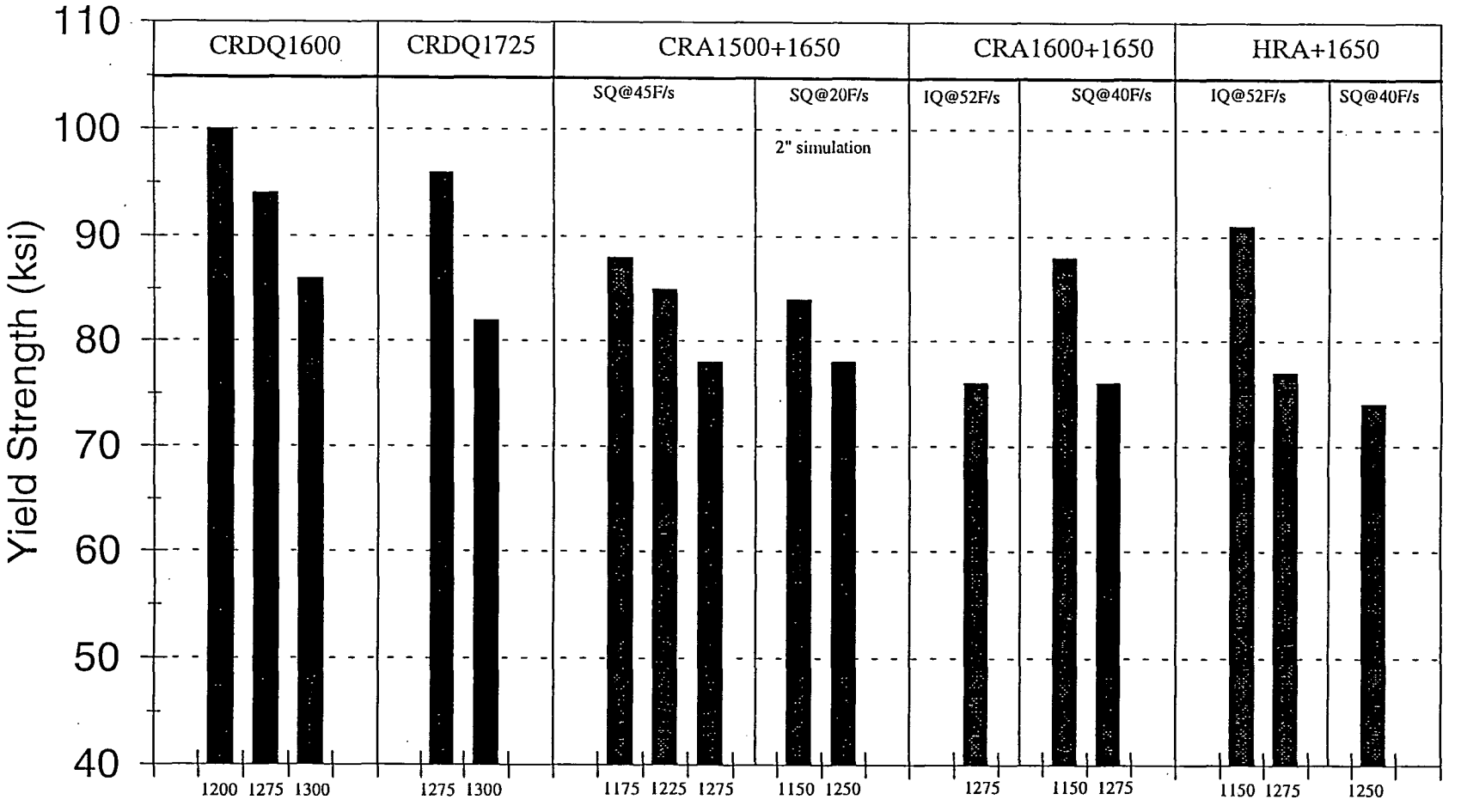


Figure 19 - Steel T yield strength at specified tempering temperatures for all TMCP practices.

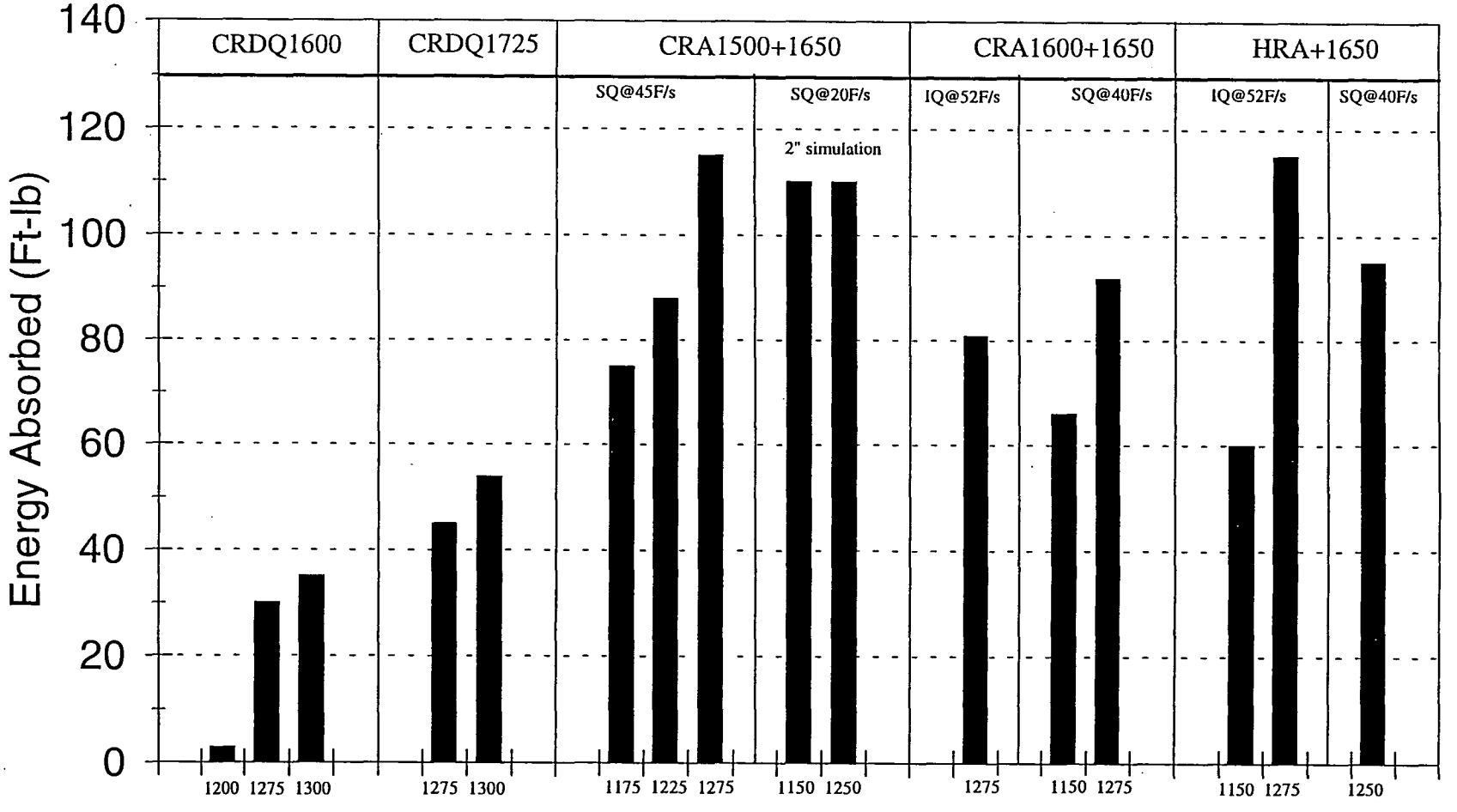


Figure 20 - Steel T -40F Charpy energy at specified tempering temperatures for all TMCP practices.

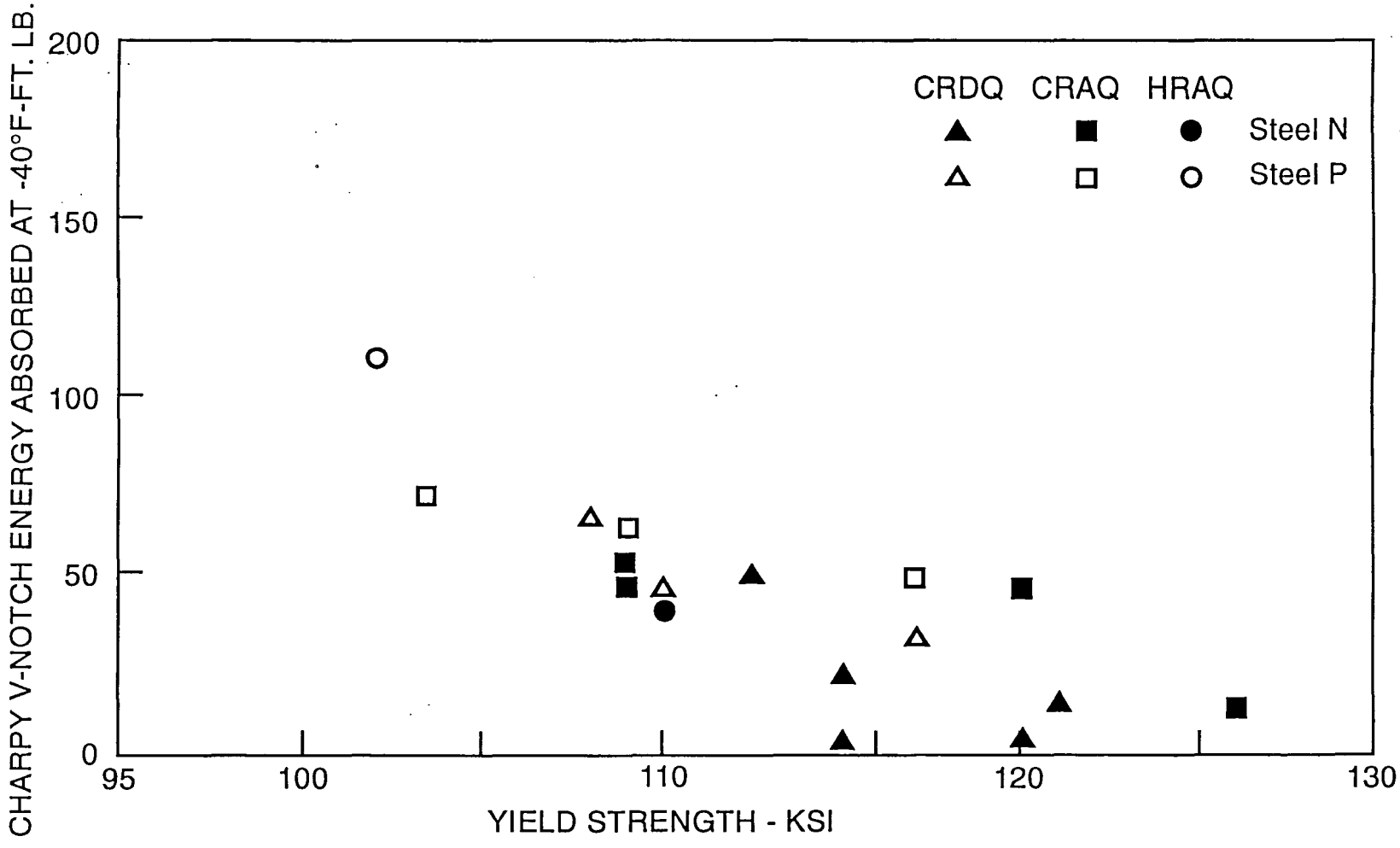


Figure 21 - Relation Between Yield Strength and Toughness for Steels N and P

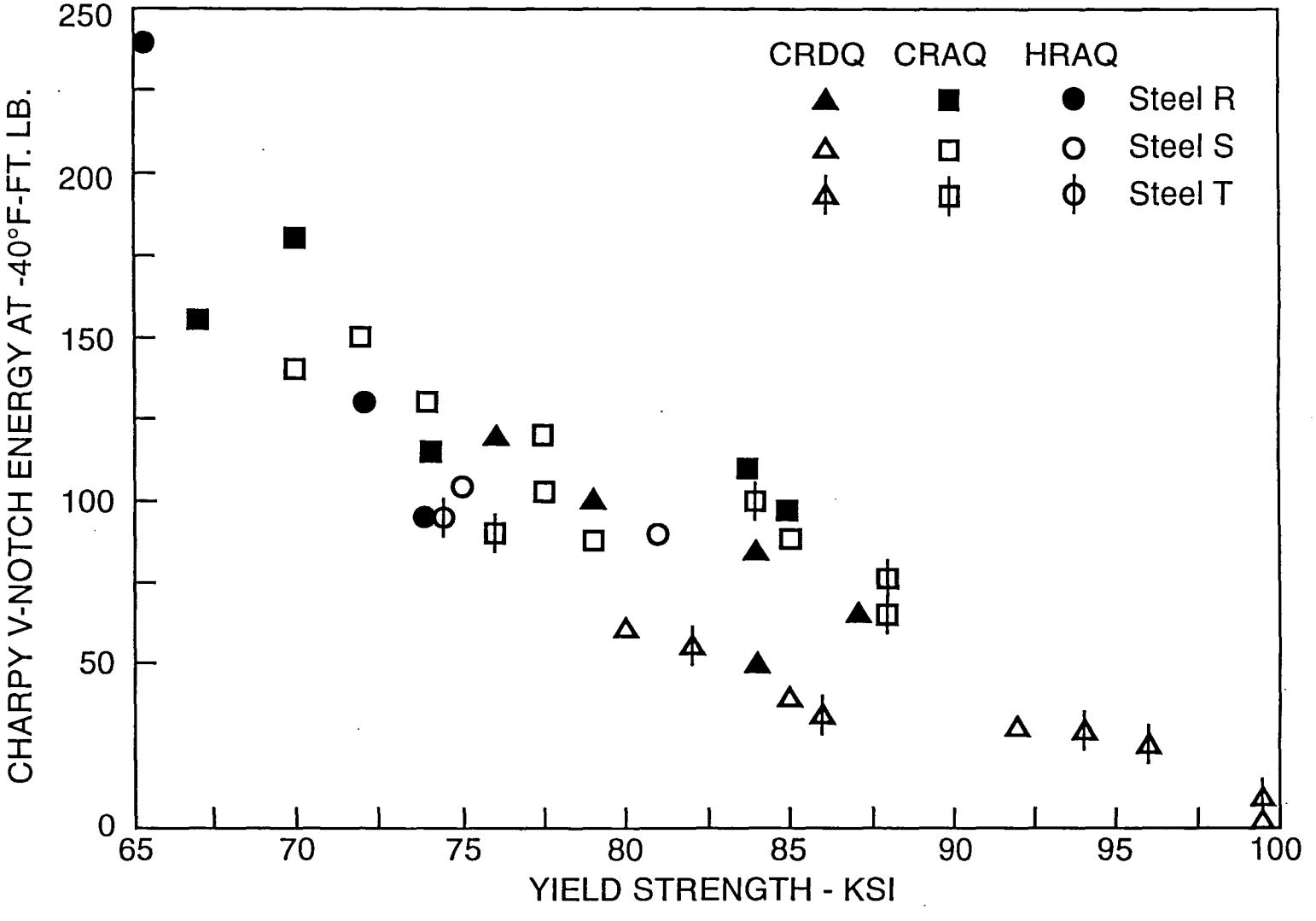


Figure 22 - Relation Between Yield Strength and Toughness for Steels R, S, and T

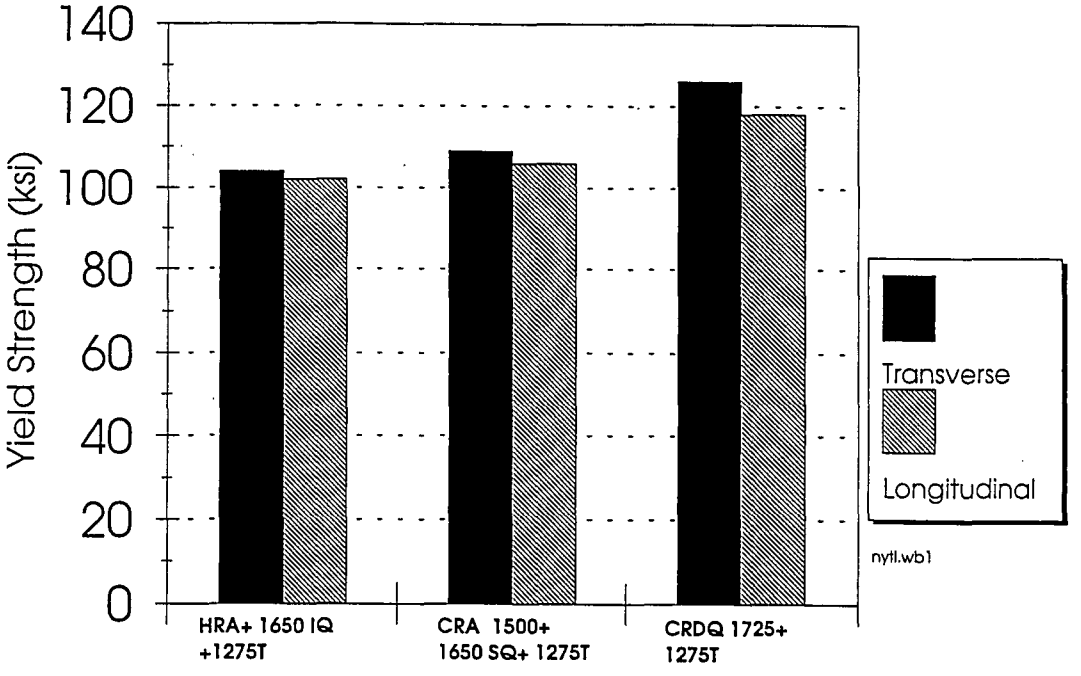


Figure 23 - Steel N: effect of anisotropy on yield strength

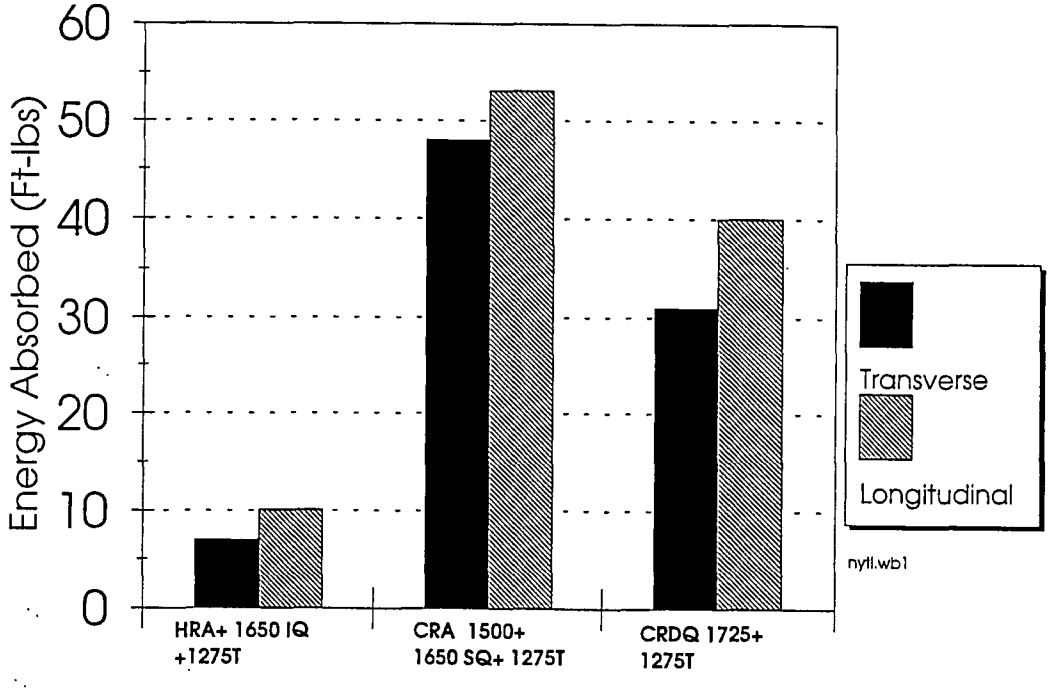


Figure 24 - Steel N: effect of anisotropy on CVN energy at -40 F

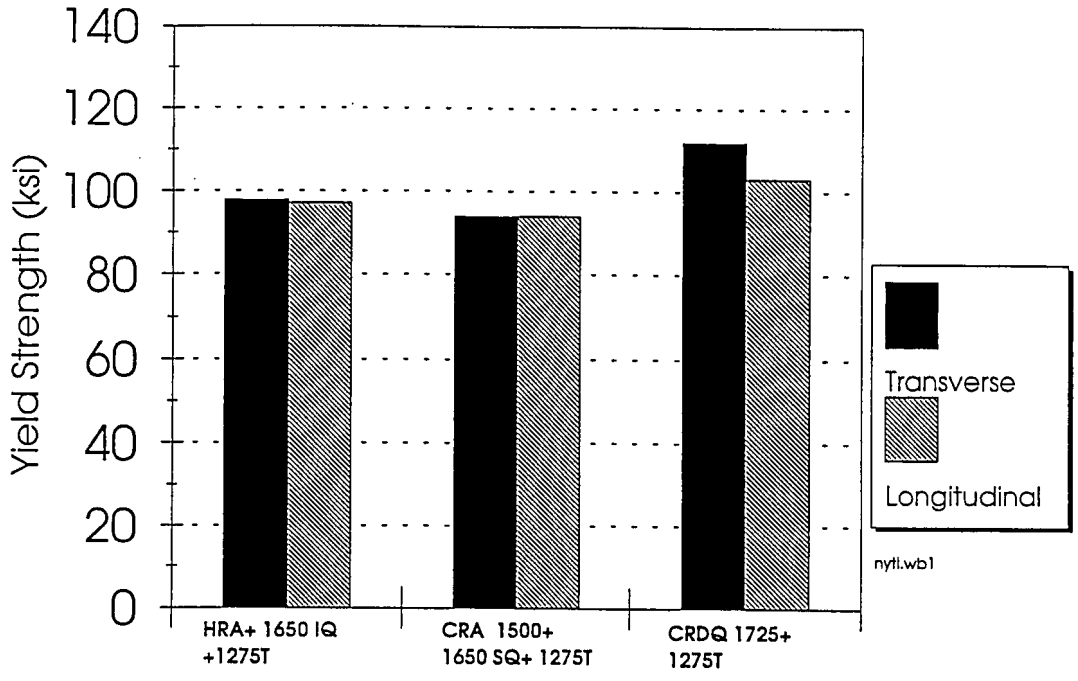


Figure 25 - Steel P: effect of anisotropy on yield strength

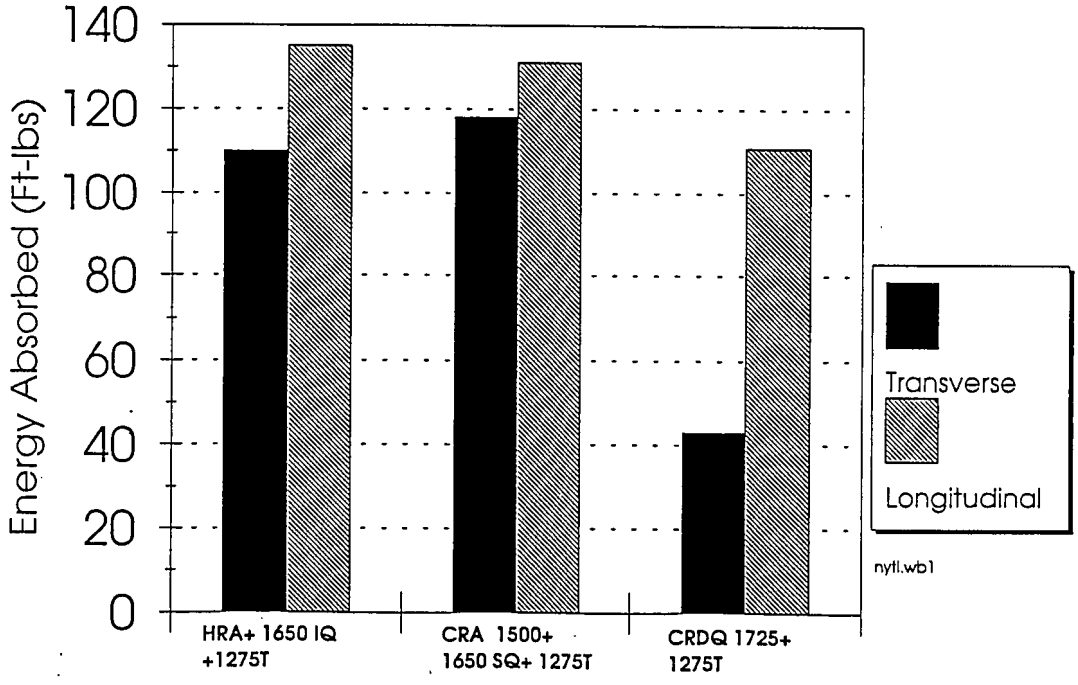


Figure 26 - Steel P: effect of anisotropy on CVN energy at -40 F

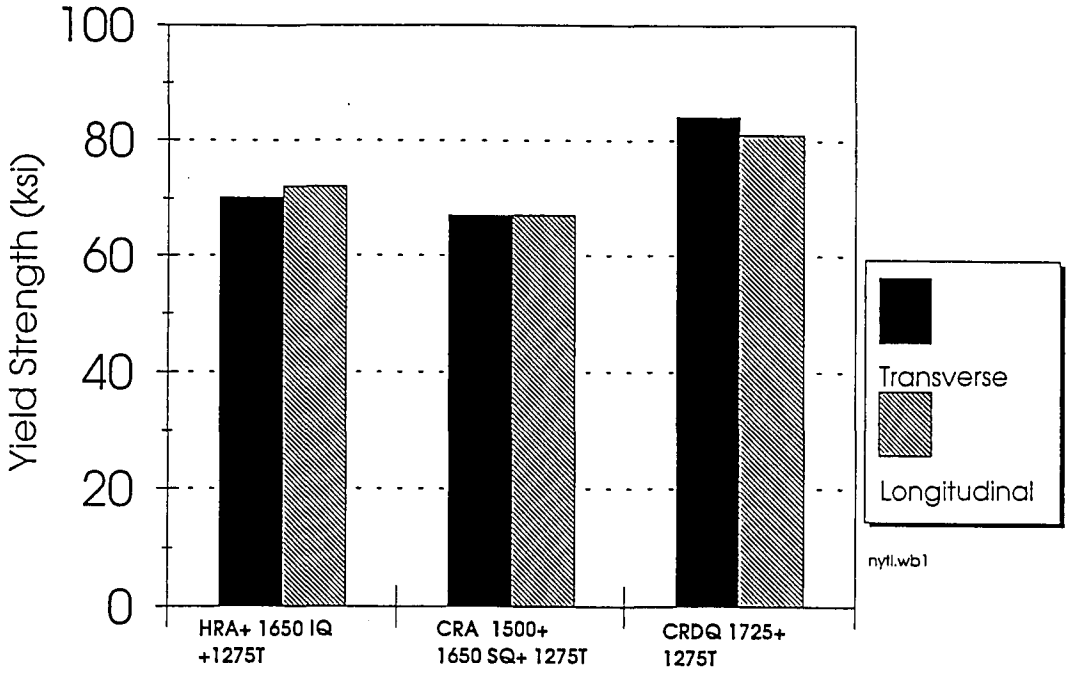


Figure 27 - Steel R: effect of anisotropy on yield strength

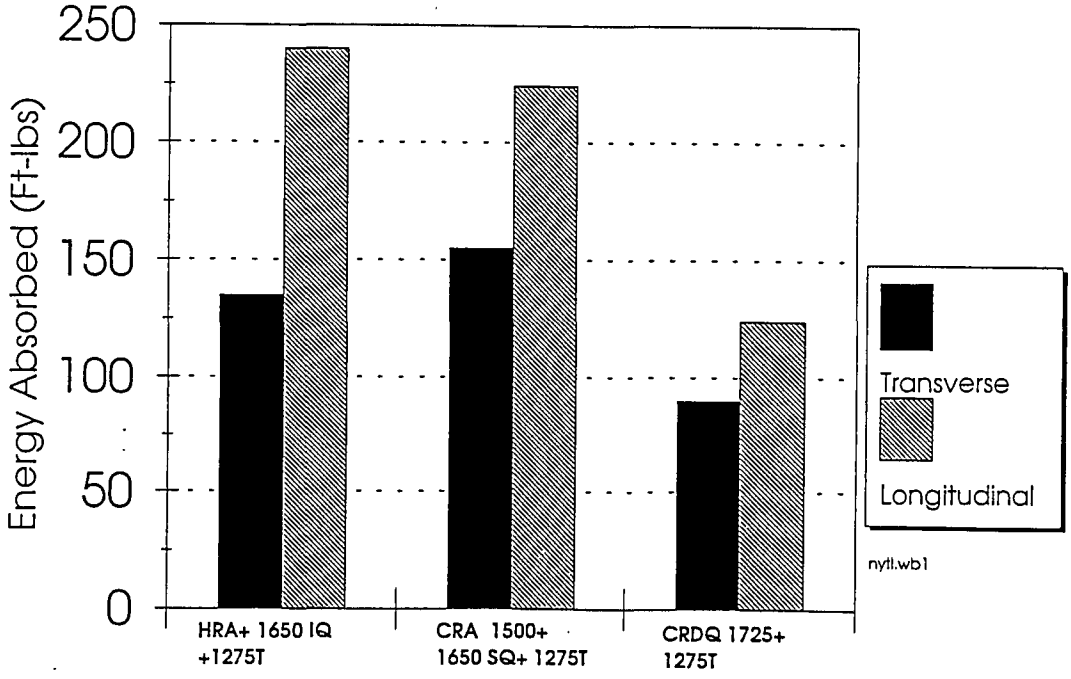


Figure 28 - Steel R: effect of anisotropy on CVN energy at -40 F

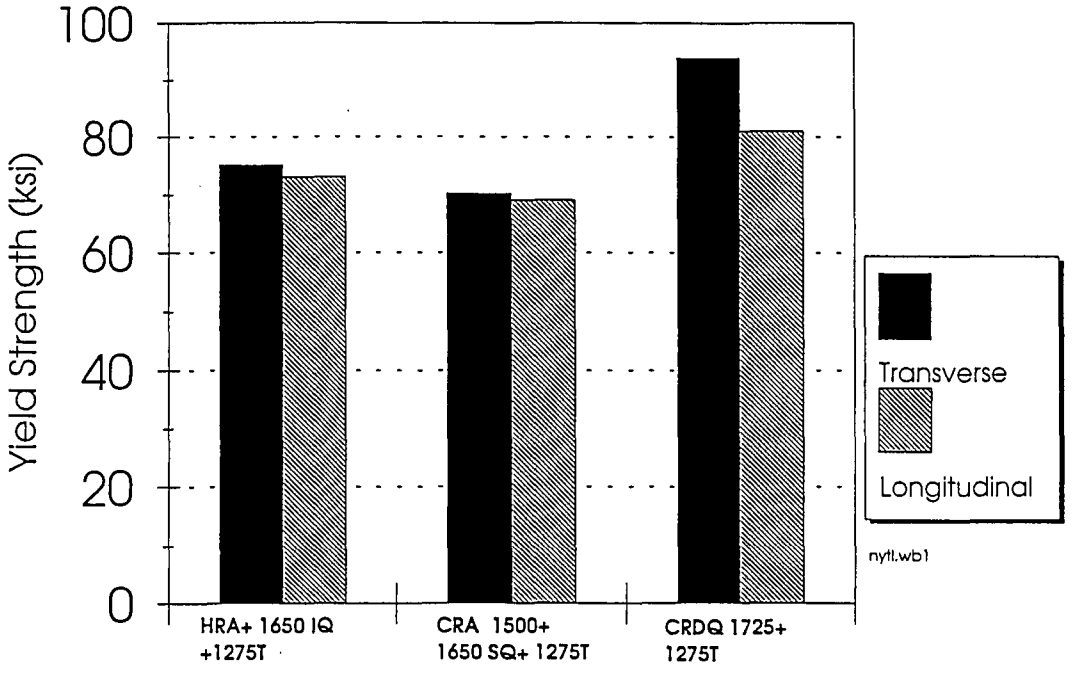


Figure 29 - Steel S: effect of anisotropy on yield strength

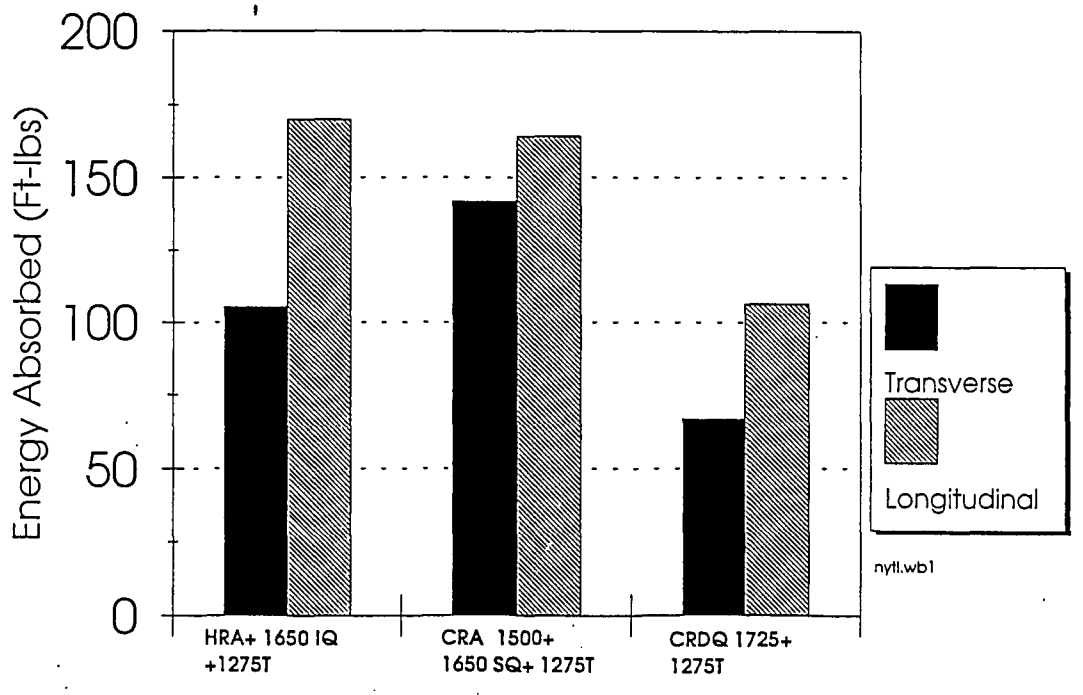


Figure 30 - Steel S: effect of anisotropy on CVN energy at -40 F

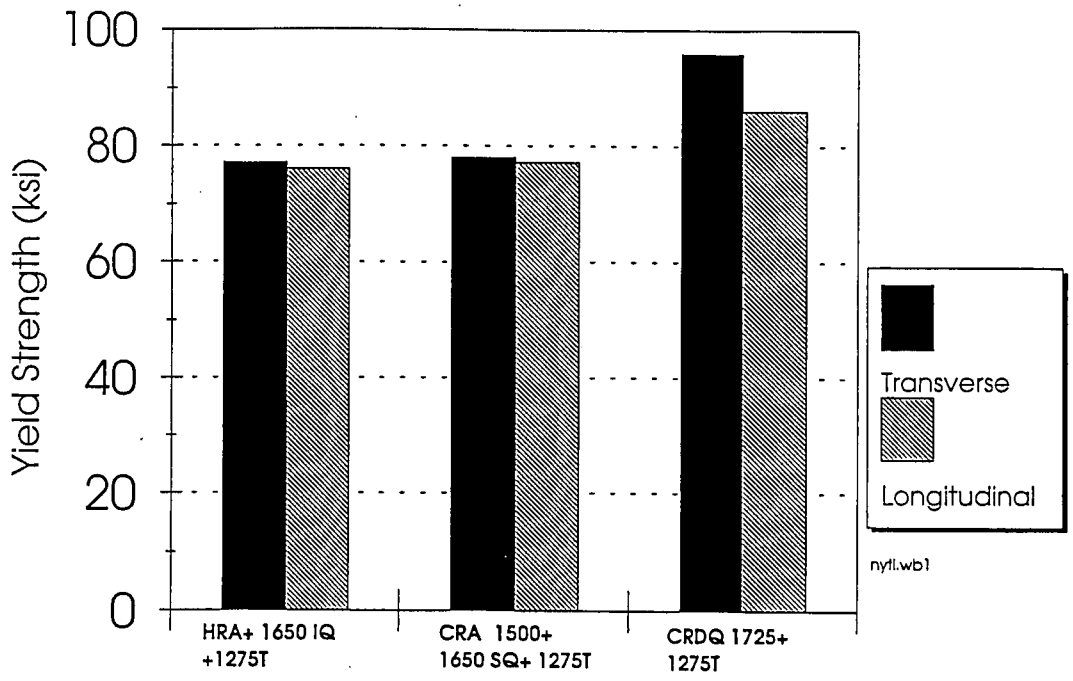


Figure 31 - Steel T: effect of anisotropy on yield strength

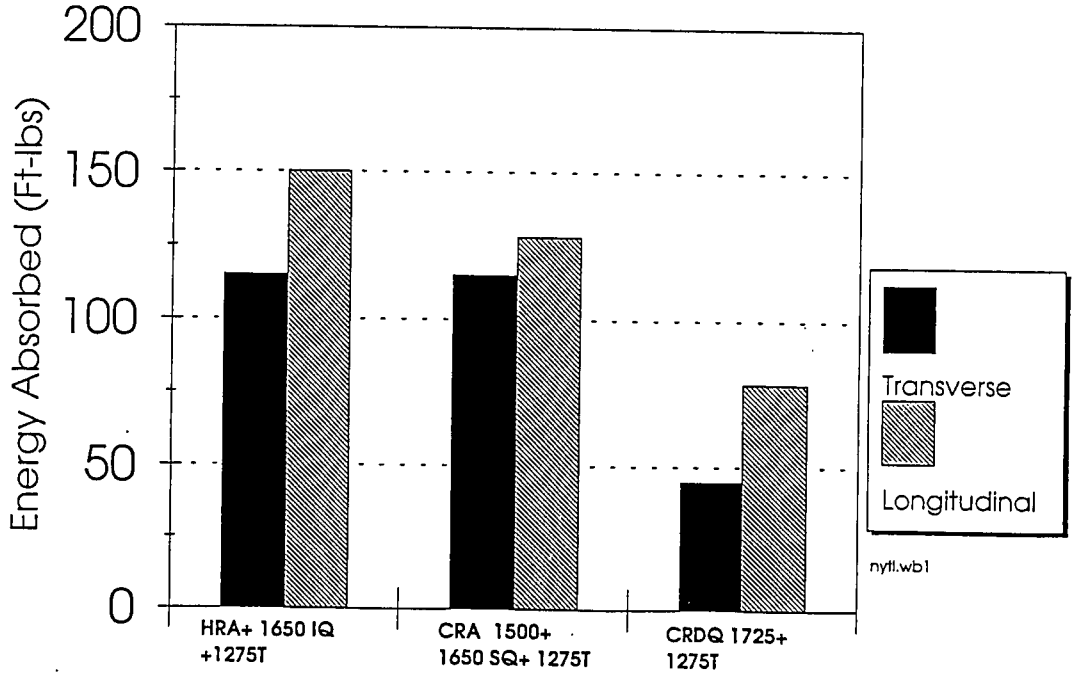


Figure 32 - Steel T: effect of anisotropy on CVN energy at -40 F

Transverse

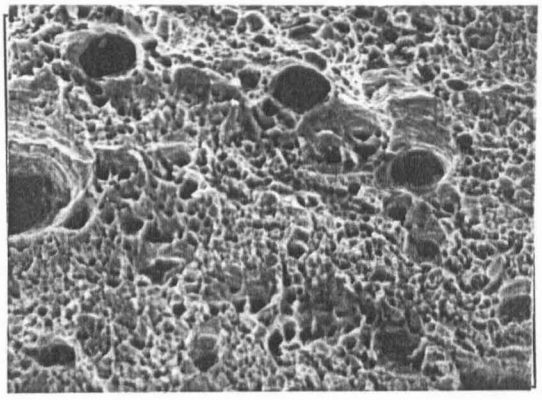

CRDQ 1725 + 1275

Longitudinal

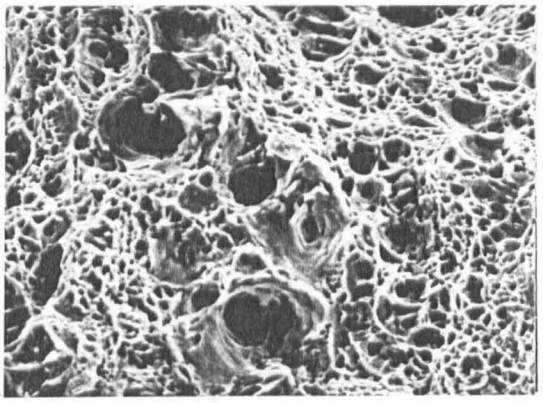

CRDQ 1725 + 1275

Transverse

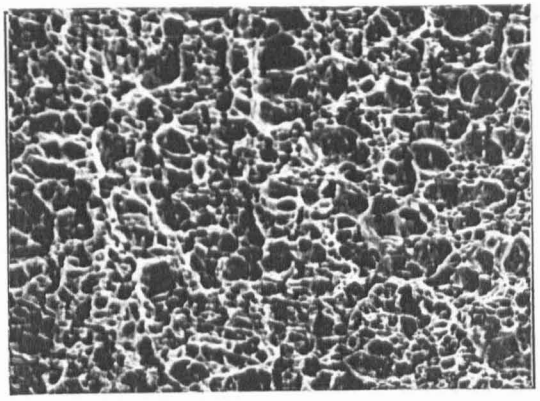

CRAQ 1500 + 1275

X1000

Longitudinal

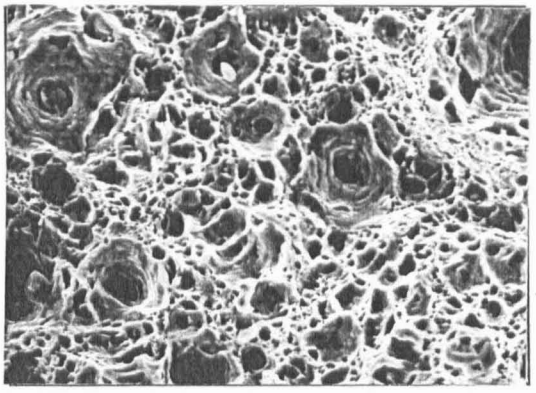

CRAQ 1500 + 1275

Figure 33 - Tensile Specimen Fracture Appearance of Steel N

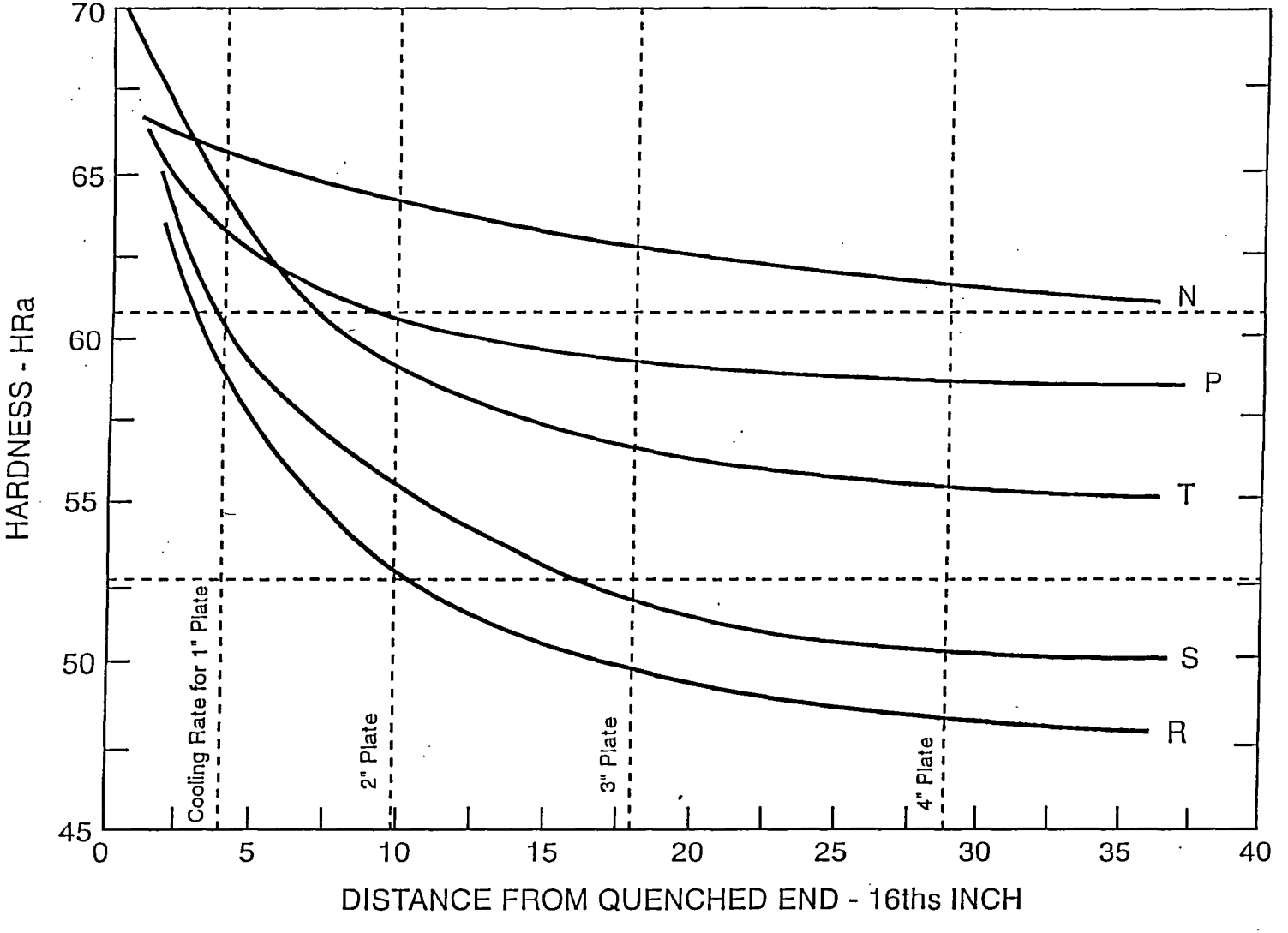


Figure 34 - Jominy end-quench curves for Steels N, P, R, S, and T

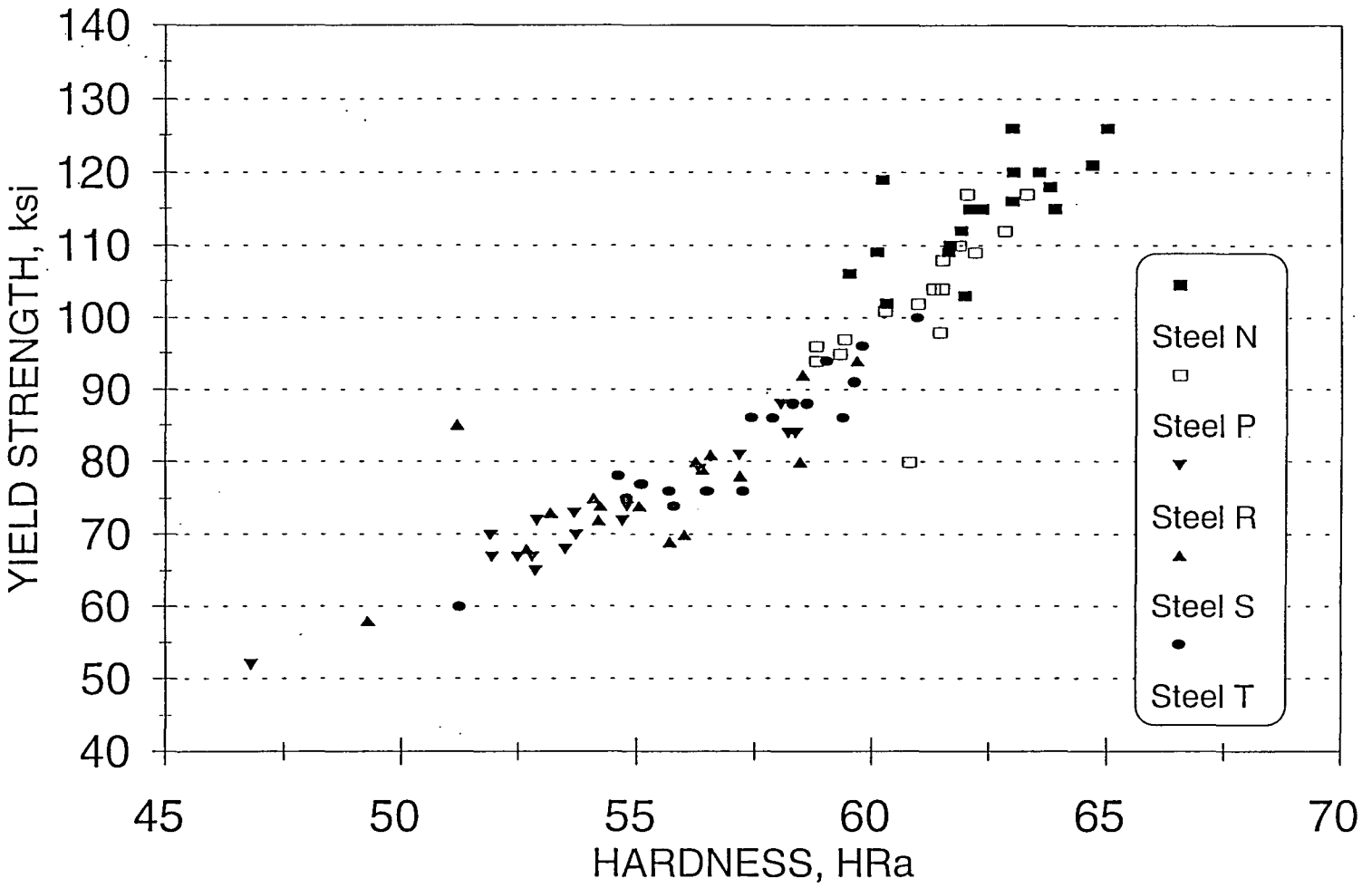


Figure 35 - Yield strength-hardness relationships

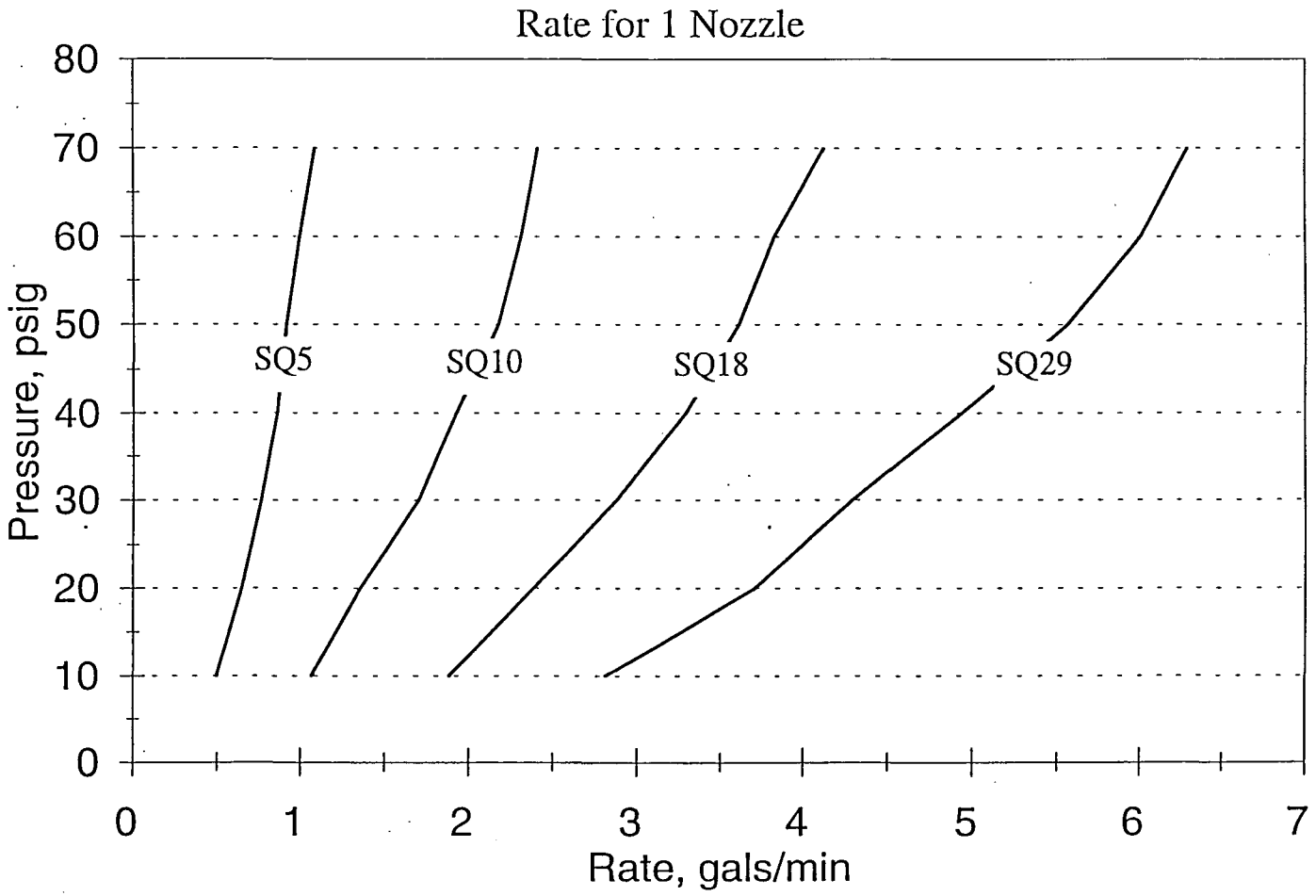


Figure 36 - Spray quench nozzle calibration

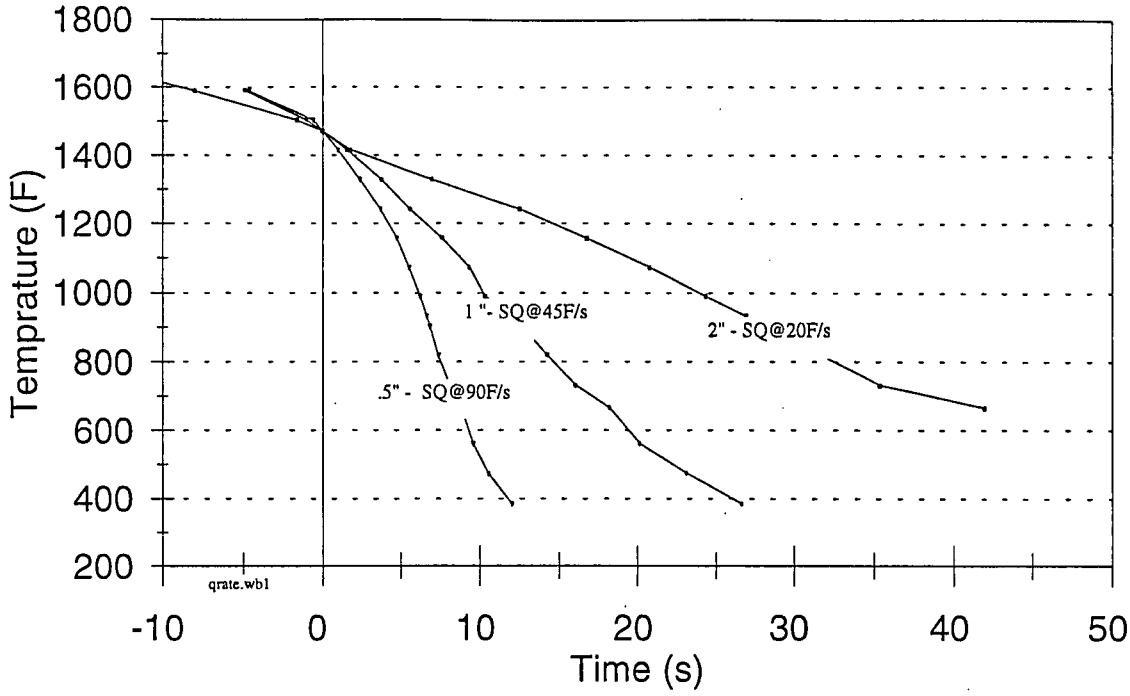


Figure 37 - Spray quenching curves for 0.5, 1, and 2 inch plates

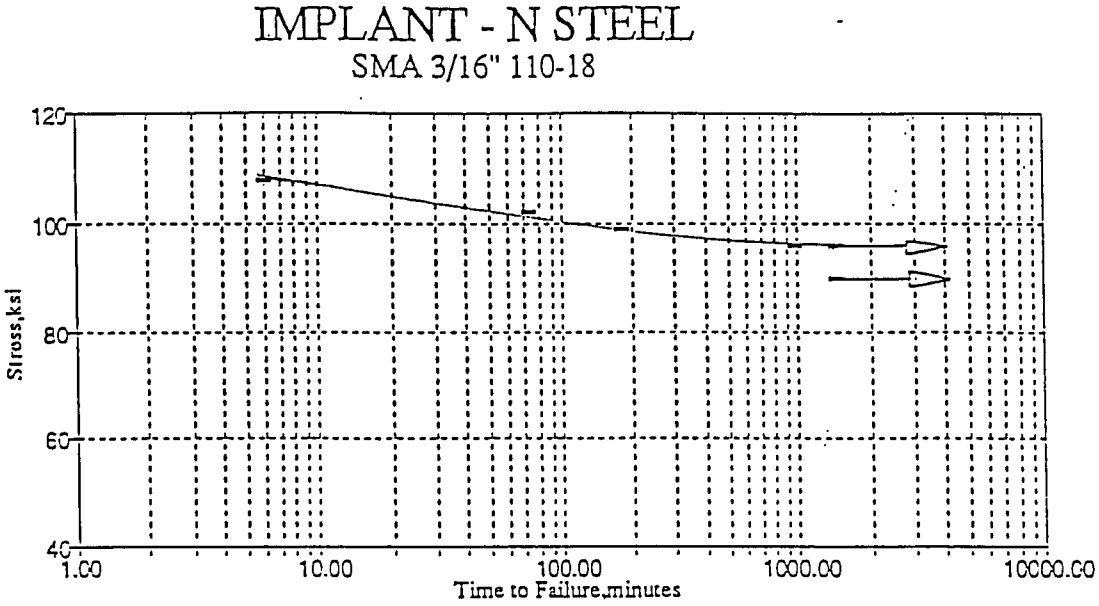


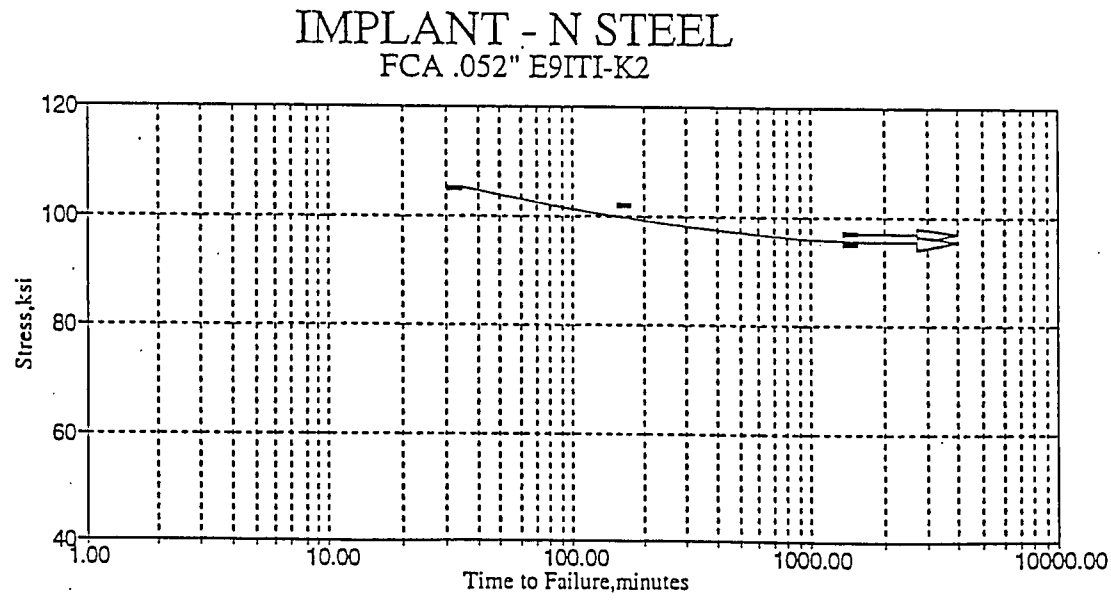


Figure 38 - Steel N implant results - SMAW and FCAW

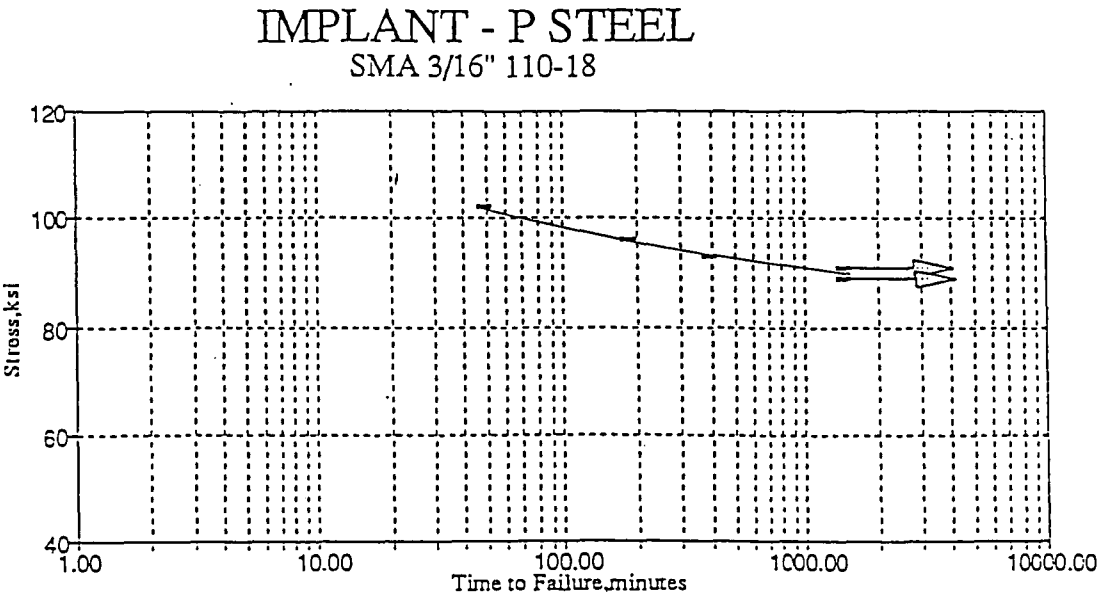


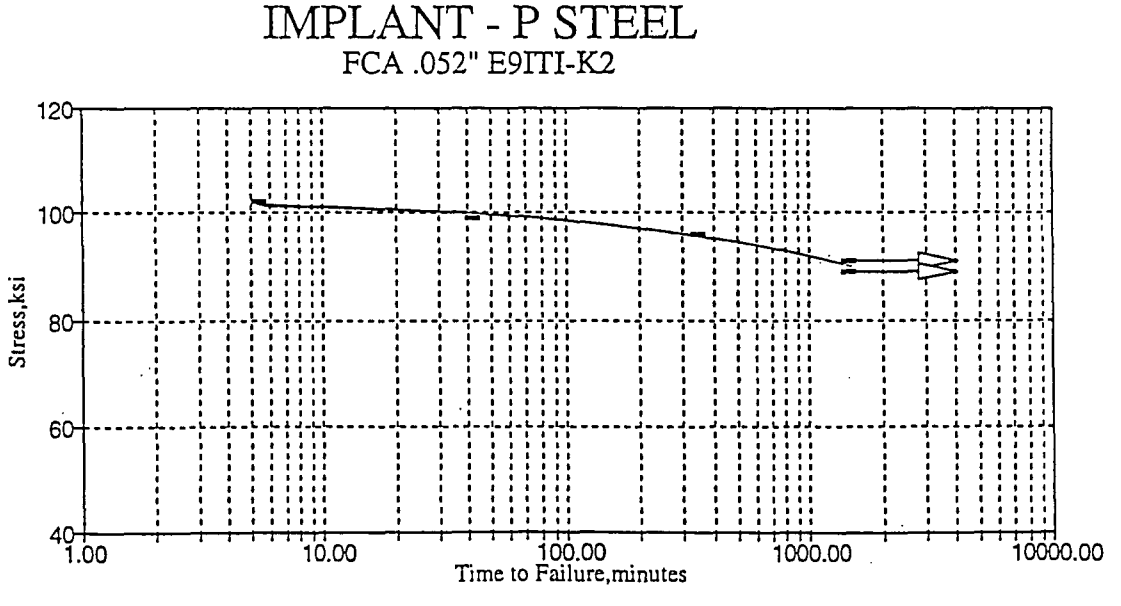


Figure 39 - Steel P implant results - SMAW and FCAW

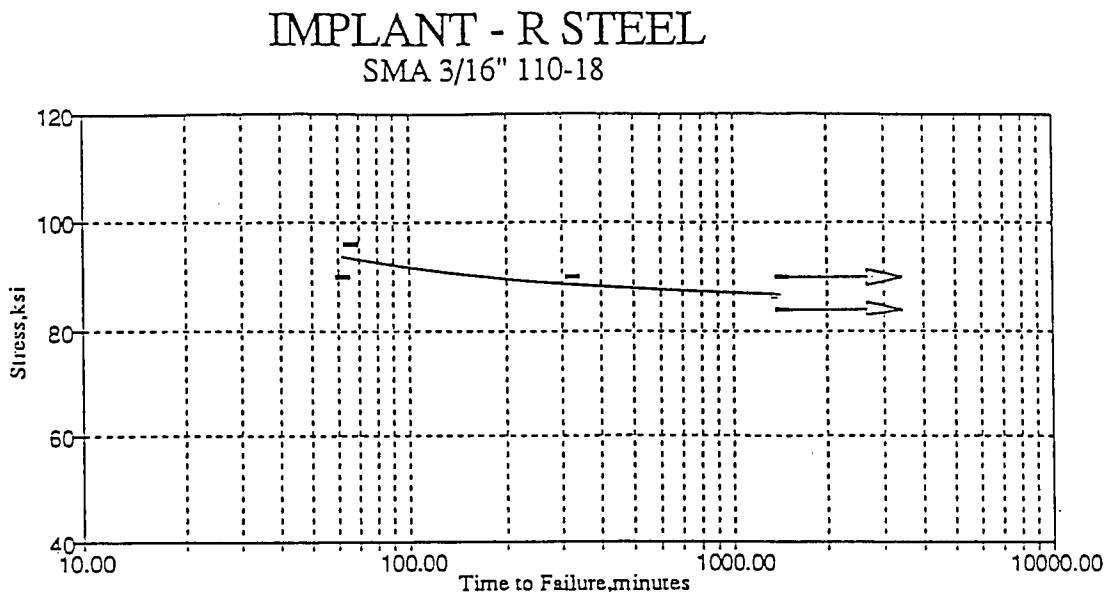


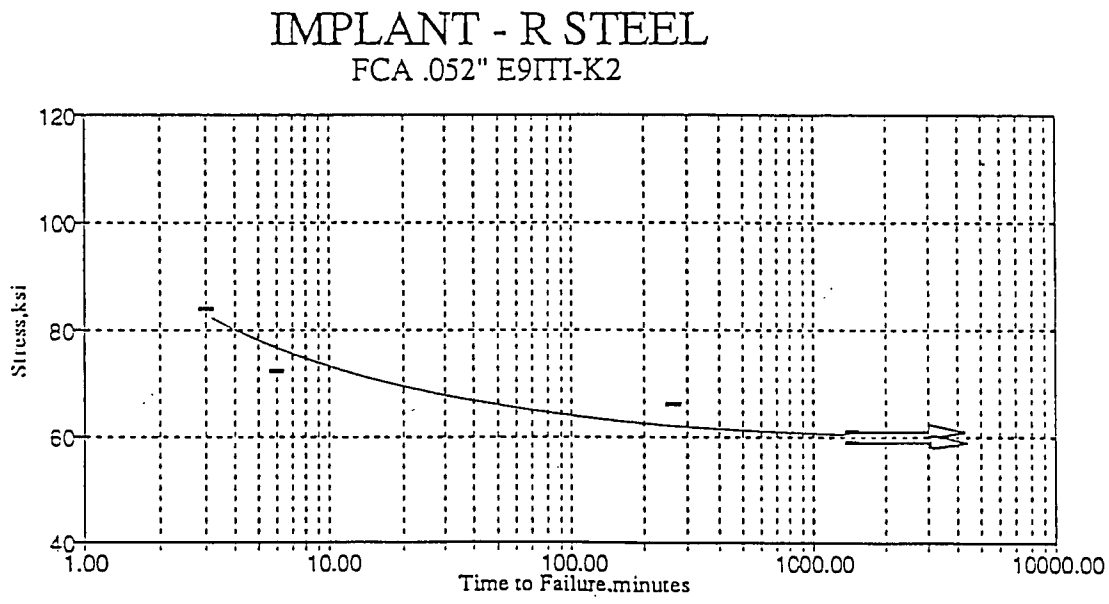


Figure 40 - Steel R implant results - SMAW and FCAW

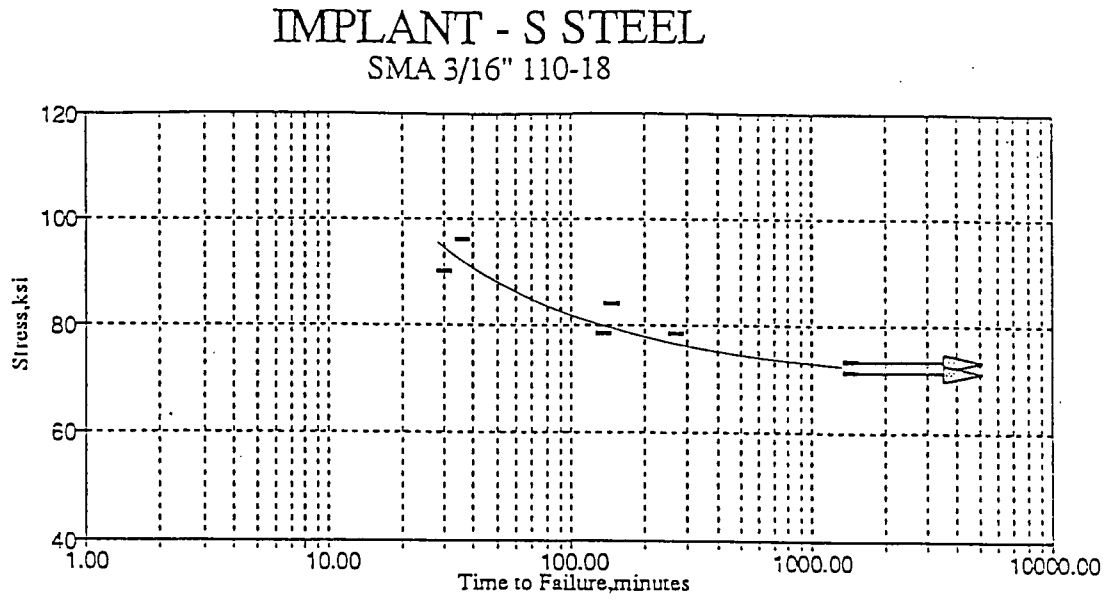


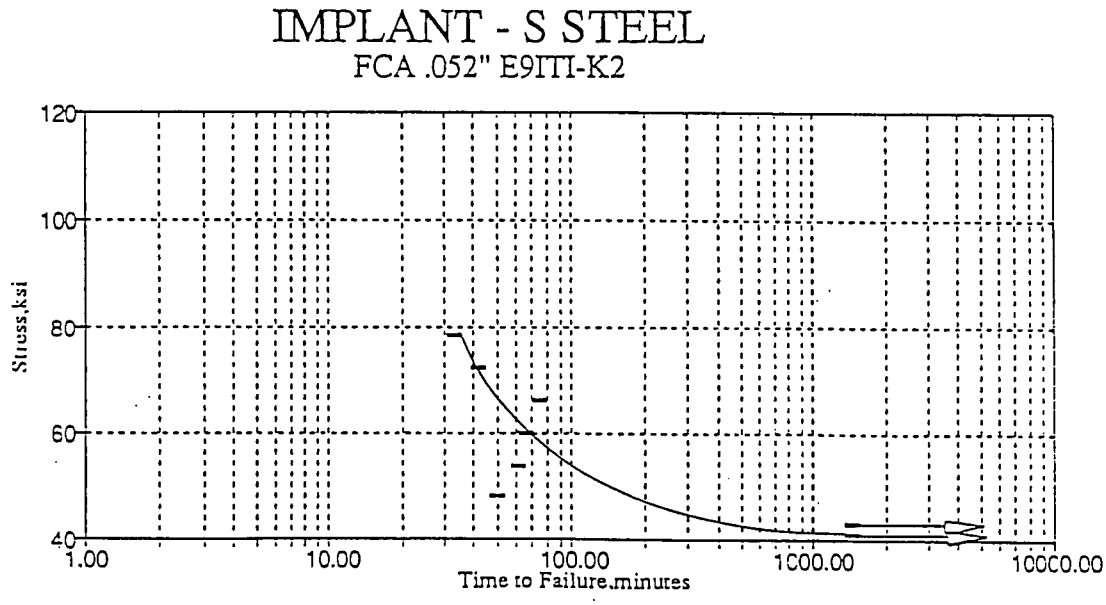


Figure 41 - Steel S implant results - SMAW and FCAW

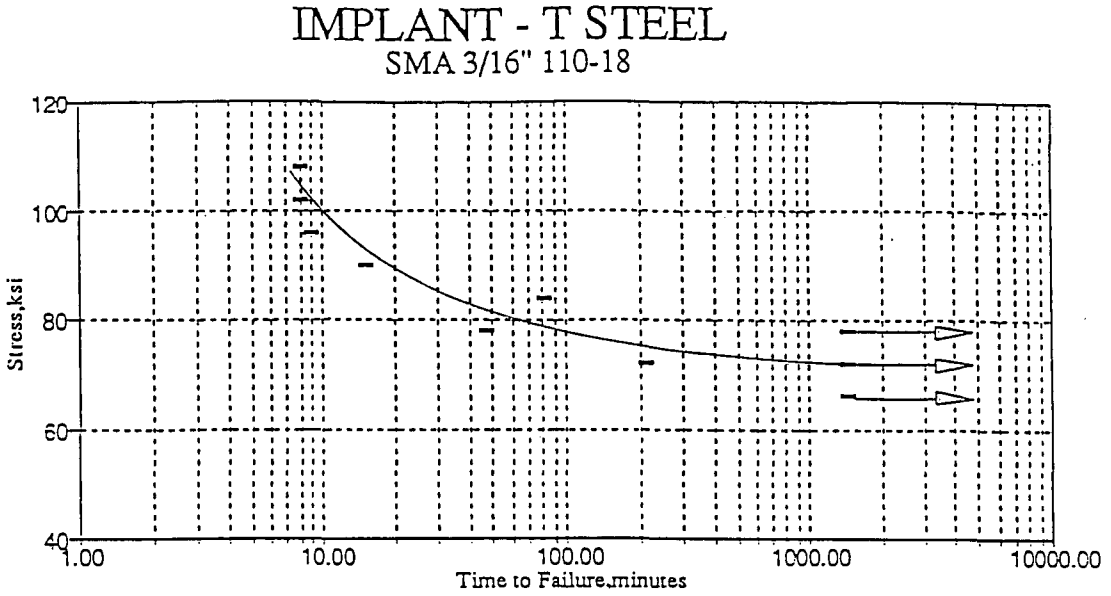


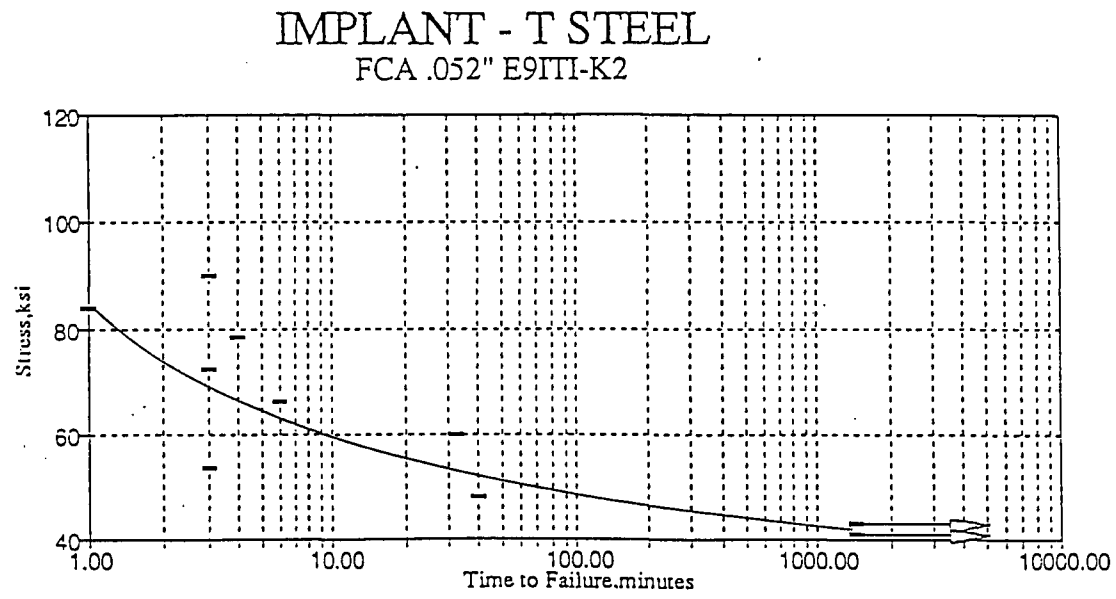


Figure 42 - Steel T implant results - SMAW and FCAW

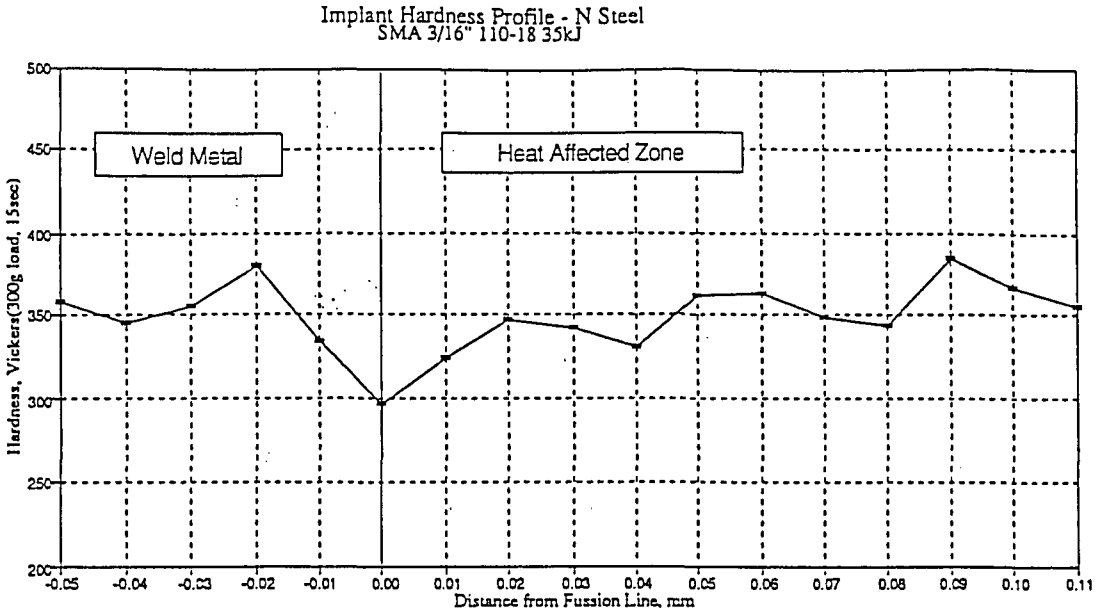


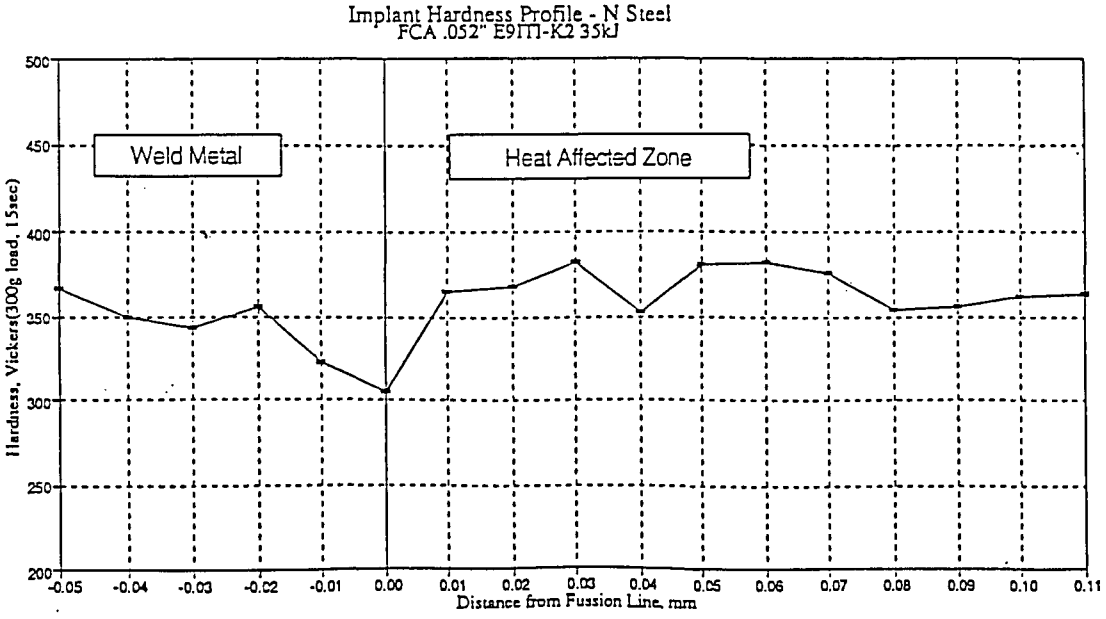


Figure 43 - Steel N implant hardness profile - SMAW and FCAW

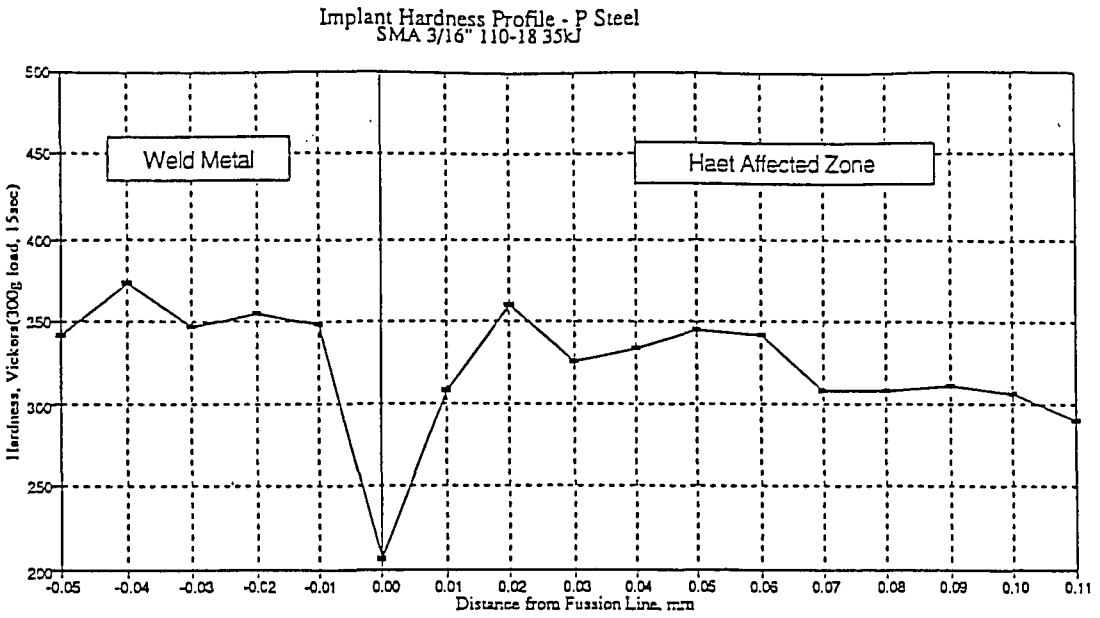


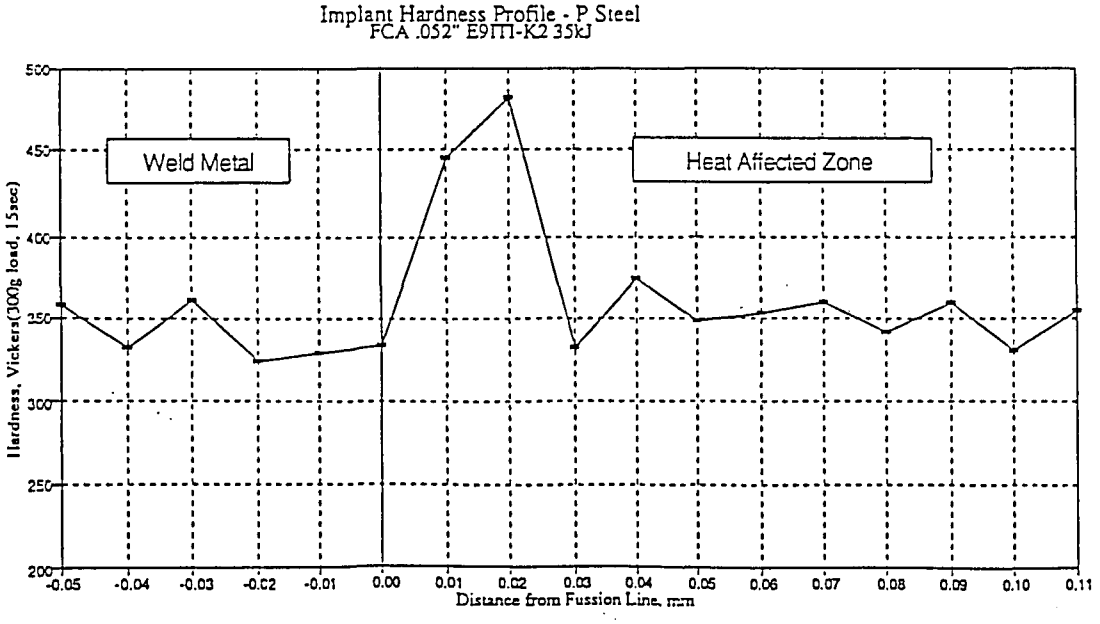


Figure 44 - Steel P implant hardness profile - SMAW and FCAW

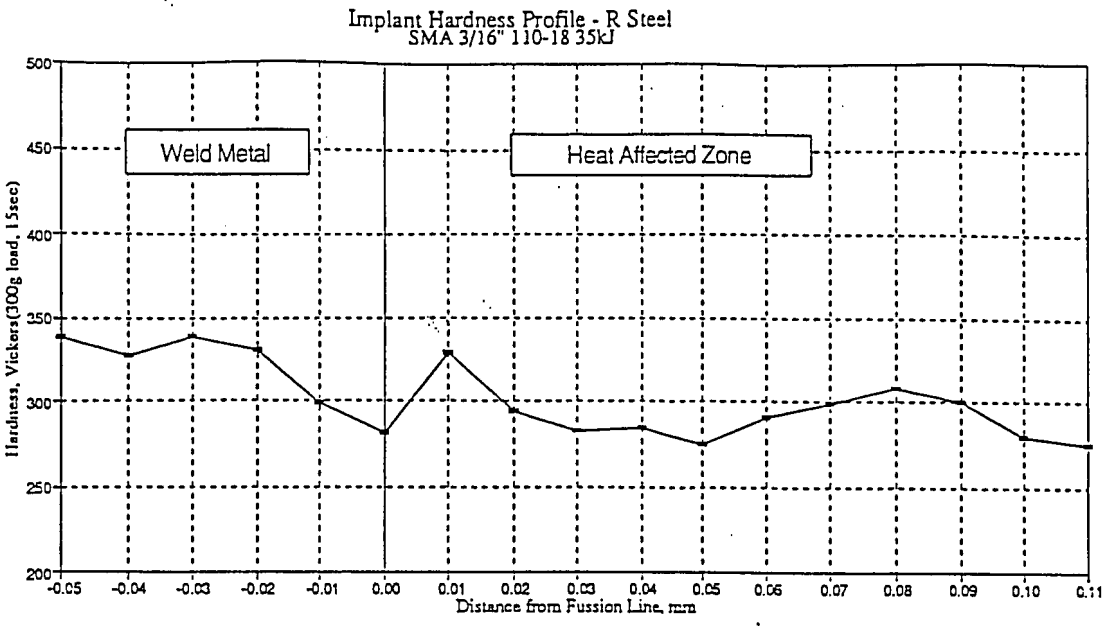


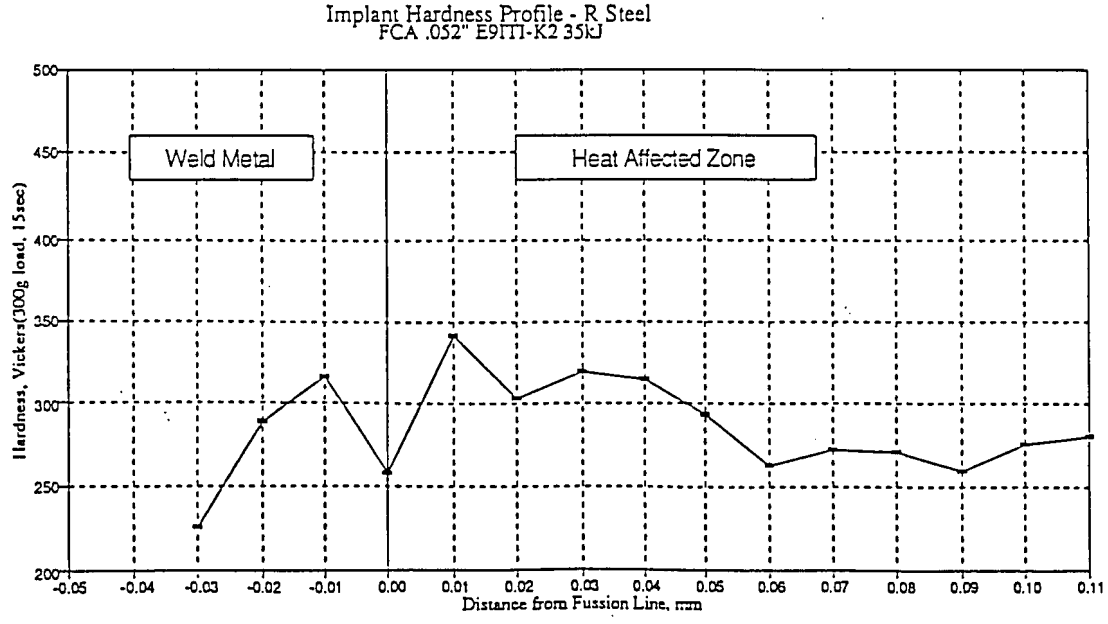


Figure 45 - Steel R implant hardness profile - SMAW and FCAW

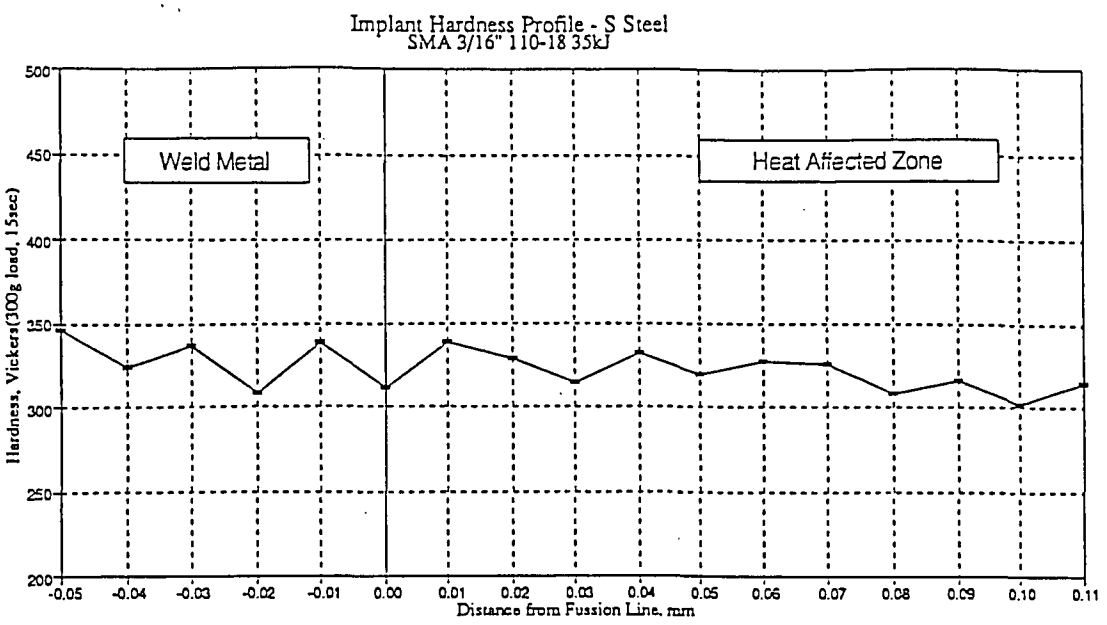


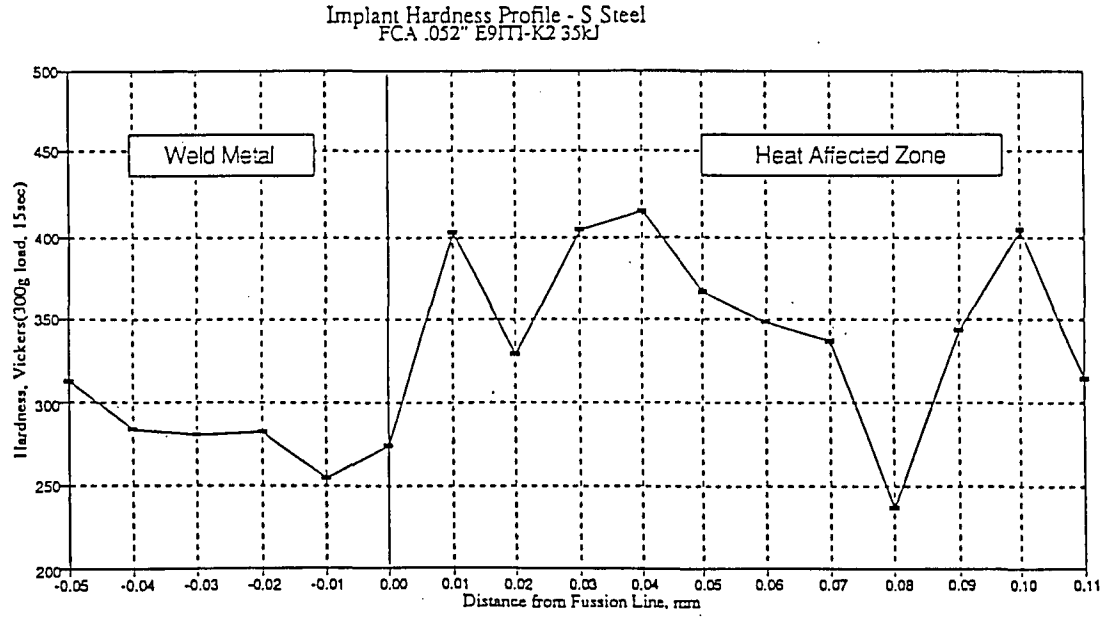


Figure 46 - Steel S implant hardness profile - SMAW and FCAW

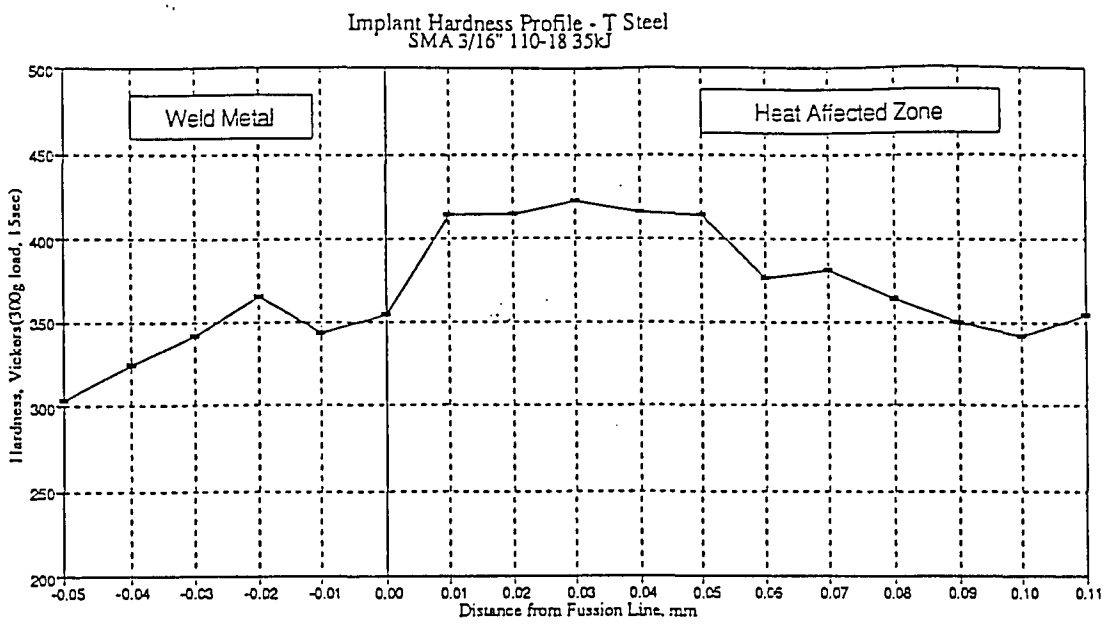


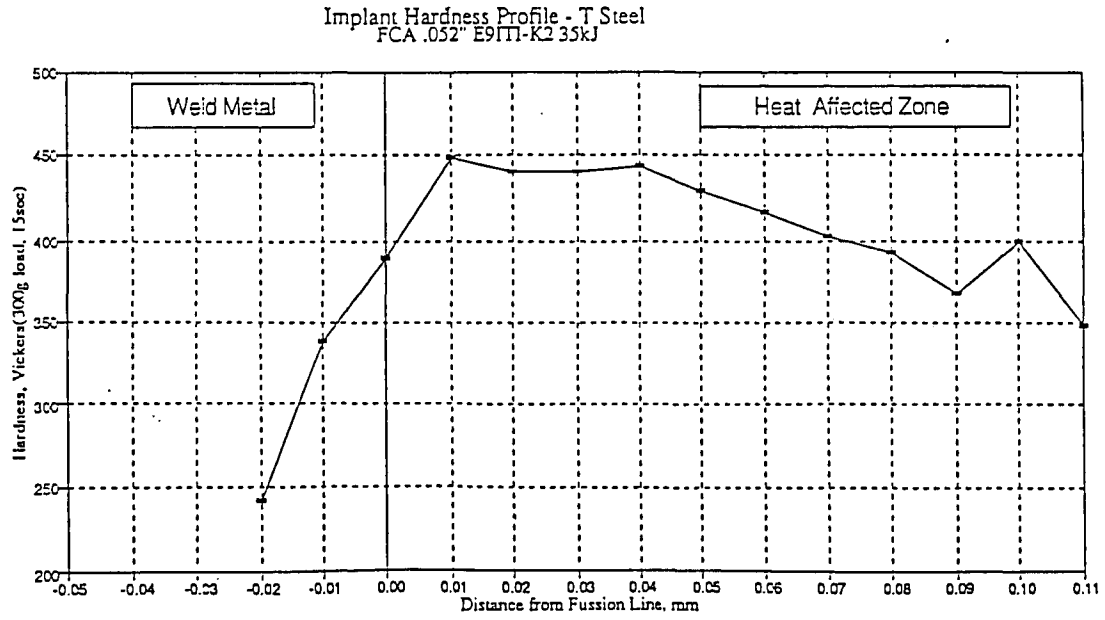


Figure 47 - Steel T implant hardness profile - SMAW and FCAW

Steel N

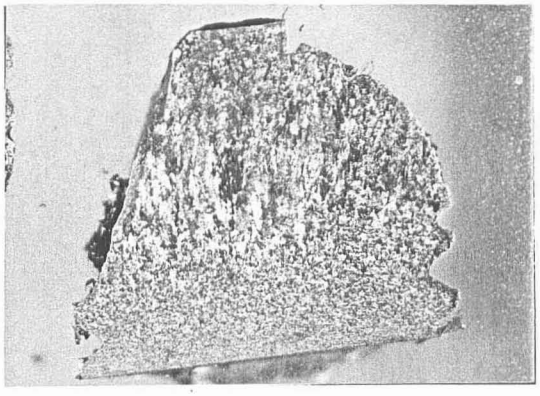

SMAW

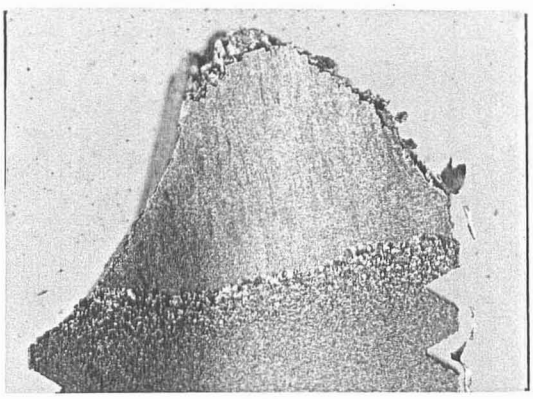

FCAW

Steel P

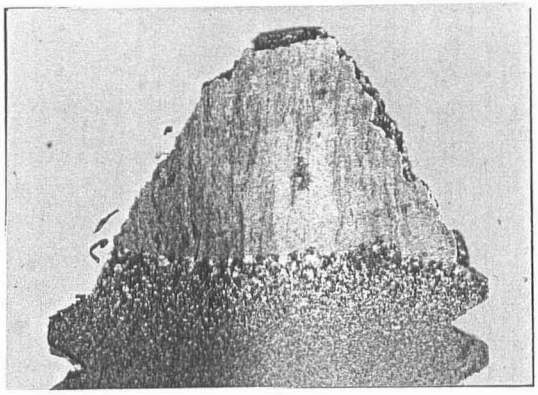

SMAW

Nital-Picral X10

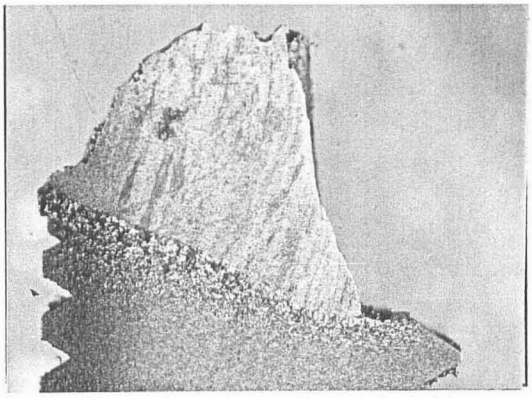

FCAW

Figure 48 - Implant cross section micrographs of Steels N and P

Steel R

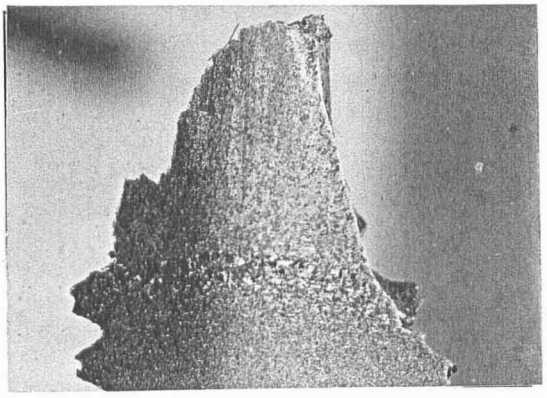

SMAW

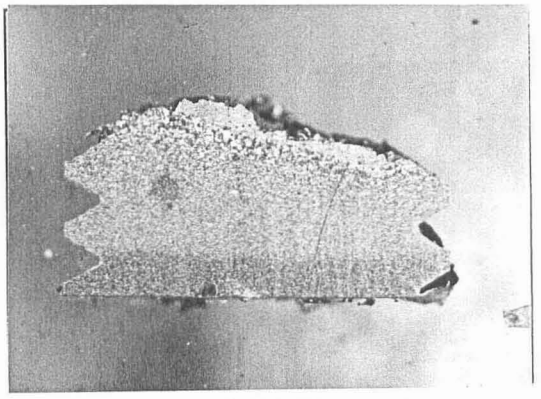

FCAW

Steel S

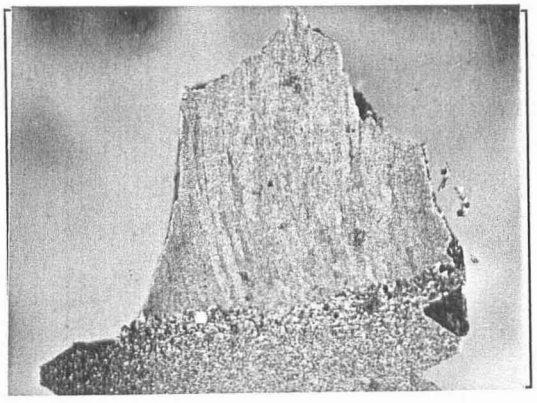

SMAW

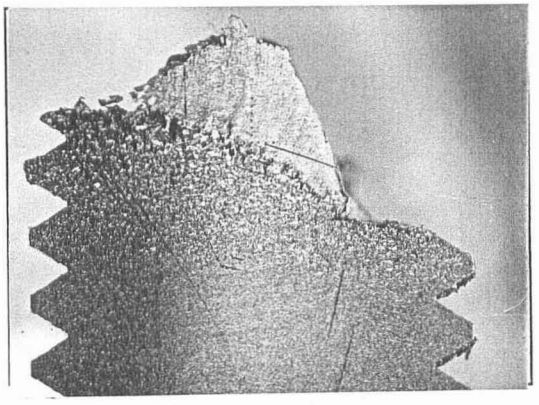

FCAW

Steel T

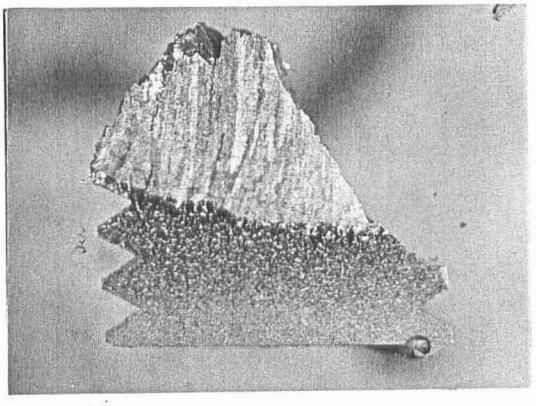

SMAW

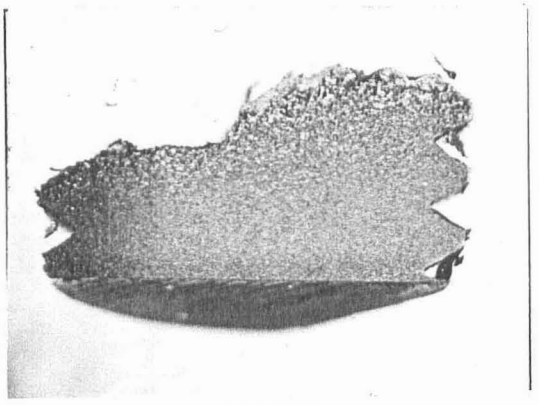

FCAW

Nital-Picral X10

Figure 49 - Implant cross section micrographs of Steels R, S, and T

a.

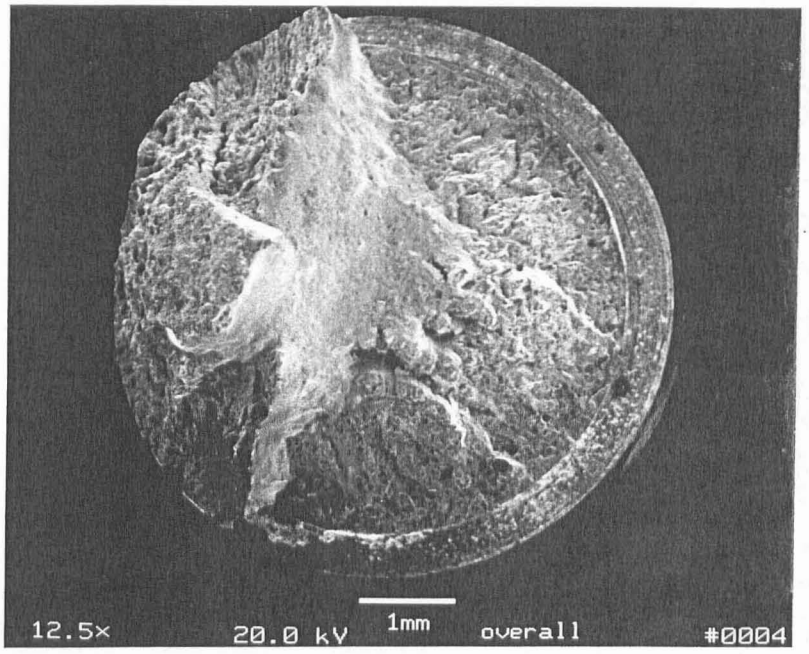


b.

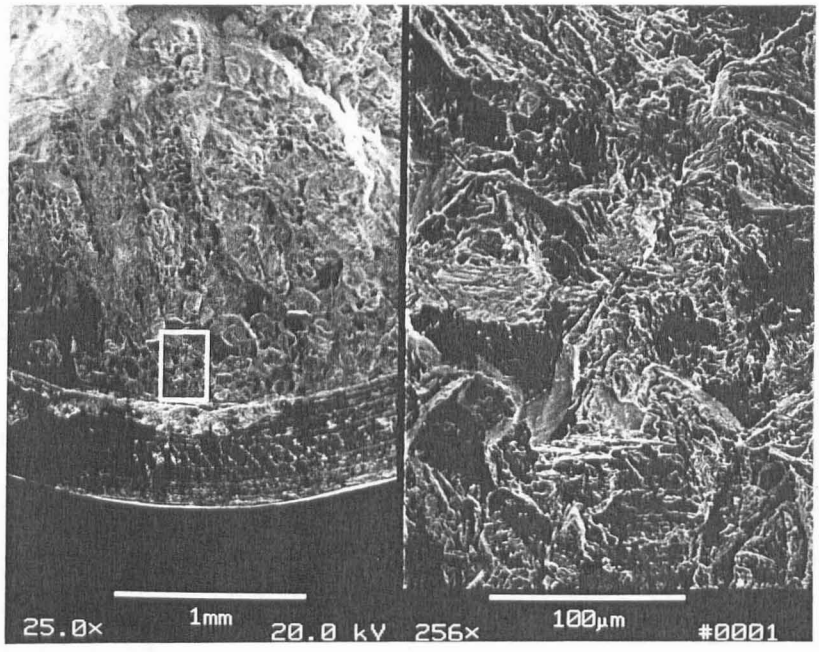


Figure 50 - Implant specimen fracture morphology of Steel R:
a. Overall view of fracture surface
b. Initiation site with intergranular fracture

c.

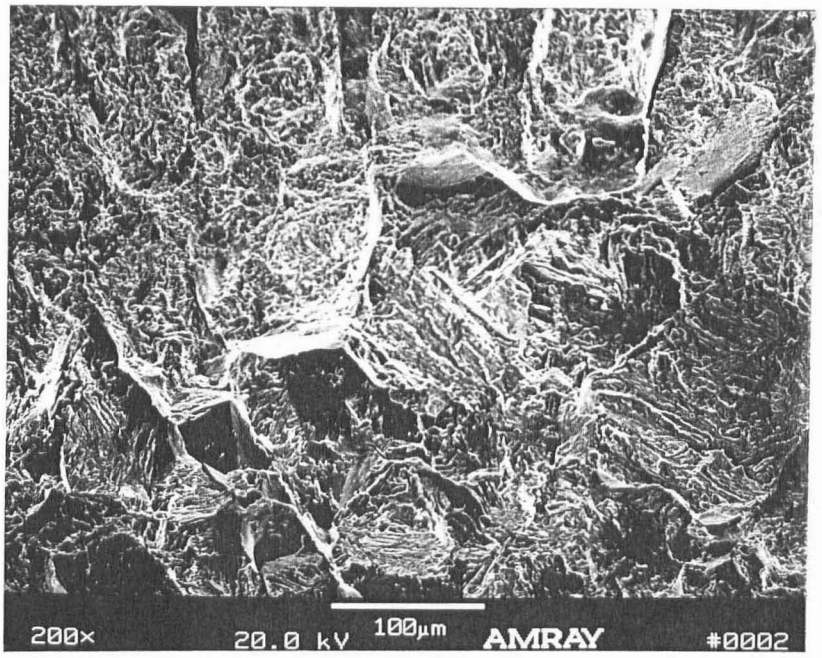


d.

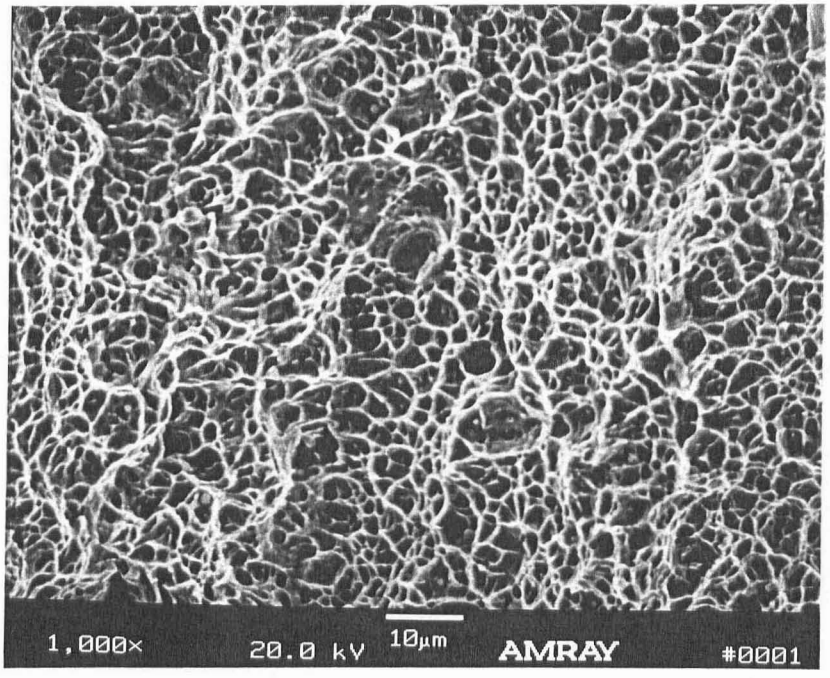


Figure 51 - Implant specimen fracture morphology of Steel R:
c. Intergranular crack propagation region
d. Area of final failure - ductile microvoid coalescence

Steel N

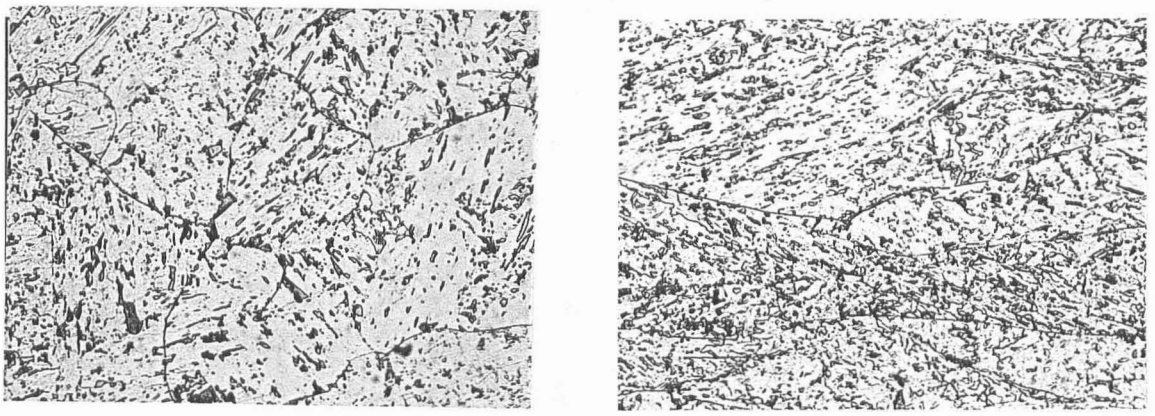

HRA 1900 CRA 1500

Steel P

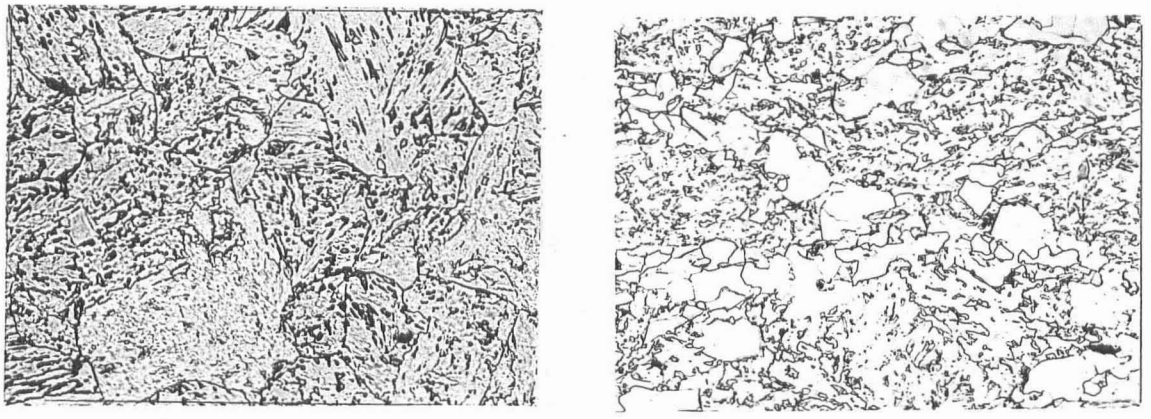

HRA 1900 Nital-Picral X400 CRA 1500

Figure 52 - Micrographs of Steels N and P, Hot-Rolled or Control-Rolled and Air Cooled

Steel R

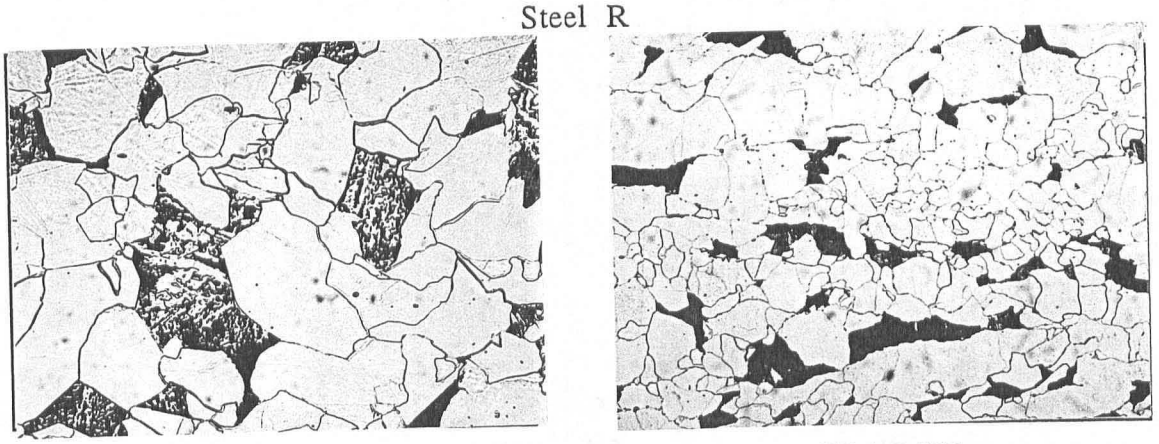

HRA 1900 CRA 1500

Steel S

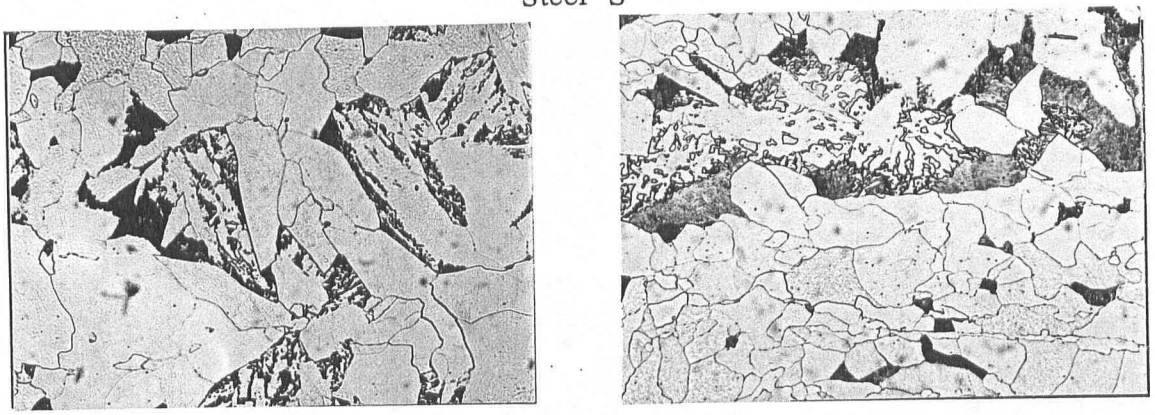

HRA 1900 CRA 1500

Steel T

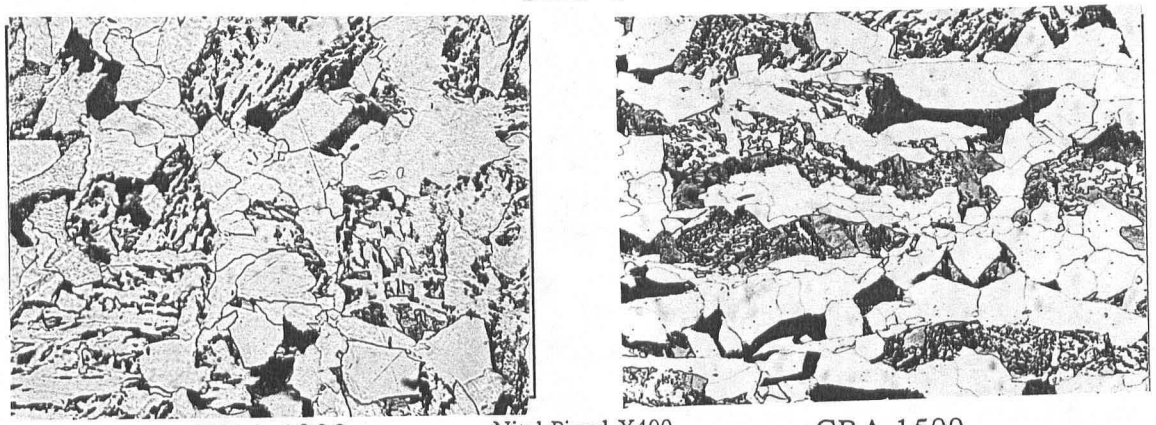

HRA 1900 Nital-Picral X400 CRA 1500

Figure 53 - Micrographs of Steels R, S, and T, Hot-Rolled or Control-Rolled and Air Cooled

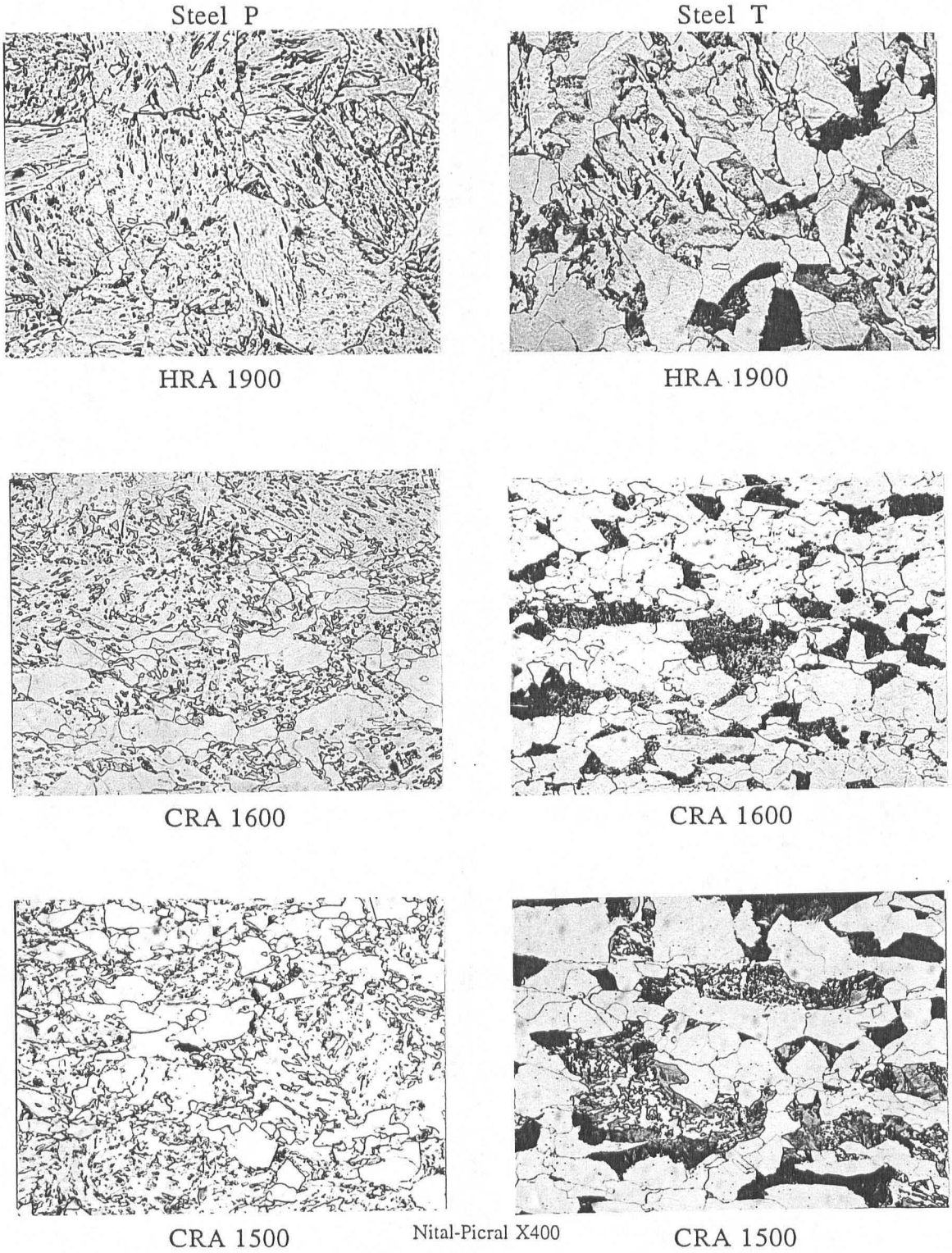


Figure 54 - Effect of Roll-Finishing Temperature on Microstructures of Steels P and T

Steel N

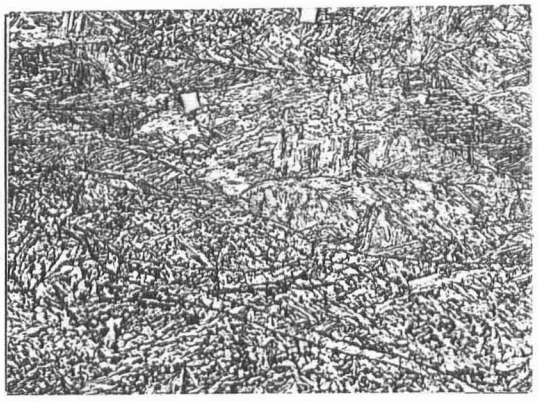

CRDQ 1600

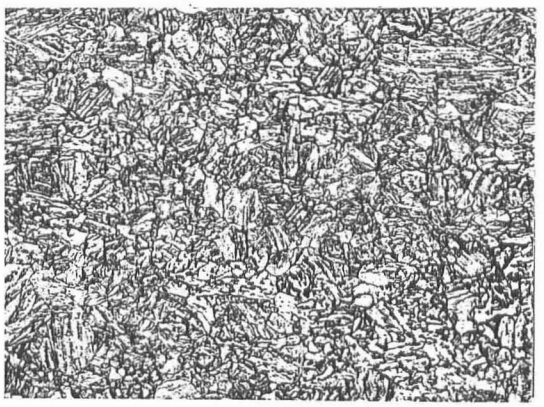

CRAQ 1600

Steel P

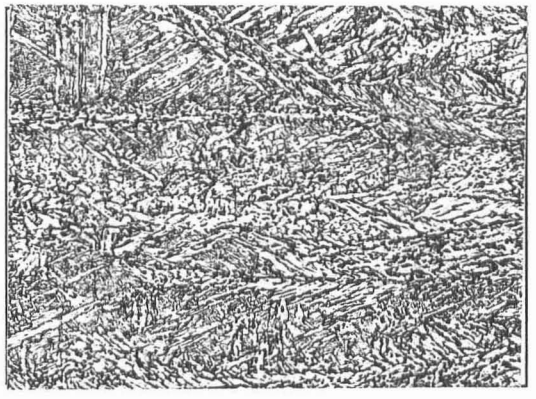

CRDQ 1600

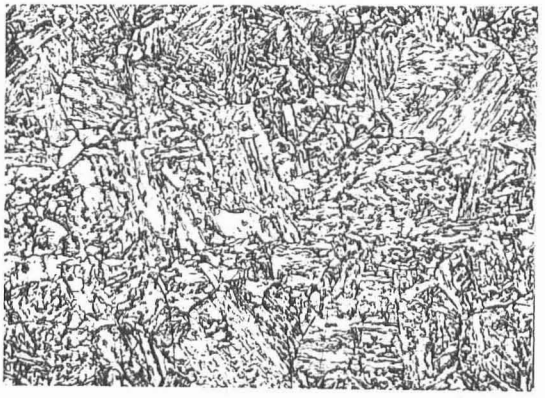

CRAQ 1600

Nital-Picral X400

Figure 55 - Micrographs of Steels N and P, Control-Rolled and As-Quenched

Steel R

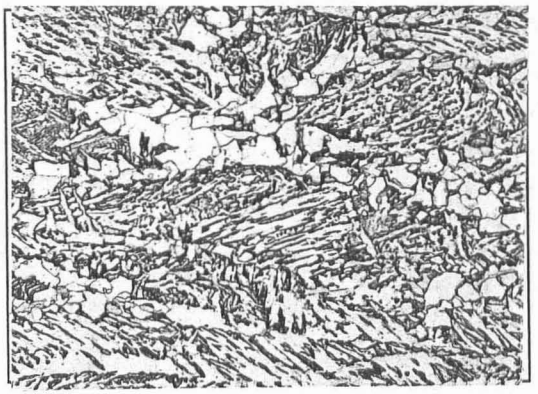

CRDQ 1600

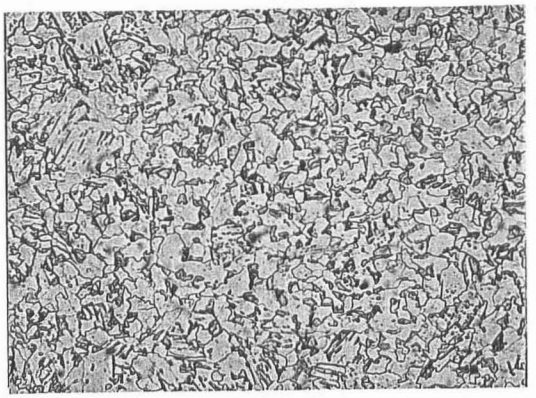

CRAQ 1600

Steel S

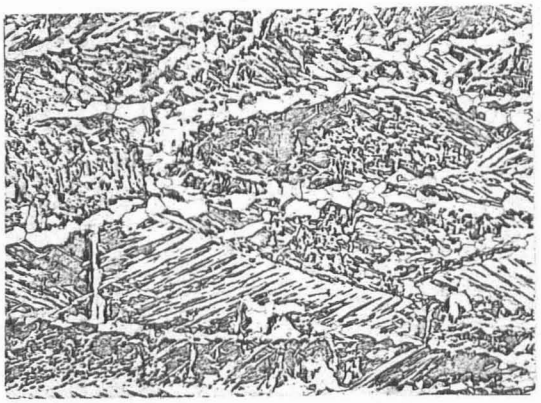

CRDQ 1600

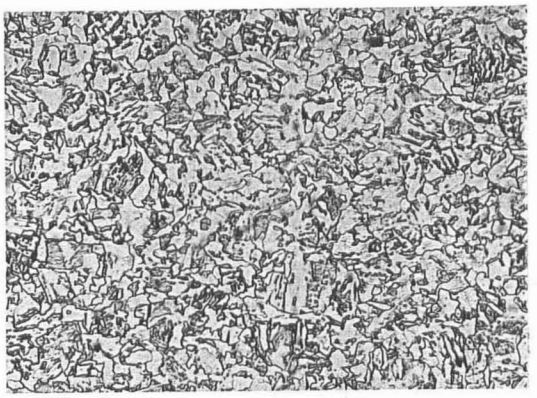

CRAQ 1600

Steel T

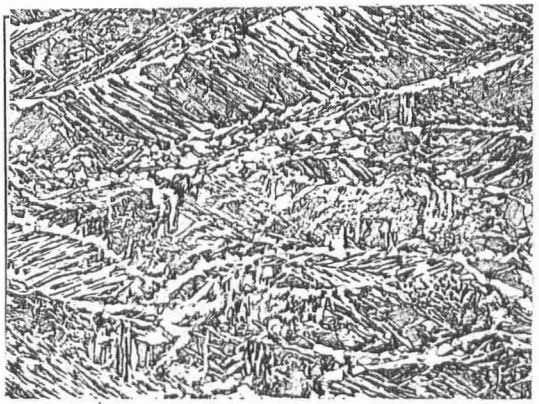

CRDQ 1600

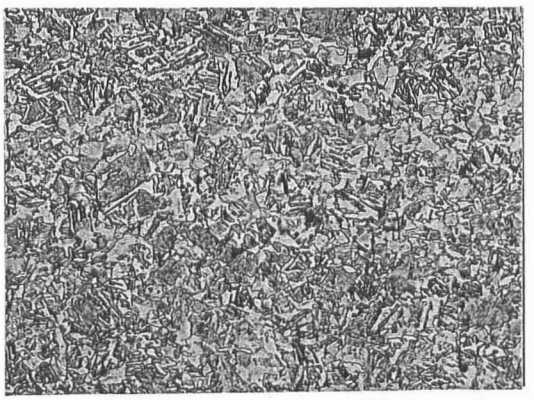

CRAQ 1600

Nital-Picral X400

Figure 56 - Micrographs of Steels R, S, and T, Control-Rolled and As-Quenched

Steel N

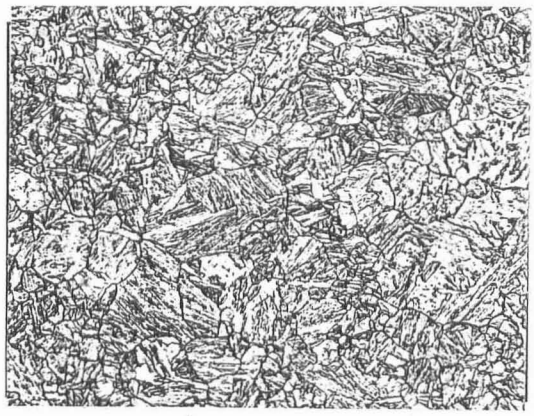

HRAQ 1900 (SQ @ 40F/S)

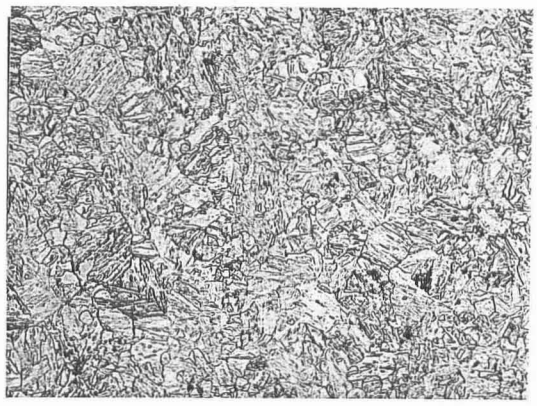

CRAQ 1500 (SQ @ 45F/S)

Steel P

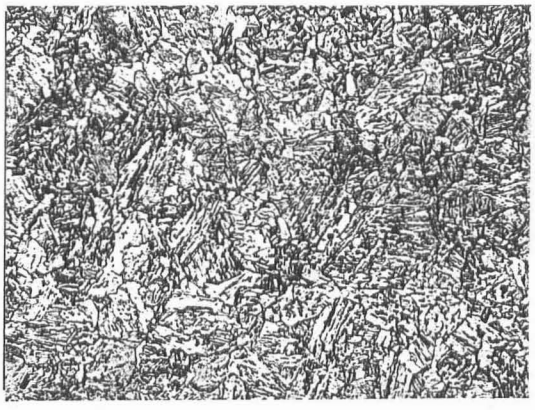

HRAQ 1900 (SQ @ 40F/S) Nital-Picral X400

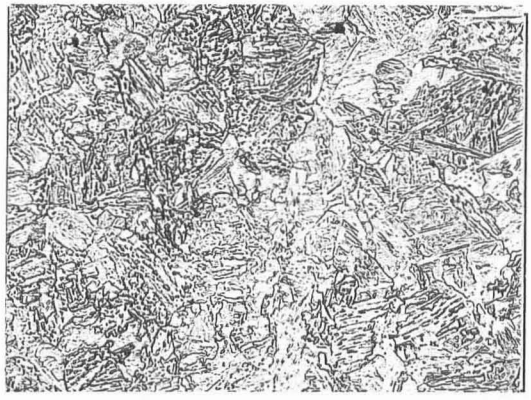

CRAQ 1500 (SQ @ 45F/S)

Figure 57 - Micrographs of Steels N and P, Hot-Rolled or Control-Rolled, Air Cooled, and Off-Line Quenched

Steel R

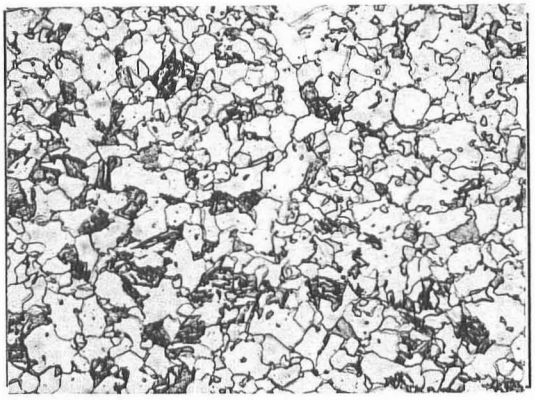

HRAQ 1900 (SQ @ 40 F/S)

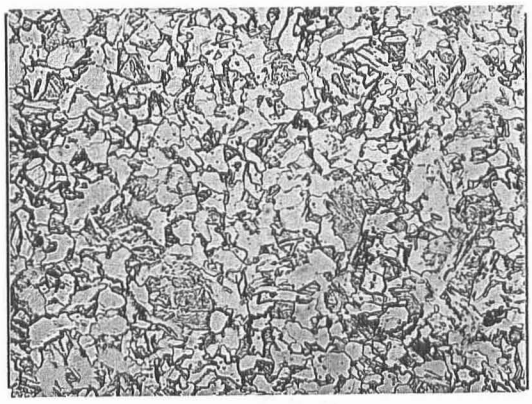

CRAQ 1500 (SQ @ 45 F/S)

Steel S

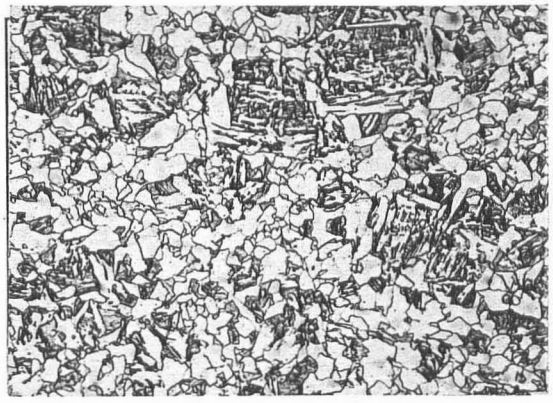

HRAQ 1900 (SQ @ 40 F/S)

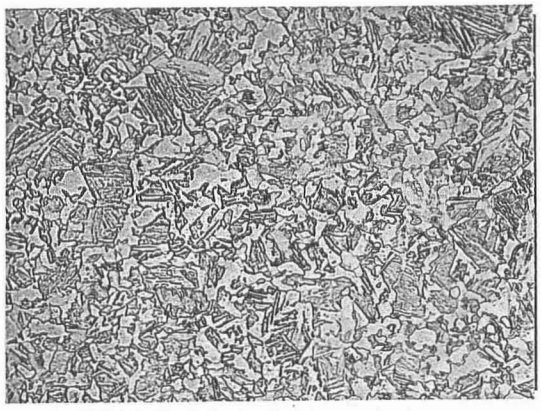

CRAQ 1500 (SQ @ 45 F/S)

Steel T

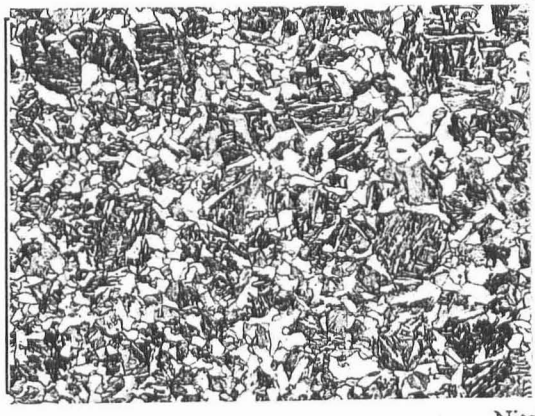

HRAQ 1900 (SQ @ 40 F/S)

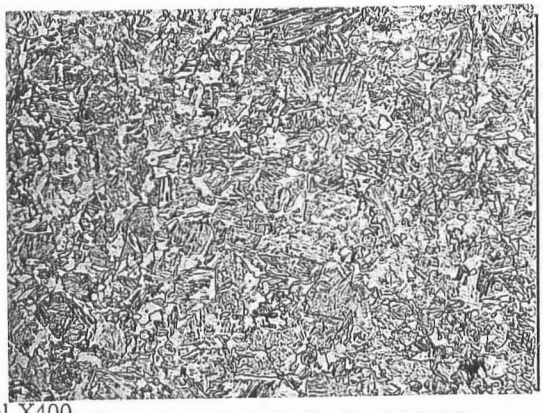

Nital-Picral X400

CRAQ 1500 (SQ @ 45 F/S)

Figure 58 - Micrographs of Steels R, S, and T, Hot-Rolled on Control-Rolled, Air-Cooled, and Off-Line Quenched

Steel N

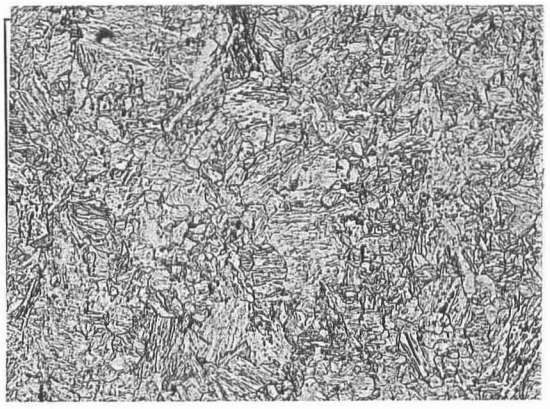

CRAQ 1500 (SQ @ 45F/S)

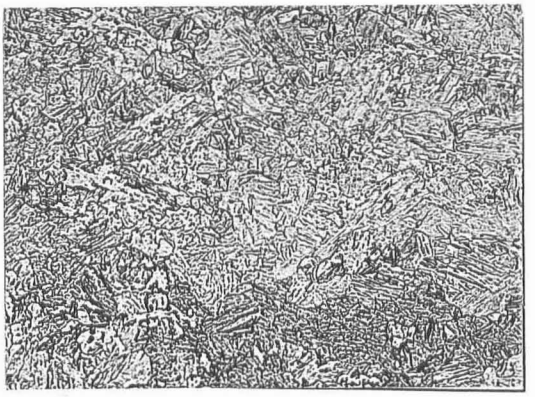

CRAQ 1500 (SQ @ 20F/S)

Steel P

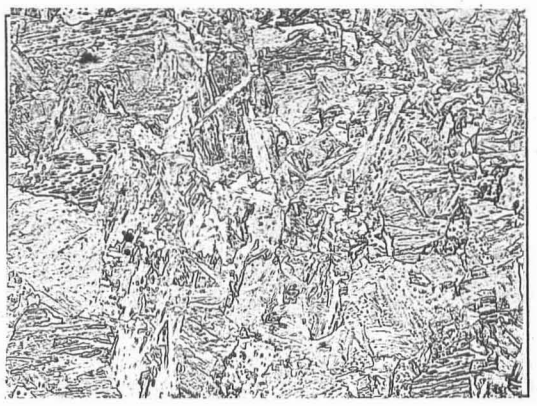

CRAQ 1500 (SQ @ 45F/S)

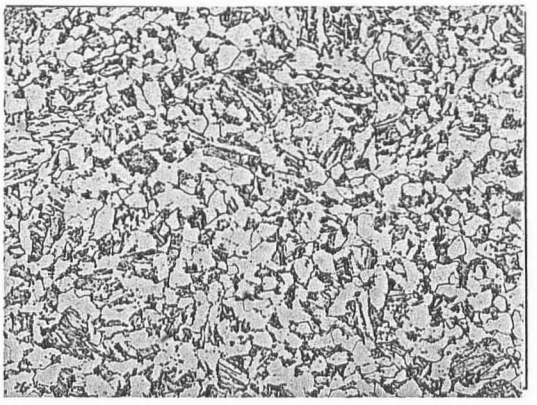

Nital-Picral X400 CRAQ 1500 (SQ @ 20F/S)

Figure 59 - Effect of Quench Rate on Control-Rolled and Off-Line Quenched Microstructure of Steels N and P

Steel R

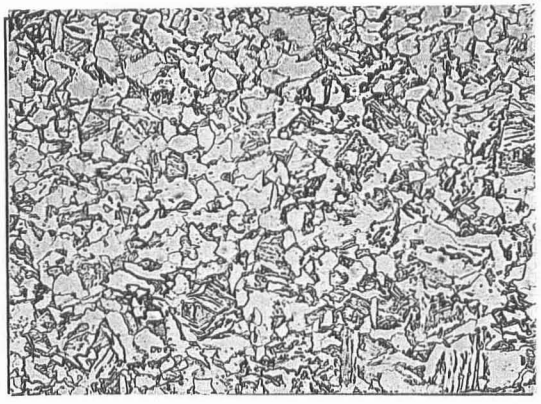

CRAQ 1500 (SQ @ 45 F/S)

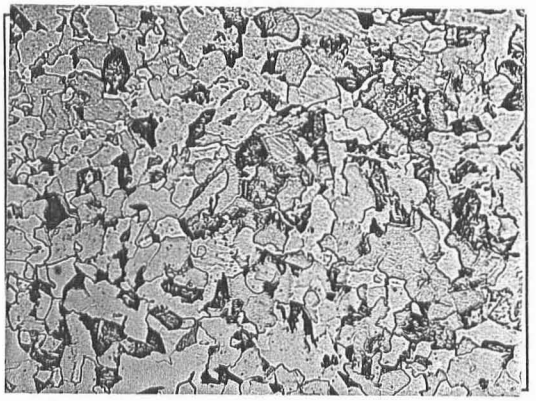

CRAQ 1500 (SQ @ 20 F/S)

Steel S

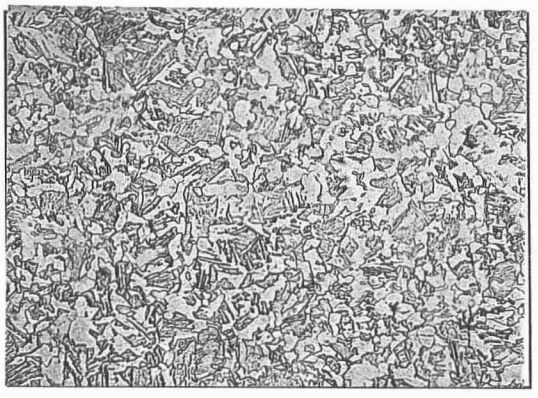

CRAQ 1500 (SQ @ 45 F/S)

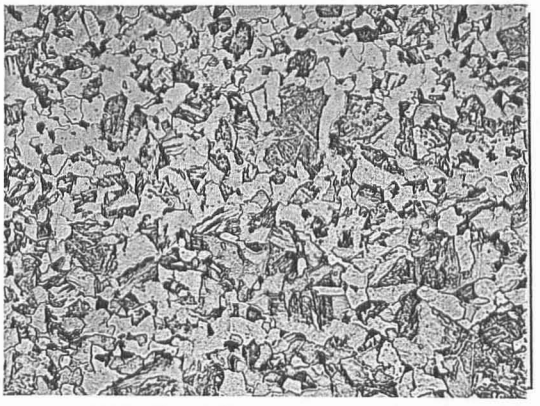

CRAQ 1500 (SQ @ 20 F/S)

Steel T

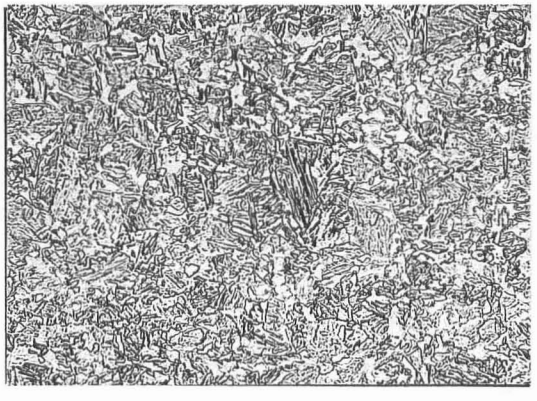

CRAQ 1500 (SQ @ 45 F/S)

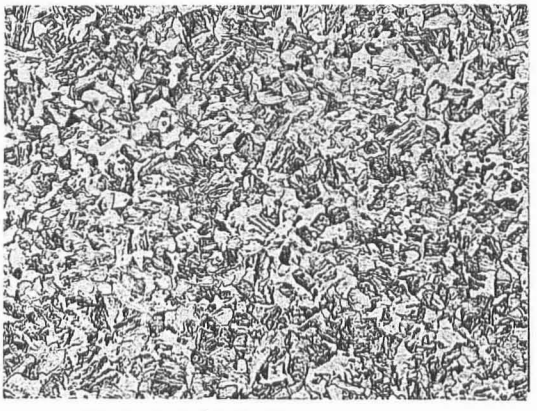

Nital-Picral X400 CRAQ 1500 (SQ @ 20 F/S)

Figure 60 - Effect of Quench Rate on Control-Rolled, and Off-Line Quenched Microstructure of Steels, R, S, and T

Steel N

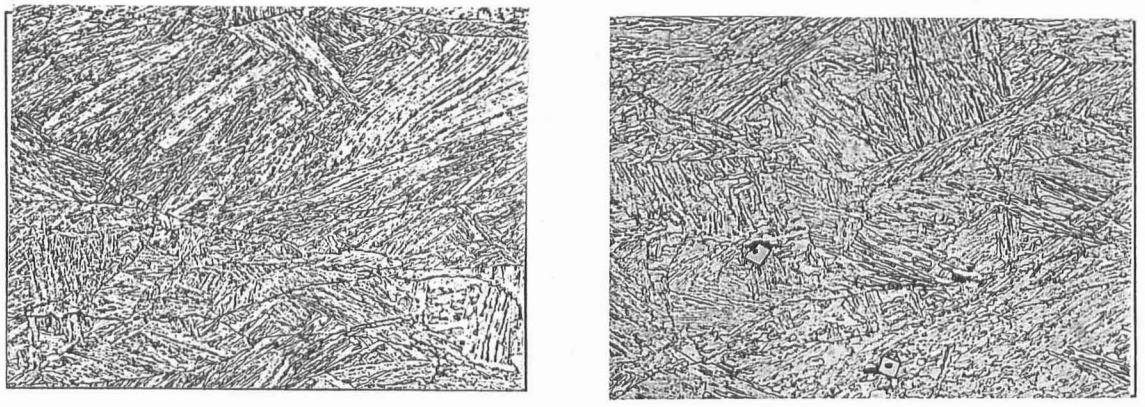

CRDQ 1725 CRDQ 1725 + T

Steel P

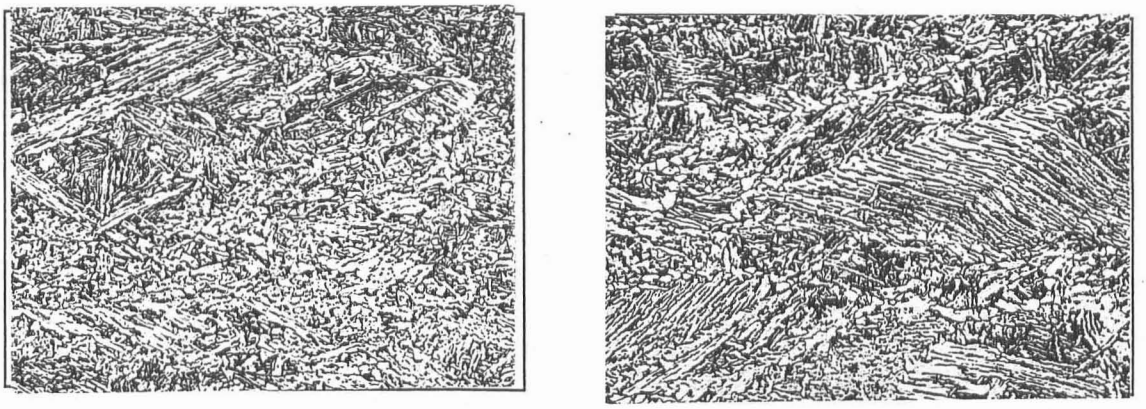

CRDQ 1725 Nital-Picral X400 CRDQ 1725 + T

Figure 61 - Effect of Tempering on Control-Rolled and Direct Quenched Microstructure of Steels N and P

Steel R

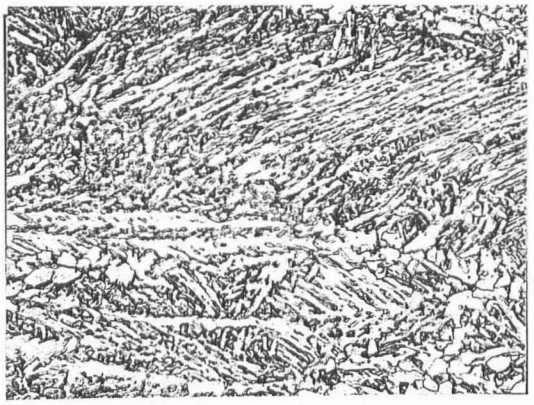

CRDQ 1725

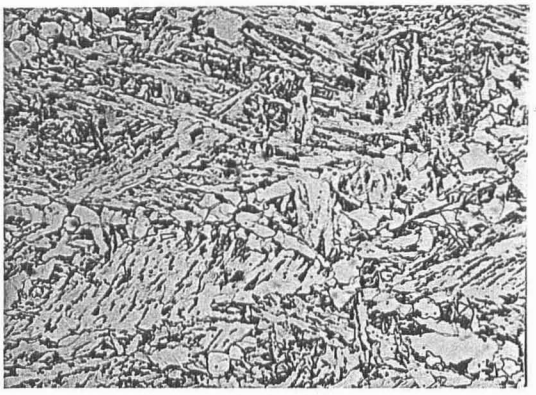

CRDQ 1725 + T

Steel S

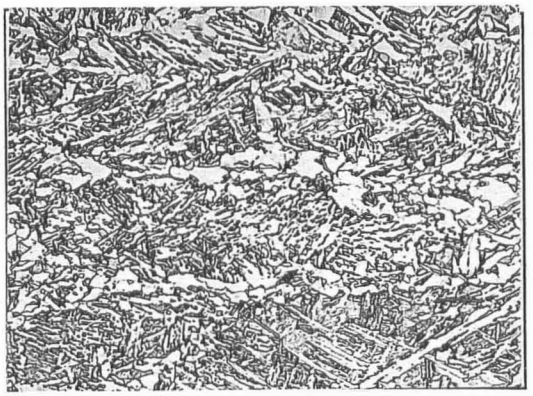

CRDQ 1725

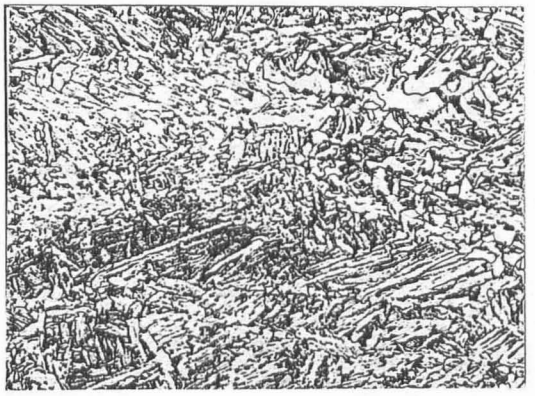

CRDQ 1725 + T

Steel T

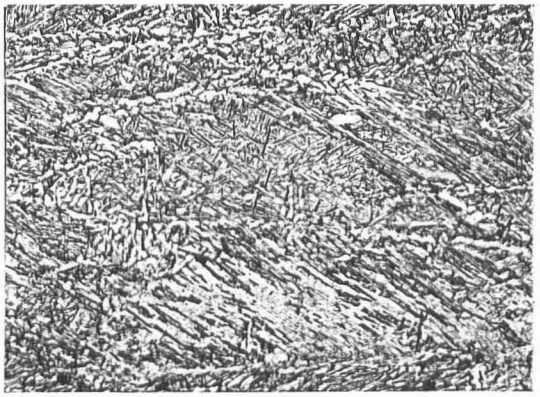

CRDQ 1725

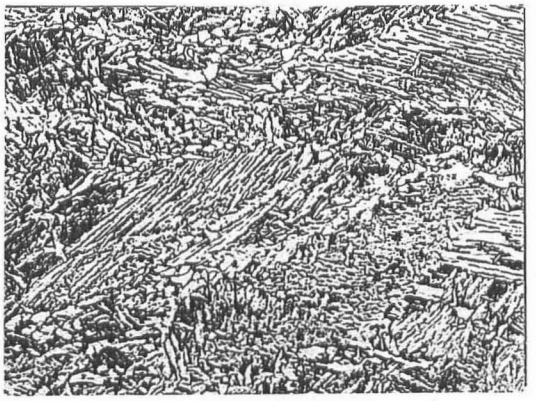

CRDQ 1725 + T

Nital-Picral X400

Figure 62 - Effect of Tempering on Control-Rolled and Direct Quenched Microstructure of Steels R, S, and T

Steel N

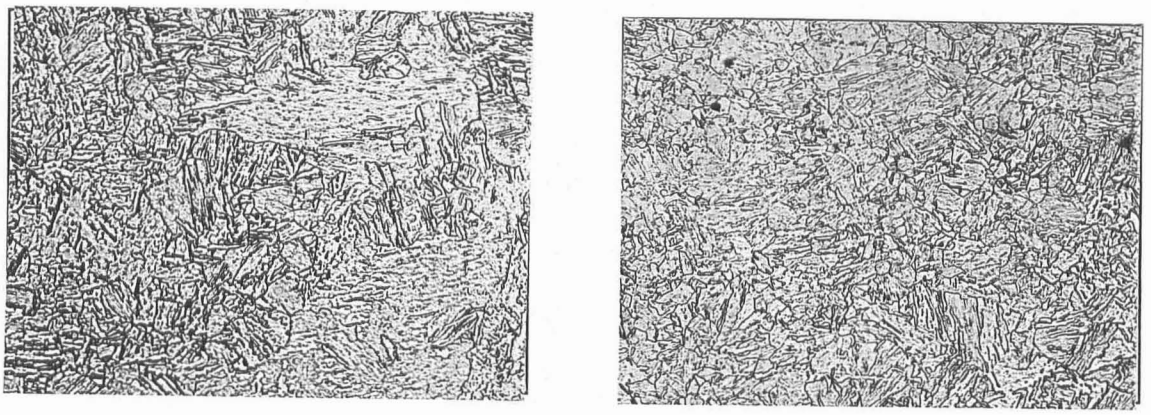

HRAQ 1900 + T

CRAQ 1500 + T

Steel P

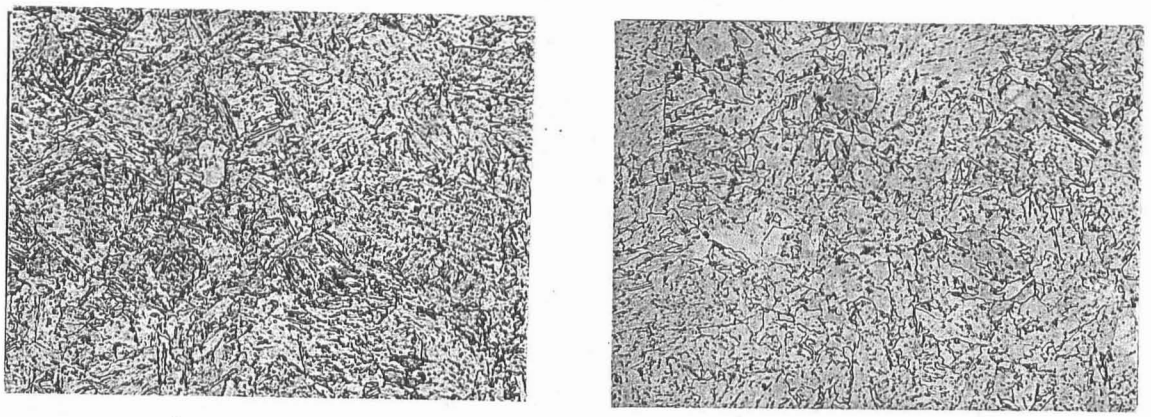

HRAQ 1900 + T

Nital-Picral X400

CRAQ 1500 + T

Figure 63 - Effect of Tempering on Air-Cooled, and Off-Line Quenched Microstructure of Steels N and P

Steel R

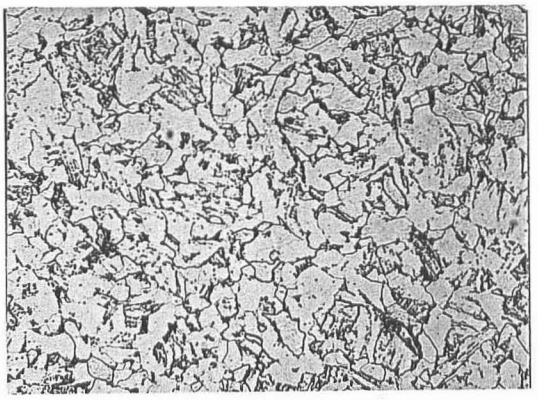

HRAQ 1900 + T

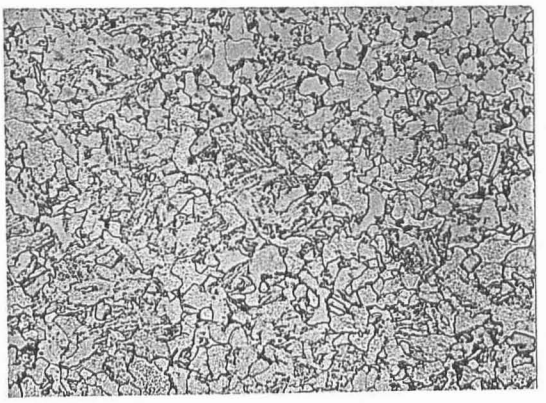

CRAQ 1500 + T

Steel S

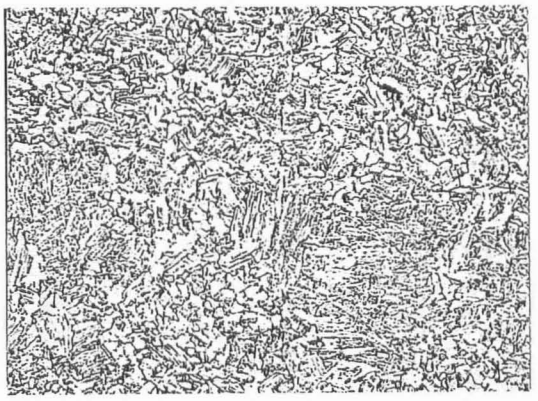

HRAQ 1900 + T

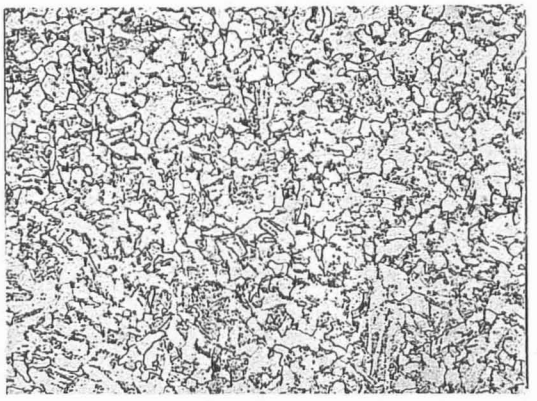

CRAQ 1500 + T

Steel T

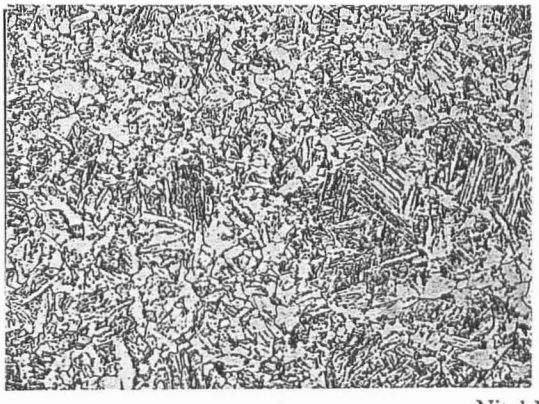

HRAQ 1900 + T

Nital-Picral X400

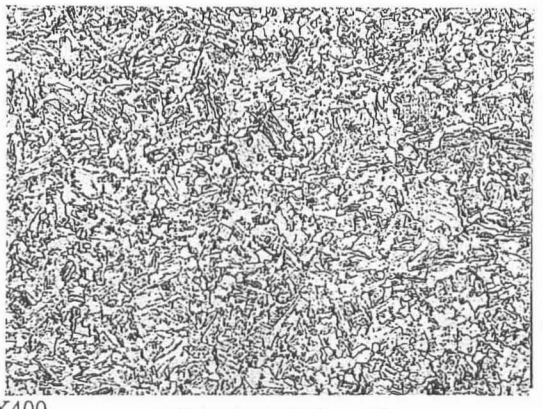

CRAQ 1500 + T

Figure 64 - Effect of Tempering on Air-Cooled, and Off-Line Quenched Microstructure of Steels R, S and T

# Bibliography


1. Shah, M. J., Infrastructure...Repairs and Inspection, American Society of Civil Engineers, New York, N.Y., 1987.

2. Albrecht, P., "Corrosion Control of Weathering Steel Bridges," Corrosion Forms and Control for Infrastructure, ASTM STP 1137, Victor Chacker, Ed., American Society for Testing and Materials, Philadelphia, PA, 1992.

3. CERF Report 94-5011, Materials for Tomorrow's Infrastructure: A Ten Year Plan for Deploying High-Performance Construction Materials and systems, CERF, Technical Report, Washington. D.C., 1994.

4. Dexter, R. J., Le-Wu Lu, Fisher, J., "Application of High-Performance Steel in New and Retrofit Structures", Proceedings of the Third Materials Engineering Conference, ASCE, Basham K. D. (Eds.), New York, NY, 1994.

5. Fisher, J. W., Fatigue and Fracture of Steel Bridges, Wiley Interscience, New York, NY, 1984.

6. Gross, J.H., Stout, R. D., *ATLSS Report No. 95-04: Report to Steering Committee - High Performance Steel (FHWA - AISA)*, Lehigh University, Bethlehem, PA, March 1995.

7. Thompson, P., Reduced Cost 100 ksi Minimum Yield Strength, Low Carbon, Low Alloy Steel Using Advanced Techniques, Lehigh University Master's Thesis, Bethlehem, PA, 1993.

8. Chrisbacher, C. J., Special Studies on the Thermo-Mechanical Processing of Low-Carbon, 100-ksi Yield Strength Steels, Lehigh University Master's Thesis, Bethlehem, PA, 1994.
9. United States Steel, The Making, Shaping and Treating of Steel, 10th ed., Association of Iron and Steel Engineers, Pittsburgh, PA, 1985.

10. Tanaka, T., "Four Stages of the Thermo-mechanical processing in HSLA Steels," TMS-AIME Conference Proceedings on High Strength Low Alloy Steels, D.P. Dunne and T. Chandra (eds.), 1984

11. Tanaka, T., Tabata, N., Hatomura, T., Shiga, C., "Three Stages of the Controlled Rolling Process," Microalloying '75, Proceedings of the International Symposium on High Strength, Low Alloy Steels, 1977, pp. 107-119.

12. Ouchi, C., "Accelerated Cooling After Controlled Rolling in HSLA Steels," TMS-AIME Conference Proceedings on High Strength Low Alloy Steels, D.P. Dunne and T. Chandra (eds.), 1984.

13. Okamoto, K., Yoshie, A., Nakao, H., "Microstructure and Mechanical Properties of Heavy Steel Plates Produced by Accelerated Cooling and Direct Quenching Process," Nippon Steel Corporation, Mechanical Working & Steel Processing XXVIII: Proceedings of the 32nd Mechanical Working and Steel Processing Conference, Cincinnati, OH, 1990.

14. Kawasaki Steel Corporation, ***MACS Multipurpose Accelerated Cooling System*** - *Kawasaki Steel's Innovative process for producing steel plates that combine excellent notch toughness with good weldability and high tensile strength*, Kawasaki Engineering Division, Japan, March 1992.

15. Stout, R. D., Weldability of Steels, 4th ed., Welding Research Council, New York, NY, 1987.

16. AWS Structural Welding Committee, 1994 Structural Welding Code - Steel, 13th ed., American Welding Society, 1994.

17. Bodnor, R. L., Cappellini, R. F., "Effect of residual Elements in Heavy Forging: Past, Present and Future," MiCon 86: Optimization of Processing, Properties, and Service Performance Through Microstructual Control, ASTM STP 979, B. L. Bramfit, R. C. Benn, C. R. Brinkman, and G. F. Vader Voort, Eds., American Society for Testing and Materials, Philadelphia, PA, 1988, pp. 47-82.

18. Gross, J. H., Stout, R. D., Czyryca, E. J., "Thermomechanical Processing of HY-130 Steel", *Welding Journal*, Vol. 74, No. 4, April 1995, pp. 53-62.

19. Brockenbrough, R. L., *Interim Report on Effect of Yield-Tensile Ratio on Structural Behavior - High Performance Steels for Construction*, ONR-AISI Agreement No. N00014-94-2-0002, Draft, Pittsburgh, PA, January 15, 1995.

20. Kuwamura, H., *Effect of Yield Ratio On Ductility of High-Strength Steels Under Seismic Loading*, This paper is part of the proceedings of the Annual Technical Session of Structual Stability Research Concil, Minneapolis, Minnesota, April 26-27, 1988.

21. Hertzberg, R. W., Deformation and Fracture Mechanics of Engineering Materials, 2nd Ed., John Wiley and Sons, New York, NY, 1989.

22. Morris, W. L., Frandsen, J. D., and Marcus, H. L., "Environmentally Induced transitions in Fatigue Fracture Mode," Fractography-Microscopic Cracking Processes, ASTM STP 600, American Society for Testing and Materials, pp. 49-61, 1976.

23. Schrader, A., Rose, A., De Ferri Metallographia - Metallographic Atlas of Iron, Steels and Cat Irons II, W.B. Saunders Company, Philadelphia, PA, 1966.

# Vita

The author was born in Phillipsburg, New Jersey on December 28, 1970 and raised in Easton, Pennsylvania by his parents Thomas and Josephine Todaro. In May of 1993 he received a Bachelor of Science degree in physics from Moravian College. He is presently attending Lehigh University in candidacy for Master of Science degree in Materials Science and Engineering. During this time at Lehigh he is working at Lehigh University's Advanced Technology for Large Structural Systems (ATLSS) Engineering Research Center as a research assistance.